2003-16

Final Report

Effects of Increasing Truck Weight on Steel and Prestressed Bridges

Research

Technical Report Documentation Page

1. Report No.	2.	3. Recipients Accession No.
MN/RC – 2003-16		

4. Title and Subtitle	5. Report Date
EFFECTS OF INCREASING TRUCK WEIGHT ON STEEL AND PRESTRESSED BRIDGES	March 2003
	6.

7. Author(s)	8. Performing Organization Report No.
Altan K. Altay, Diego S. Arabbo, Eric B. Corwin, Robert J. Dexter, and Catherine E. French	

9. Performing Organization Name and Address	10. Project/Task/Work Unit No.
University of Minnesota Department of Civil Engineering 122 CivE, 500 Pillsbury Dr. S.E. Minneapolis, MN 55455-0116	11. Contract (C) or Grant (G) No. (c) 74708 (wo) 76

12. Sponsoring Organization Name and Address	13. Type of Report and Period Covered
Minnesota Department of Transportation Research Services Section 395 John Ireland Boulevard Mail Stop 330 St. Paul, Minnesota 55155	Final Report 2000
	14. Sponsoring Agency Code

15. Supplementary Notes

http://www.lrrb.gen.mn.us/PDF/200316.pdf
Appendix A, Effects of Increasing Truck Weight on Prestressed Concrete Bridges; Appendix B, Effects of Increasing Truck Weight on Steel Bridges; and Appendix C, Effects of Increasing Truck Weight on Reinforced Concrete Decks for this report are available by contacting Mn/DOT Research Services Section.

16. Abstract (Limit: 200 words)

Any increase in legal truck weight would shorten the time for repair or replacement of many bridges. Five steel girder bridges and three prestressed concrete I-girder bridges were instrumented, load tested, and modeled. The results were used to assess the effects of a 10 or 20% increase in truck weight on bridges on a few key routes through the state. Essentially all prestressed girders, modern steel girders, and most bridge decks could tolerate a 20% increase in truck weight with no reduction in life. Unfortunately, most Minnesota steel girder bridges were designed before fatigue-design specifications were improved in the 1970's and 1980's. Typically, an increase in truck weight of 20% would lead to a reduction in the remaining life in these older steel bridges of up to 42% (a 10% increase would lead to a 25% reduction in fatigue life). Bridge decks are affected by axle weights rather than overall truck weights. Transverse cracks in bridge decks are primarily caused by shrinkage soon after construction and are not affected by increasing axle weight. However, decks with thickness less than 9 inches or with girder spacing greater than 10 ft may be susceptible to longitudinal flexural cracking which could decrease life.

17. Document Analysis/Descriptors		18.Availability Statement
truck weight	axle load	No restrictions. Document available from: National Technical Information Services, Springfield, Virginia 22161
prestressed concrete	steel	
bridge deck	girder	
cracking	deterioration	
fatigue		

19. Security Class (this report)	20. Security Class (this page)	21. No. of Pages	22. Price
Unclassified	Unclassified	129	

Effects of Increasing Truck Weight on Steel and Prestressed Bridges

Final Report

Prepared by

Altan K. Altay
Diego S. Arabbo
Eric B. Corwin
Robert J. Dexter, P.E.
Catherine E. French, P.E.
Department of Civil Engineering
University of Minnesota

March 2003

Published by

Minnesota Department of Transportation
Office of Research Services
395 John Ireland Boulevard MS 330
St. Paul, MN 55155

This report represents the results of research conducted by the authors and does not necessarily reflect the official views or policies of the Minnesota Department of Transportation and/or the Center for Transportation Studies. This report does not contain a standard or specified technique.

ACKNOWLEDGEMENTS

Funding for this research was provided by the Minnesota Department of Transportation (Mn/DOT). We would like to thank the many people from Mn/DOT who have helped with this research including Gary Peterson, Erik Wolhowe, Kevin Anderson and Charles Deutsch for providing information on bridges in the state, Curtis Dahlin for providing weigh-in-motion data, Lowell Johnson, Cliff Moening and the Bemidji and Crookston maintenance crews, Brad Johnson and the Duluth maintenance crews, and Mark Pribula and the Metro maintenance crews.

We would also like to thank all the people from the University of Minnesota that helped in this project, especially Paul Bergson for the field work, and also Eli Rupnow for his help with strain gages, field tests, and AutoCAD drawings, and Joel Ray and Nels Ojard for their help with the field tests.

TABLE OF CONTENTS

LIST OF TABLES

LIST OF FIGURES

EXECUTIVE SUMMARY

A significant increase in truck loads, i.e. maximum legal gross-vehicle weight (GVW), maximum axle weight, and/or maximum permit loads, would shorten the time before which many bridges would need to be repaired or replaced, and even increase the number of bridges that must be repaired or replaced immediately. This study was conducted to investigate the impact of an increase in truck loads on the bridge structures along Interstate T.H. 35 as well as U.S. T.H. 2 and Minnesota T.H. 200 between Duluth and North Dakota. A methodology to estimate the cost impacts of increasing truck weight on individual bridges and extrapolate these impacts to a network of bridges was developed in a recently completed National Cooperative Highway Research Program project (NCHRP 12-51). This study builds upon the methodology proposed in NCHRP 12-51, addressing several remaining uncertainties including: 1) the mechanisms of deterioration and how they are affected by increasing loads; and 2) the structural analysis to determine girder moments. Possible mechanisms of deterioration were identified from the literature. Typical Mn/DOT bridge configurations were evaluated to see which of these mechanisms would likely govern, i.e. be the first to lead to significantly increased deterioration due to increasing truck loads. For prestressed girders and bridge decks, the governing mechanisms were different from those assumed in NCHRP 12-51.

Three-dimensional beam grillage models of the bridges were used to assess the effect of truck weights on bridges. The models were refined and verified by comparing their results to strain measurements from load tests on five steel girder bridges and three prestressed concrete I-girder bridges. The refined models were then used to investigate the effect of present trucks at the legal limit as well as the same vehicle configurations with a proportionate 10 or 20% increase in axle weights. Parametric studies were used to extrapolate the results to other bridges on these routes. A methodology was proposed to extend findings from this research to other bridges in the State of Minnesota.

The governing deterioration mechanism for steel bridges is fatigue. Fatigue is insensitive to loading that occurs less frequently than 0.01% of all load cycles – such a special permit loads. However, annual permits are issued in Minnesota for an unlimited number of trips with almost twice the present legal GVW An increase in the allowable weight of these annual permit vehicles could become significant for steel bridges if they exceed 0.01% of the truck traffic at a

particular bridge. However, assuming that is not the case, the critical issue for steel bridges is a possible increase in the maximum legal GVW, rather than permit loads or axle loads.

The effect of increasing truck weight on steel girders depends on when the bridge was designed. Steel girders designed before improved fatigue design specifications were introduced in the 1970's and 1980's (unfortunately most of the steel bridges in Minnesota) often feature poor fatigue details such as welded cover plates. Many of these bridges are already experiencing fatigue cracking. The cost impact of an increase in legal GVW on bridges that are already experiencing fatigue cracking depends strongly on the action taken, e.g. replacement or repair. If repair is the approach taken, it can be estimated that the frequency of the repairs will increase 33% if the legal GVW increased by 10%; and the frequency of the repairs will increase 73% if the legal GVW increased by 20%. The present costs for maintenance and repairs of bridges already experiencing fatigue cracking would be expected to increase at least as much as the repair frequency increases.

For bridges with some remaining life before fatigue cracking begins to occur, the remaining life can be reliably calculated if the fatigue life is due to cracking from primary loads on poor fatigue details such as cover plates. For these bridges, an increase in legal GVW of 10% would lead to a reduction in the remaining fatigue life of 25%; whereas an increase in GVW of 20% would lead to a reduction in the remaining fatigue life of 42%. The impact of the decrease in life will be accelerated costs for inspection and repair, and possibly even replacement.

If the fatigue life is limited by distortion-induced cracking such as at web-gap details, the remaining life is not presently quantifiable. However, the treatment for this deficiently is typically repair, and therefore the increase in the frequency of the repairs are the same as stated above for a 10% and 20% increase in legal GVW. Therefore, the present rate of spending on repairs for distortion-induced cracking can be expected to increase 33% or 73% if the legal GVW increased by 10% or 20%, respectively. Steel girders designed since 1985 are typically not susceptible to fatigue at present truck weights and should be able to tolerate a 20% increase in truck weight without reducing the expected fatigue life to less than 75 years.

Typical Minnesota prestressed concrete girders and concrete decks were found to be not susceptible to fatigue for present or even 20% increased truck weights. If the loads were increased on the prestressed-concrete girders, the first deterioration mechanism to occur that is significantly affected by increasing loads would be shear cracking. Shear cracking is a serviceability problem and there is significant additional capacity in shear before failure could occur. However, shear cracking could increase the rate at which water can penetrate the girders and increase the rate of corrosion of the prestressing strands and other reinforcement.

Unlike fatigue, cracking of concrete is a single event due to a single load, and therefore could be caused by increases in permit loads as well as increases in legal load limits. Various truck configurations were investigated for typical Minnesota prestressed concrete I-girders. In all cases, the particular truck configuration that gave the worst-case shear would have to increase weight by more than 20% before shear cracking and associated reduction in service life would occur. Flexural cracking and fatigue of the prestressing strands and other reinforcement and fatigue of the concrete were also investigated but these phenomena would require even greater increases in truck weight before they would occur.

Bridge decks are affected by axle weights rather than overall truck weights. The first adverse phenomenon to occur in bridge decks due to increasing axle weights would be longitudinal flexural cracking. As in prestressed concrete girders, cracking of bridge decks will increase the potential for corrosion. Transverse cracks are more common than longitudinal cracks in bridge decks. However, transverse cracks are primarily caused by shrinkage during or soon after construction and are not affected by increasing truck weight. However, the spacing of transverse cracks may influence the potential for longitudinal cracking. Typically, standard 9-inch-thick (225 mm) decks with girder spacing less than 10 feet (3 m) should not be affected by an increase of up to 20% in axle weights. However, more flexible decks (thinner and/or wider girder spacing) with pre-existing transverse cracks spaced less than 5 feet (1.5 m) apart may be susceptible to longitudinal flexural cracks even from present truck traffic.

CHAPTER 1 – INTRODUCTION

1.1 PROBLEM STATEMENT

The State of Minnesota is frequently requested to allow for an increase in weight of commercial truck traffic. However, increasing truck weight (i.e. increasing maximum legal GVW, the maximum permit loads for annual or special permits, and/or the maximum legal axle load) may significantly increase deterioration in Minnesota's bridge system. Increased vehicle loads on steel bridges may cause a reduction in the fatigue life of critical details. The increased vehicle loads could potentially lead to cracking of bridge decks or prestressed concrete I-girders, which could then lead to increased reinforcement corrosion and possibly fatigue of the prestressing strand. A combined analytical and experimental study was performed to investigate the effect of increased truck weight on Minnesota steel bridges, prestressed concrete I-girder bridges, and bridge decks.

1.2 APPROACH AND SCOPE

The general objective of this research was to investigate the impact of increasing allowable truck weight on Minnesota bridges and to develop a general procedure to estimate the potential reduction in bridge life associated with an increase in the allowable gross vehicle weight (GVW).

The objective of this research is to address this problem within the following scope:

Field Tests

- Three prestressed concrete I-girder and five steel girder bridges were instrumented and load tested. Four bridges were located on Interstate 35 and one bridge was located on each of the following highways: U.S. Highway 2, Minnesota T.H. 200, Minnesota T.H. 36, and Interstate 535. The bridges were selected on the basis of ease of access, bridge characteristics, and location.

- Strain gages were placed on several locations on the girders and deck for each bridge. The bridges were then subjected to loaded trucks of known weight and dimensions. Bottom fiber strains and strains along the depth of the girders and strains on the bottom surface of the deck were recorded during the load tests.

Analytical Study

- Each tested bridge was modeled using a finite element approach. The models were calibrated to the response of the real bridge using the test data.

- Parametric studies were conducted to investigate the effect of several variables on the response of each bridge.

- For steel bridges the procedures developed by Moses et al. (1987) in National Cooperative Highway Research Program Report 299 (NCHRP 299) were used to evaluate the remaining fatigue lives. These procedures provide reasonable estimates when a sufficiently accurate analysis of the stresses is used.

- For prestressed concrete girder bridges, the possibility that the increase in truck weight would lead to cracking of the girders was investigated. Strand stress ranges were calculated, and the number of cycles to fatigue failure of the girders was determined.

- For bridge decks, two possible causes for cracking were investigated: fatigue and overstressing (i.e. susceptibility to longitudinal cracking). For each problem, the effects of different variables were determined. The characteristics of bridges most susceptible to deck deterioration from the possible increase in the current truck weight limits were identified.

- On the basis of the research findings, a methodology was proposed to extend findings from this research to other bridges in the State of Minnesota.

1.3 OVERVIEW OF REPORT

The main body of this report is separated into five chapters and summarizes the findings reported in the appendices. The report also contains additional information that is general to the three appendices. Appendix A contains "Effects of Increasing Truck Weights: Prestressed Concrete Bridges" by Arabbo (2002), which examines the effect of increased truck weight limits on prestressed concrete bridges. Appendix B contains "Effects of Increasing Truck Weights: Steel Bridges" by Corwin (2002), which focuses on the effect on steel bridges. Appendix C contains "Effects of Increasing Truck Weights: Bridge Decks" by Altay (2002), which investigates the effect of increased truck weight limits on reinforced concrete decks.

Chapter 2 provides background information on several topics. This includes:

- design and evaluation specifications related to the fatigue and service lives of bridges.
- analysis methods that were used or considered to be used for evaluation.
- information on truck loads.
- deterioration issues related to the three aspects of this report; prestressed concrete girders, steel girders, and reinforced concrete decks.

Chapter 3 describes the field testing of the eight bridges, including selection, instrumentation, and truck tests. Chapter 3 also describes the analytical modeling and compares these results with the measured results. In Chapter 4, the effect of increased truck weight on these and other bridges is determined. Chapter 5 summarizes and presents the conclusions from this research.

CHAPTER 2 – BACKGROUND

Chapter 2 is composed of four main sections. In Section 2.1, the design and evaluation procedures are presented with an emphasis on the service and fatigue limit states. Section 2.2 discusses different analysis methods. In Section 2.3, a discussion is provided on loads, including limits, configurations, and histograms. Section 2.4 describes the issues that are related to deterioration and fatigue of prestressed concrete and steel girder bridges and reinforced concrete decks.

2.1 DESIGN AND EVALUATION PROCEDURES

As part of the process of understanding the bridge structures that were studied, an extensive review of the design provisions governing the design of the bridges was performed. In the subsections that follow a general overview of the limit states and distribution factors found in the design provisions is presented.

2.1.1 Limit States

The 1998 American Association of State Highway and Transportation Officials (AASHTO) LRFD Bridge Design Specifications (AASHTO 1998) recognize the following four limit states:

- *Service Limit State*: Restricts stress, deflection, and crack width, under regular service conditions.
- *Fracture and Fatigue Limit State*: The fatigue limit state restricts stress ranges for a particular number of stress range cycles, as produced by a single design truck. The fracture limit state is a set of material toughness requirements as they are described in the AASHTO Material Specifications.
- *Strength Limit State*: The purpose of this limit is to ensure local and global strength and stability of a structure when faced with the different load combinations likely to occur during the structure's lifetime.

- *Extreme Event Limit State*: This limit state is in place to ensure the survival of the structure when faced with extreme events, such as earthquakes, floods, collision of a vessel, vehicle, or ice flow.

The study described herein focused on the service and fatigue limit states for prestressed concrete girders and reinforced concrete decks, and the fatigue limit state for steel bridges.

2.1.2 Design Specifications

Many older bridges in Minnesota were designed for much lower loads and do not meet present design criteria for either strength or service for today's legal loads. For example, most Minnesota bridges designed in the 1960's have poor inventory ratings, i.e. the calculated remaining live-load strength capacity. Fortunately, the ratings arte typically very conservative, especially since they are carried out with simplified line girder analysis models and girder distribution factors that consistently overestimate the flexural stresses in the girders (see Section 2.2.1 below).

Design specifications used to be based on allowable stresses, checked at service load levels (without load factors). Serviceability and fatigue specifications are still typically based on service loads. However, load-factor design (LFD) surpassed allowable stress design (ASD) for strength calculations. In 1994, the Load and Resistance Factor Design (LRFD) Specification was introduced

2.1.2.1 Prestressed Concrete Design

Typically, the design of prestressed concrete bridge girders is governed by the limiting allowable stresses. Allowable stress design is a limit state design based on limiting anticipated stresses in the structure under different stages of loading. For precast members such as prestressed bridge girders, the allowable stresses are checked at three distinct loading stages. The first stage corresponds to the time when the member is loaded by the prestress only, with no superimposed external loads present. During this stage, the stresses are limited in order to prevent cracking and crushing of the concrete. The second stage involves the transportation and erection of the members, and stresses during this stage are also checked to ensure the member does not crack. The third stage corresponds to the actual external loading of the members. During this last stage

the anticipated stresses are limited to prevent cracking, and in addition the member is checked to meet ultimate strength and ductility requirements.

The process of design typically begins with the determination of the required prestressing level to limit member stresses during various loading stages. At service load conditions, all prestress losses are assumed to have taken place, and the deck is assumed to act compositely with the girder. Live loads used in design include various design trucks and/or distributed lane loadings. Typically, the live load is multiplied by the corresponding live load distribution factor and impact factor, and is then applied on a single simply supported beam, where the beam is assumed to act compositely with a corresponding effective deck portion, and the desired response is computed (moment, shear, etc).

Following the check of allowable stresses, the entire member is then checked for ultimate strength under factored loads, using load factor design.

2.1.2.2 Steel Bridge Design

In steel structures, compact members that were able to fully develop their plastic capacity would often be governed by the serviceability criteria under overloads, where flange stresses were limited to a value slightly less than the yield point. For steel structures, the fatigue life or number of cycles to failure, is governed primarily by the nominal stress range and the detail category as reflected in the AASHTO S-N curves (Figure 2.1), which show the number of cycles to failure, N, for a given constant stress range, S. There are individual S-N curves for different categories of details, and each of these S-N curves is based on extensive laboratory data (Fisher et al. 1970 and Fisher et al. 1974). There is a great deal of scatter in fatigue test data, consequently the life predicted for a given stress range by these S-N curves represents a lower bound with a 97.5% probability of exceedence. If a constant stress range is below the constant amplitude fatigue limit (CAFL), the detail is expected to have theoretically infinite fatigue life. The CAFL for each detail is shown in Figure 2.1 by the horizontal dashed lines.

Both the 1989 AASHTO Standard Specifications (AASHTO 1989) for Highway Bridges and the 1998 AASHTO LRFD Bridge Design Specifications use the S-N curves in Figure 2.1. However, these specifications use the curves in slightly different ways. The AASHTO LRFD Specifications use the stress ranges from the HS-20 vehicle with constant 30 ft. (9.1 m) rear axle spacing with a factor of 0.75 on the load. The Standard Specifications use the same vehicle without a factor to reduce the gross vehicle weight for fatigue. The AAHSTO LRFD Specifications check for infinite fatigue by comparing the stress range at the detail with one-half of the CAFL stress range. The Standard Specifications design for infinite fatigue life (defined as over two million cycles in this Specification) by requiring that the stress range from the design vehicle be less than the CAFL for redundant members.

Further discussion on the fatigue design of steel bridges is presented in Chapter B2.

2.1.2.3 Reinforced Concrete Deck Design

Before the 1994 AASHTO Design Code provisions, concrete bridge decks were only orthotropically reinforced in the U.S. In this design approach, different reinforcement ratios are applied in the perpendicular and parallel directions to the traffic. Greater amount of reinforcement is required in the perpendicular direction to traffic, because the orthotropic reinforcement design does not take two-way slab action into account in the bridge deck; it assumes that the deck behaves as transverse strips along the length.

Studies in Ontario in the late 70's (Hewitt et al., 1975, Batchelor et al., 1978) developed isotropically reinforced bridge decks, which accommodated the two-way slab action by the requirement for equal amounts of reinforcement in both directions. It was observed in laboratory tests during the development of this design approach that the desired ultimate and fatigue strengths could be attained even with levels of reinforcement required only for shrinkage and temperature in conventional design (Batchelor et al., 1978). The design procedure proposed by Batchelor et al. (1978) was first included in the Ontario Highway Bridge Design Code (OHBDC), 1991. It was adopted into the AASHTO LRFD Bridge Design Code (1998) as the "Empirical Bridge Deck Design Method."

In the State of Minnesota, the existing bridge decks are constructed with orthotropic reinforcement patterns. In future bridge decks, the construction of isotropic decks may be more common due to the development of the procedure in AASHTO LRFD Bridge Design Code (1998) and the ease of design.

2.2 ANALYSIS METHODS

In this section, several methods of bridge analysis are discussed, including line girder analysis and more refined methods, such as the finite element method.

2.2.1 AASHTO Line Girder Analysis

The purpose of the distribution factors used in the 1989 AASHTO Standard Specifications method of lateral distribution is to reduce the complex analysis of a bridge subjected to one or more vehicular loads to a simple analysis of a beam. The distribution factors are used to distribute wheel loads to adjacent girders. The method is based on the assumption that the maximum load effects on a girder or strip of unit width (in the case of a slab bridge), can be determined by treating it as a one dimensional beam subjected to the load of one line of wheels of the design vehicle multiplied by a load fraction.

In the case of the method of lateral distribution found on the 1989 AASHTO Standard Specifications for Highway Bridges, the load fraction is equal to S/D, where S is the girder spacing and D is a factor given in the specifications for different bridge types. D is in essence a measure of how each bridge distributes load. This type of method is often coined D-type method of load distribution, and was originally developed by Newmark in 1948 (Newmark, 1948). The method, as it is currently found in the 1989 AASHTO Standard Specifications, was developed in the 1970's by Sanders and Elleby (Sanders and Elleby, 1970). A detailed description of the S/D method is given in Section A2.2.1.

The 1998 AASHTO LRFD Design Specifications introduced more detailed equations for computing live load distribution factors. The new distribution factors and load fraction equations

were calibrated to accurately represent the loading produced by a new HL93 design truck and by the existing HS20 design truck. These equations and distribution factors were only included in the 1998 AASHTO LRFD Bridge Design Specifications and were revised for both moment, and shear. They were based on the assumption that no interior diaphragms were present within the span. Where transverse diaphragm were present within the span, the 1998 AASHTO LRFD Design Specifications recognized that an improvement in load distribution would likely take place, and allowed the use of an acceptable method of structural analysis to evaluate the improvement.

The advantages of the new equations is that they resulted in load distribution factors that more closely resemble the load distribution pattern of the structure, and that they represented new truck configurations much more accurately than the old equations. The main disadvantage of the new equations and factors is that they were specifically calibrated for the HL93 and HS20 design vehicles, and hence are not applicable to other types of trucks (such as the newly proposed NAFTA truck) and tandems. The new equations are given in Section A2.2.2

When looking at fatigue, the 1998 AASHTO LRFD Bridge Design Specifications addresses load redistribution in different manners based on the method of analysis used. When using a refined method of analysis, such as finite elements or the grillage analogy method, Section 3.6.1.4.3a of the LRFD Bridge Specifications requires that the design vehicle be positioned longitudinally and transversely on the bridge in order to maximize the stress range on the critical components. By making the position of the design vehicle independent of the location of traffic and design lane, the code accounts for uncertain future traffic patterns. This results in an inherently conservative fatigue limit state because it is highly unlikely that the structure will see a large number of stress range cycles in the transverse direction. When using an approximate method, the 1998 AASHTO LRFD Specifications requires that the distribution factor for one lane be used. This is in addition to the various distribution factors used by each approximate method.

2.2.2 Refined Methods of Analysis

An integral part of this project was the numerical analysis of the selected bridges in order to predict bridge responses to different loadings and load patterns. The bridge responses were used for the assessment of fatigue limits on members, connections, details, and ultimately – the bridge as a whole.

Presently, there are many different approaches to bridge analysis. These range from the very complex, such as finite element analysis with solid three-dimensional elements, to very simple, two-dimensional methods such as the method of joints or method of virtual work.

What follows is a short description of each of four refined methods of analysis currently available. Table 2.1 shows the applicability of three of the four methods of analysis discussed based on three main parameters: type of deck, plan geometry, and support conditions.

2.2.2.1 Articulated Plate Method

This method is best suited for bridges in which the transverse distribution of load occurs mainly through shear forces, with very little involvement of transverse bending stiffness (Bakht and Jaeger, 1985). This method is ideally suited to cellular and multi-cell bridges. Essentially, the bridge is divided into longitudinal strips that are joined along longitudinal seams. The transverse distribution of loads occurs mainly through shear forces acting at the seams.

2.2.2.2 Orthotropic Plate Method

The orthotropic method consists of replacing an actual bridge deck with an equivalent plate for the purpose of determining the distribution of stresses. The orthotropic plate is defined as a plate with different specified elastic properties in two orthogonal directions. Two forms of orthotropy exist: material orthotropy and shape orthotropy. Most bridges are orthotropic because of shape orthotropy (Cusens and Pama, 1975).

This method is best suited for cases in which load distribution occurs mainly through flexure and torsion in the longitudinal and transverse directions. Deflections due to shear should be small,

and thus negligible. The use of the orthotropic method of analysis on cellular and multi-cell bridges requires that the method be modified to account for the deformations due to shear present in these bridge types (Bakht and Jaeger, 1985).

2.2.2.3 Finite Element Modeling

Finite Element Modeling (FEM) is the most powerful and accurate of the methods of analysis discussed here. This method is an extension of the direct stiffness approach to structural analysis. The method utilizes an assemblage of two- and three-dimensional members to represent a structure. The members are connected at nodal points which posses a prescribed number of degrees of freedom.

The finite element method can be broken down into three phases (Clough, 1965):

Structural idealization. The structure is modeled as an assemblage of discrete "elements". Each element has finite dimensions and properties, and force-displacement relationships need to be established for each element (i.e. material properties, restraint conditions at each node). Then a mathematical approximation is selected for the elements (this could be in the form of an equation of any order).

Evaluation of Element Properties. In this step the shape of the approximating element is selected. This shape could be triangular or quadrilateral, and the elements can be both planar and solid. The shape chosen depends on the convergence property of each element, the geometry of the structure and the importance of local features such as stress concentrations. In general, the greater the level of detail and accuracy required, the finer the mesh.

Structural analysis of the element assemblage. By using matrix methods of analysis, certain requirements are to be satisfied:

- Equilibrium of the internally and externally applied forces at each node of an element.
- Geometric fit or compatibility of element deformations, in such a way as to have nodes of adjacent elements meet without discontinuities in the loaded configuration.

- Establish internal force-displacement relationships with each element as governed by the existing geometry and material property characteristics.

By satisfying the above requirements it is possible to obtain nodal displacements, and hence stresses and strains at each node.

The main advantages of the FEM are its accuracy, the flexibility to adapt to any geometry in two or three dimensions, and the wide availability of software and capable computers that can effectively perform the calculations.

The disadvantages of the FEM lie in its complexity. This translates into lengthy data preparation and an increase in computing time as the number of elements increases.

2.2.2.4 Grillage Method of Analysis

The grillage method works by idealizing a structure as a discrete grillage of beams in a two-dimensional plane interconnected by rigid or flexible joints. The beams are often chosen so as to coincide with the actual beams and transverse diaphragms present in the bridge. The idealized beams combine the contribution of the torsional rigidity and stiffness, both transverse and longitudinal of the actual beams and bridge deck.

Load distribution is easily performed with the grillage method. Wheel loads are treated as point loads acting perpendicular to the grillage and are distributed to adjacent grillage beams in proportion to the distance to each beam.

As with the orthotropic plate, this method is suitable for cases in which load distribution occurs mainly through flexure and torsion in the longitudinal and transverse directions. As before, the deflections due to shear should be small enough as to be considered negligible. This type of analysis can be used with solid slab, slab-on-girder, and voided slab type of bridges (the analysis on cellular and multi-cell bridges requires that the method be modified to account for deformations due to shear (Bakht and Jaeger, 1985). In addition, the method can easily be adapted to bridges exhibiting heavy skews, edge stiffening, isolated supports, or other

complicating features. The grillage method can also handle two and three-dimensional analyses (space trusses).

2.2.2.5 Method of Analysis Used

When considering girders (steel and prestressed concrete), the grillage method was used. Several reasons made this method a better choice over the other methods of analysis:

- The grillage method can be easily adapted to work with almost any type of bridge (the analysis on cellular an multi-cell bridges requires that the method be modified to account for the deformations due to shear (Bakht and Jaeger, 1985). Because the joints of the grillage can be given any form of restraint to movement, support conditions can easily be accounted for with the grillage method (Cusens and Pama, 1975).
- In addition, the grillage method can be applied to bridges exhibiting heavy skews, edge stiffening, isolated supports, or other complicating features.

In the case of the investigation of the flexural deck stresses, an efficient methodology combining the grillage method and three-dimensional FE modeling was applied. The deck region considered to have susceptibility to longitudinal cracking is modeled using the quadrilateral shell elements, and the other regions are modeled using the principles in the grillage method. Therefore, the accuracy of the three-dimensional finite element method and the time-efficiency of the grillage method are combined. More detail can be found in Section 3.6.3 and Chapter C5.

2.3 LOADS

In this section loads are discussed, including design loads, truck GVW and axle regulations, and histograms.

2.3.1 Design Loads

Most of the bridges considered in this study were designed using HS20 or higher design load (HS20 with modification or HS25). The HS20 design load has a gross weight of 72 kips (320 kN) was developed in the early 1950's and represents the typical service load level at that time. As truck weights and demand on the structural performance of bridges increased, the representative loads for service level were increased for design, leading to the development of the HS25 loading with Load Factor Design Code (1989), which has a gross weight of 90 kips (400 kN).

The live load model (named as HL93 loading) in the recent AASHTO LRFD Specifications (1998), consisting of both a truck or tandem coincident with a uniformly distributed lane load of 640 pounds per foot (9.3 kN/m) was developed as a notional representation of shear and moment produced by a group of vehicles routinely permitted on highways of various states under grandfather provisions. In states with grandfather provisions (e.g. Michigan), higher loads than current limits are allowed. He lane load is equivalent to a legal 90 kip (356 kN) truck every 125 feet (38 m).

To determine an optimum model for the force effect on bridges of various span lengths from grandfather vehicles, the envelope of maximum moment and shear was calculated and compared to the corresponding force effect from an HS20 loading (AASHTO LRFD Bridge Design Code, 1998). The bias factor, defined as the ratio of maximum force effect from the envelope of grandfather vehicles to the corresponding force effect from the HS20 vehicle, was calculated and plotted against span length. A constant bias factor of 1.0 across all span lengths would only be possible if a complete match of force effects existed, indicating that the HS20 was an accurate and representative model of the loads regulated with grandfather provisions would be indicated by. However, the bias factor was observed to vary from about 0.9 for very short span lengths to about 1.8 for span lengths in the 80 to 120 ft range (24 to 37 m). These results proved that the HS20 loading was not representative of the loads on highways in states with grandfather provisions.

The model, consisting of either the HS20 truck plus the uniform lane load or the tandem plus the uniform lane load (designated as HL93 loading) resulted in a bias factor between 0.9 and 1.1 for all force effects over all span lengths. It was also demonstrated that the HL93 loading and the load factor applied to the live load were independent of span length. Therefore, for design purposes, the HL93 loading represents current service load levels better than the HS20 loading.

2.3.2 Weight Regulations

Considerable concern over the deterioration of the existing bridge infrastructure in the United States combined with pressure from the trucking industry to increase weight limitations, created a need to regulate the truck weights to guarantee the safety and serviceability of bridges. For this purpose, federal legislation introduced a program called "Federal-Aid Highway Act." This legislation restricts the gross vehicle weight and the weights of different axle types. The Federal-Aid Highway Act restricts truck weights on Interstate Highways through (a) gross vehicle limit of 80,000 lb. (356 kN); (b) limits on axle loads (20,000 lb. (89 kN) for single axles, 34,000 lb. (150 kN) for tandem axles); and (c) a bridge formula that specifies the maximum allowable weight on any group of consecutive axles based on the number of axles in the group and the distance from first to the last axles (FHWA 1994). The axle group weights are regulated based on the truck weight formula or Formula B (Equation 2.1a for customary U.S. units and Equation 2.1b for SI units).

$$W = \frac{BN}{2(N-1)} + 6N + 18 \qquad \text{(U.S. Customary)} \qquad 2.1a$$

or

$$W = 2.2\left(\frac{0.305BN}{N-1} + 12N + 36\right) \qquad \text{(SI units)} \qquad 2.1b$$

where W is the overall weight of the axle group of two or more axles, B is the length of the axle group (the units in Equation 2.1a are pounds and feet, and newtons and meters in Equation 2.1b), and N is the number of axles in the axle group. Formula-B was calibrated to avoid girder

overstressing of HS20 bridges by more than 5% and of H15 bridges by more than 30%. Figure 2.2 shows examples of legal loads that meet this formula and are commonly used for rating.

Critics in the truck industry and transportation agencies have focused on the high conservatism of Formula B due to the experiences in some states and the province of Ontario in allowing higher truck weights (Ghosn 2000). Grandfather Provisions in the federal statutes allow some states to retain higher limits than the limits found from Formula B, if the higher limits were in effect prior to the enactment of the federal statutes. Exemptions to federal weight limits are determined based on interpretations of state laws rather than on the likely consequences of granting the exemptions. Minnesota allows a winter increase of GVW of 10% during dates set by the transportation commissioner based on a freezing index. Many states have increased their legal loads above the 80,000 lb. (356 kN) limit. Michigan, for instance, allows loads up to 154,000 lb. (685 kN), most western states allow loads of up to 131,000 lb. (583 kN).

A study supported by the Federal Highway Administration (FHWA) developed another truck weight formula, known as the TTI formula (James et al. 1986). The TTI formula is based on the same girder overstressing criterion as the Formula B. The formula is given by:

$W = 34 + B$ (kips)	for $B < 56$ ft	(U.S. Customary)	2.2a
$W = 62 + 0.5B$ (kips)	for $B > 56$ ft	(U.S. Customary)	2.2b
or			
$W = 4.4\ (34 + 3.28\ B)$ (kN)	for $B < 17$ m	(SI)	2.2c
$W = 4.4\ (62 + 1.64\ B)$ (kN)	for $B > 17$ m	(SI)	2.2d

As demonstrated in Figure 2.3, the TTI formula (Equation 2.2) allows higher weights for short vehicles, and tandem and tridem axle groups compared to the current bridge formula, Formula B. For longer vehicles, however, the TTI formula allows smaller GVWs than Formula B. In 1990, TRB (1990) proposed a modification on the TTI formula, which would reduce the limits on axle loads while allowing higher gross weights, as demonstrated in Figure 2.3. The modified TTI formula only established stress limits on HS20 bridges and did not consider the overstressing criterion in the bridges designed with H15 loading. The formula is given by:

$W = 26 + 2.0\ B$ (kips)	for $B < 23$ ft	(U.S. Customary)	2.3a
$W = 62 + 0.5\ B$ (kips)	for $B > 23$ ft	(U.S. Customary)	2.3b
or			
$W = 4.4\ (26 + 6.55\ B)$ (kN)	for $B < 7$ m	(SI)	2.3c
$W = 4.4\ (62 + 1.64\ B)$ (kN)	for $B > 7$ m	(SI)	2.3d

Furthermore, the traffic allowed in the North American Free Trade Agreement (NAFTA) created a need to change the weight limit regulations because of the higher legal limits in Canada. As shown in Figure 2.4, the legal load configuration in Canada violates the modified TTI formula. In order to allow Canadian legal trucks to circulate in the U.S., the U.S. legal load limits on GVW and tridem axles would have to be increased by 20%.

In summary, to allow the Canadian traffic and to apply the TTI formulas will increase deterioration in different components of the bridges in Minnesota. This research addresses the effects of these scenarios on steel and concrete components of bridge superstructures.

2.3.3 Weigh-In–Motion Data

Weigh-in-motion (WIM) sites collect data on the classification and weights of trucks and axles that pass the WIM site. The data that are collected include the number of vehicles in a GVW range for each classification as well as similar information on axle loads such as the number and weight of the axles. The data from WIM sites can be used to: calculate effective truck weights, estimate traffic volume, determine the composition of the traffic, or to find the maximum GVW or axle weight at the site.

The effective truck weight can be calculated from WIM data by using Equation 2.4, where f_i is the fraction of gross weights within interval i and W_i is the mid-width of interval i. The effective truck weight can be used as the weight of an equivalent fatigue truck for evaluation of nearby bridges. The 54 kip (240 kN) fatigue truck (Figure 2.5) that is described in National Cooperative Highway Research Program Report 299 - Fatigue Evaluation Procedures for Steel Bridges

(Moses et al. 1987) (hereafter referred as NCHRP 299), and which is based on extensive nationwide WIM data, can be used for bridges located in routes for which no WIM data is available.

$$W = \sqrt[3]{\sum_i f_i \cdot W_i^3} \qquad 2.4$$

In the State of Minnesota, weigh-in-motion data were available for US T.H. 2 near Bemidji, and at the Mn/ROAD research site on Interstate 94. WIM data were not available for Interstate 35. Because of this, the gross vehicle and axle weight distributions of the I-94 truck traffic were assumed to be representative of the truck traffic in the metro area on major highways. In this way, the WIM data collected at the Mn/ROAD site was used to characterize the truck traffic on the Interstate 35W, which has the highest truck volume in the metro area of the Twin Cities and is the most critical route in terms of fatigue.

Data from the WIM site on T.H. 2 corresponded to the months of January, April, August, and October of 1992. WIM data from the I-94 site was also from 1992, and corresponded to the months of February, May, June, and October.

These two data sets were used to estimate the effective and maximum truck and axle weights. The effective weights represent the load that should be used for fatigue evaluation. The upper tail of the load distributions from the WIM data can be used to estimate the maximum GVW and axle weights and was important for some deterioration issues related to concrete components (i.e. in the investigation of the load causing deck overstressing and girder cracking for prestressed concrete members).

From the WIM data, it was found that about 70% of the truck traffic consisted of 5-axle semi trailers. Figure 2.6 shows the percent of the truck traffic for each truck classification for T.H. 2 and I-94, and also shows that the distribution of truck configurations is similar for the two sites (it should be noted that the data from these two sites are from different months). However, it is

considered a coincidence that the average percent of 5-axle semi trailers were identical for the two locations (the averages for each month ranged from 68% to 74%).

The data for T.H. 2 were separated into traffic traveling in the westbound and eastbound lanes. It was found that there was a significant difference in the weights of the vehicles based on the direction of travel. A gross vehicle weight histogram for this site from the four months of WIM from 1992 is presented in Figure 2.7. From these data, it was found that the effective truck weight was approximately 66 kips (293 kN) for eastbound traffic, and approximately 45 kips (200 kN) for westbound traffic. It was believed that this difference was due to trucks traveling eastbound fully loaded towards Duluth, and then returning empty. Due to the large differences in effective truck weight, only the data from the eastbound direction should be used for fatigue evaluation, because the bridges for this direction of traffic will experience larger loads.

Figure 2.8 shows the GVW histograms for the eastbound data on T.H. 2 near Bemidji for each of the four months with data. This figure shows that during the month of January there were heavier trucks. The effective truck weight for the month of January was 73 kips (325 kN), while for the other months, the effect weights were only 66 kips (294 kN), 61 kips (271 kN), 63 kips (280 kN) for April, August, and October respectively. These differences suggest that for T.H. 2, there are seasonal changes in the truck weights, with heavier trucks traveling during the winter. This is expected because Minnesota allows a winter load increase of GVW of 10%.

Figure 2.9 shows the GVW histograms for data on I-94 at the Mn/ROAD site for each of the four months with data. Unlike the data from T.H. 2, there were no significant differences in the seasonal data. The effective weight from these months was about 58 kips (258 kN), and the effective weights only ranged from 57 to 59 kips (254 to 262 kN).

2.3.4 **Live Loads Considered for Prestressed Concrete Bridges**

As discussed in Section 2.4.1 of this report, girder cracking could lead to fatigue deterioration and increased corrosion of prestressing reinforcement. Thus, live loads that could lead to possible girder cracking were considered for prestressed concrete bridges.

Two of the three tested prestressed concrete bridges had relatively short spans (bridges #9731 and #9603), thus for these bridges, trucks with short overall axle spacing and large GVWs were considered critical for flexural and shear cracking. The third tested prestressed concrete bridge (bridge #04006) was longer than the first two bridges. Therefore, for this bridge it was possible that a truck with longer overall axle spacing and large GVW could be more critical for flexural or shear cracking than a truck with a smaller overall axle spacing and smaller GVW.

Because the purpose of this study was to assess the effects of an increase in allowable GVW on prestressed concrete bridges in the State of Minnesota, it was important to assess how current legal loads affected the prestressed concrete bridges. Then, on the basis of the findings from current legal loads, the results could be extrapolated to find the percent increase in GVW that would lead to girder cracking.

The legal trucks selected as critical for prestressed concrete bridges are shown in Figure 2.10 and Figure 2.11. The 3-axle rigid body truck shown in Figure 2.10 is the test truck that was used for the three tested prestressed concrete bridges. For the axle spacing and GVW shown, the truck slightly exceeds Formula B and its GVW represents 94% of the maximum allowable GVW under Formula B for 3-axle trucks (54 kips (240 kN) on a minimum overall axle spacing of 24 ft (7.3 m). Because the 3-axle rigid body truck had a small overall axle spacing and large GVW, it gave the worst-case loading for flexural cracking.

The 5-axle tractor semitrailer body truck shown in Figure 2.11 represents a typical hauling vehicle (Laman and Ashbaugh, 2000). The truck also represents the maximum allowable GVW for a 5-axle truck under Formula B. Because this vehicle is longer and heavier than the 3-axle rigid body truck, it gave the worst-case loading for shear cracking. The results from investigating the 5-axle truck can be scaled to approximately examine the effects of heavy rating permit vehicles, such as the 159 kip (700 kN) GVW Standard C vehicle. This Standard C vehicle has approximately the same wheelbase but with groups of four axles where the tandems are located in a typical 5-axle truck. Longer permit vehicles would not be expected to govern due to the limited span length for these prestressed bridges.

2.3.5 Live Loads Considered for Steel Bridges

For steel bridge fatigue evaluation, a fatigue truck that approximates the damage caused by all of the truck loads is used. The effective truck weight from WIM data can be used as the weight of the fatigue truck. From national WIM data, Moses et al. (1987) found that the average effective weight was about 54 kips (240 kN) and that four and five-axle semi trailers cause over 90% of the fatigue damage in typical U.S. bridges. From Moses' data, the axle spacing and load distribution of the fatigue truck used for evaluation in NCHRP 299 (Moses et al. 1987) was developed (which is illustrated in Figure 2.5). This truck is also used for fatigue design in the 1998 AASHTO LRFD Specifications.

With an increase in the allowable gross vehicle weight, the frequency of heavier loaded trucks will increase. This suggests that the fatigue truck should also increase to account for this change. To estimate this new fatigue truck's gross weight, we will use a truck weight histogram. A truck weight histogram gives a breakdown of the number of miles traveled for each type and weight of truck. By knowing how many trucks of each load are traveling the highways, an equivalent fatigue truck can be created. This was done for two Minnesota sites that have collected weigh-in-motion data (WIM), which is described in Section 2.3.3.

2.3.6 Live Loads Considered for Decks

Previous research has demonstrated that the axle weights have a more significant effect than the GVW in the deterioration of reinforced concrete bridge decks (Batchelor et al., 1978, Kostem et al., 1978, and James et al. 1988). Therefore, the investigation of deck deterioration focused on the increase in the limits for single, tandem, and tridem axle weights.

As seen in Figure 2.3, the proposed TTI formula would lead to an increase in the current tandem axle weight limit by 10%. Furthermore, to allow legal trucks in Canada to enter the U.S., the current legal tridem axle weight needs to be increased by 20%. From this point of view, 10 and 20% increases in legal limits of single-, tandem-, and tridem-axle weights were considered as possible future scenarios.

Fatigue and overstressing due to truckload are affected by the load distribution at a specific site in different ways. The effective axle load (i.e. weighted average of axle load distribution) controls deck fatigue. An increase in the allowable axle loads results in a shift of the entire axle load distribution towards higher axle loads and an associated increase in the effective axle weight. On the other hand, the axle load that was used to evaluate overstressing was the upper load interval in the WIM data, which represented the largest 8% of the axle loads in the WIM data for the total of the representative months in 1992 as shown in Table 2.2. This axle weight was always greater than the maximum legal axle weights (in other words, an illegal load – more than 20-kip single axle, 34-kip tandem axle, or 42-kip tridem axle) and thus would not be necessarily directly affected by an increase in the legal GVW or axle weights. However, it was assumed that an increase in the legal limits might embolden the illegal operators to try a proportional increase in the illegal loads. Note that, in the event of an increase in the legal GVW or axle weight limits, the proportion by which the extreme once-in-a-lifetime axle weight increases is not likely to be the same as the proportion by which the effective axle weight increases.

To investigate these two different effects of axle load histograms, the WIM data of Interstate route I-94 was analyzed. The details of the WIM data analysis can be found in Section C4.2.

2.4 DETERIORATION ISSUES

This section contains a discussion of the deterioration issues that could lead to a reduced service life for Minnesota bridges. First, the deterioration issues for prestressed concrete I-girder bridges will be discussed. Then the fatigue of steel structures is discussed along with the evaluation procedures that were used. In section 3.1.3, the deterioration in bridge decks under truckloads is described.

2.4.1 Prestressed Concrete I-girder Structures

An extensive literature review was performed on the issues affecting the service life of prestressed concrete girders, including a review of analytical and field studies on the fatigue behavior of prestressed concrete girders. All the studies reviewed are given in Section B2.3.

From the literature review, the critical issue leading to the fatigue of prestressed concrete girders was identified as girder cracking. All but two of the mentioned studies in Section B2.3, established a connection between fatigue related failures of reinforcement and cracks in prestressed girders. It was found that flexural cracks in prestressed concrete girders led to increased stress ranges in the strands, increasing the possibility of fatigue failure and decreasing the service life of the girders, and the bridge structure as a whole. In addition, the presence of cracks in prestressed concrete girders could lead to increased strand corrosion. Consequently, it is important to determine whether increased truck loads in Minnesota would result in cracking of the prestressed concrete I-girders, as this may lead to a reduction in the service life of prestressed concrete I-girder structures.

To predict the number of cycles to fatigue failure for prestressed concrete I-girders, Equation 2.5, proposed by Overman et al. (1984) was used. Equation 2.5 relates the strand stress range to number of cycles to fatigue failure for prestressed concrete girders.

$$\text{Log } N = 11.0 - 3.5 \text{ Log } S_r \qquad 2.5$$

where: N = fatigue life in number of cycles

S_r = strand stress range; maximum stress – minimum stress (ksi)

2.4.2 Steel Bridges

Improved fatigue design specifications for steel bridges were developed in the 1970's largely as a result of research performed for the National Cooperative Highway Research Program at Lehigh University (Fisher et al. 1970, Fisher et al. 1974). The fatigue design procedures are included in the AASHTO specifications for bridges (Fisher 1984, Fisher 1997). Further refinements of the fatigue design specifications were introduced in 1985 to require connection plates to be connected to girder flanges, a problem which was causing web-gap cracking (Fisher et al. 1990). Using these specifications, it is possible to identify and avoid details that are expected to have low fatigue strength (Dexter and Fisher 1999). Steel bridges that have been built in the last two decades have not had and will not have significant problems with fatigue, because of these fatigue design specifications (Fisher 1997). However, most of the steel bridges in Minnesota (approximately 85%) were built before 1986, indicating that a large number of the steel bridges are potentially susceptible to fatigue damage.

If the structural member only undergoes compressive cyclic loading, if a crack is present, it will arrest and is not structurally significant; therefore, only members or connections that have at least some tension need to be assessed for fatigue (Dexter and Fisher 1999). There have also been very few if any failures related to details that have a fatigue strength greater than category C (Dexter and Fisher 1997).

The welds at the ends of partial length cover plates are a common fatigue problem in steel bridges. Cover plates were originally used to enable local increases in moment capacity with a constant girder depth throughout the span. Therefore cover plates did not span the whole length of the girder. This detail is a category E or E' depending upon the flange thickness. These poor details were rarely used in bridges constructed after the fatigue design specifications were revised in the mid 1970's.

However, another common source of fatigue cracking, web-gap cracking or distortion-induced fatigue, was not addressed in the specifications until 1985. Distortion-induced fatigue is the result of secondary loading that is not normally recognized in design. Most distortion-induced fatigue cracks occur where connection plates for diaphragms or floor beams are not welded to

the tension flange due to unfounded reluctance to weld to the tension flange (Dexter and Fisher 1997, Jajich et al. 2000). The cracks manifest in the web of the girder in the gap between the vertical welds on the connection plate and the longitudinal fillet weld joining the web to the flange and typically propagate in the girder longitudinal direction, at least initially. Since 1986, it has been required that connection plates be rigidly attached to both flanges, eliminating this type of cracking in new bridges.

Due to the complex and unexpected stress ranges that are experienced at these locations, it is currently extremely difficult to predict the life of web gap details without field measurements. A few bridges with these details are susceptible to cracking under current truck loads, more will be susceptible to cracking with increased allowable GVW, and some of these bridges will experience infinite fatigue lives. However, if an estimate of the remaining lives of bridges with distortion-induced cracking can be made, it is then possible to determine the percentage reduction in those lives due to increasing truck weight using the methods in Appendix B. Fortunately, distortion-induced cracking is rarely an immediate threat the structural integrity of the bridge and it can typically be repaired. However, the cost of these repairs may be substantial.

Recent research is beginning to make it possible to determine which bridges will experience larger differential deflection and thus more distortion induced fatigue without performing field measurements or complex analyses or modeling (Berglund and Schultz 2002). This research performed finite element modeling of bridges to determine the parameters that influence differential deflection. The parameters that were found to have a significant effect on differential deflection were angle of skew, span length, girder spacing, and deck thickness. Berglund and Schultz (2002) also presented equations that can be used to estimate the differential deflection for bridges that have skew angles of 20^{o}, 40^{o}, and 60^{o} and are also functions of girder spacing and main span length. However the findings from this research only apply to skewed bridges that have staggered diaphragms. There was a currently funded Mn/DOT research project on web gap stresses from differential deflection of non-skew bridges with back-to-back diaphragms and skewed bridges with X-diaphragms.

Chapter B2 provides more information about the fatigue issues for steel bridges. This chapter also describes issues related to the field measurements of steel bridges and their comparison with analytical results.

The 1990 AASHTO Guide Specifications for Fatigue Evaluation of Existing Steel Bridges were used for the fatigue evaluation of steel bridges. The purpose of the 1990 AASHTO Guide Specifications for Fatigue Evaluation of Existing Steel Bridges is to provide procedures for calculating the remaining fatigue life of existing steel bridges using concepts of probabilistic limit states. The fatigue evaluation procedures in the AASHTO Guide Specifications for the Fatigue Evaluation of Existing Steel Bridges were adopted from and identical to the proposed procedures presented in NCHRP 299 (Moses et al. 1987). The effects of repeated loading on the fatigue life of an existing bridge is defined in terms of the remaining life of the structure. This means that the effect of exceeding the allowable fatigue stress is a reduction on the remaining fatigue life of the structure rather than immediate failure.

There are two levels that the remaining fatigue life can be calculated at, the remaining safe life and the remaining mean life. The remaining safe life provides a much higher level of safety. The safe life represents has an exceedence probability of 97.7% for redundant members (the same probability inherent in using the basic design S-N curves). The mean remaining life, however, is the best estimate of the actual remaining fatigue life of the detail under consideration. The mean life has an exceedence probability of 50%.

The safe life is used for design and for a first screening analysis. The impact of reaching the safe life equal to zero should be relatively minimal, for example having to repair just a few percent of the details on a bridge. In this case, the calculated mean life may be used to determine when the cracking will be so pervasive that half the details will be cracking, requiring extensive retrofitting or possibly replacement of the bridge. If the remaining life that is estimated is not satisfactory, there are four options: recalculate the fatigue life more accurately (possibly using load testing), restrict truck traffic on the bridge, repair or modify the detail, and/or perform more frequent inspections of the detail.

The procedures in NCHRP 299 are the best available procedures for predicting the number of years before substantial fatigue cracking *may* occur at a detail. It is difficult to accurately predict all of the variables that the bridge will experience over its remaining life, such as past, present, and future truck volumes and stress ranges, which can also vary with changing truck weights over time. The procedures and equations of NCHRP 299 are described in detail in Chapter B2.

2.4.3 Bridge Deck Deterioration

There is no consideration given to structural rating of the performance of bridge decks in the current rating and evaluation code, the 1994 AASHTO Manual for Condition Evaluation of Bridges (AASHTO 1994), although there has been extensive research on the deterioration of bridge decks under truckloads. The evaluation of bridge decks is limited to visual inspections. Chapter C2 discusses the research related to overstressing (i.e. susceptibility to longitudinal cracking) and fatigue.

There were extensive studies on the fatigue behavior of reinforced concrete girders before the 1960's, although specific deck fatigue received attention after the late 1970's. In the girder fatigue tests, it was observed that the girder tested had a fatigue load limit of 60-70% of the static ultimate strength for a life of one million cycles of loading (Nordby, 1958). Reinforcement fracture and diagonal tension failure were common failure modes observed at the end of the girder fatigue tests, and compression failure was very rare. An accumulation of residual deflections was observed, but the recovery of the deflection was reported in rest periods. A relationship between the fatigue life of the girder and the reinforcement was concluded. In other words, the endurance limit of the reinforcement and the fatigue strength of the reinforcement as a fraction of the static strength were related to those of the girders in these laboratory tests.

It should be noted that substantial differences exist in the structural responses of reinforced concrete beams and slabs due to geometry, reinforcement pattern, and load distribution characteristics. Therefore, it is questionable whether fatigue behavior observed in reinforced concrete beams can be extended to slabs. Slabs are relatively shallow reinforced concrete

structures, and they have the capability to distribute the applied load in two-way action compared with the one-way behavior of beams.

In previous research on deck slabs subjected to different types of repetitive loading in laboratory tests (Batchelor et al., 1978, Okada et al., 1978, Kato et al., 1978, Azad et al., 1986, Fang et al., 1990, Petrou et al., 1994, and Youn et al., 1998), different crack patterns, failure modes, and fatigue strengths were observed for the different loading types. The literature is summarized in Chapter C2 according to the loading type, i.e. stationary pulsating load and moving wheel load.

Although the overstressing phenomenon was not specifically addressed in the laboratory fatigue test studies, in most of the studies, the applied repetitive load was higher than the legal load limits. Therefore, in the review, overstressing issues are also discussed with respect to their effect on the deterioration of the decks in these tests.

In conclusion, the simulation of the truck axle load by the stationary pulsating load did not yield the cracking pattern observed in the field (Okada et al., 1978, Kato et al., 1978, and Petrou et al., 1994). Instead of map cracking as the reflection of the reinforcement, such types of tests resulted in radial cracks emanating from the load patch area, as observed for punching failure modes under static loading. Also, it was always observed that the tests with stationary pulsating load simulation overestimated the fatigue life compared to the moving pulsating or wheel load simulation. In the selection of the fatigue model for the study described herein, one of the most important factors was the appropriateness of the load simulation in the fatigue tests considered.

Another important factor that affected the results of the fatigue tests was the simulation of the boundary conditions of the loaded deck part. Most of the laboratory fatigue tests were performed with single deck panels supported by elastic beams (Azad et al., 1986, Okada et al., 1978, and Kato et al., 1978). It is believed that the restraining effects at the boundaries were not simulated in a proper way in those models because the panels tested in these studies lacked the significant in-plane restraining effect from the adjacent deck parts and the adjacent girders. Therefore, the selection of the fatigue model for the study described herein focused on the simulations of the deck in bridge structural systems.

All of the studies reviewed in Section C2.3.1 concluded an endurance limit of 0.4 to 0.6P_u at 2-3 million cycles of loading. Most of these laboratory fatigue tests did not continue beyond three-million cycles of loading. However, in the study described herein, the number of truck axle repetitions was predicted to be more than 100 million cycles for some of the metro area bridges during their design life. Therefore, to assume the endurance limit at as high as 0.5-0.6P_u may be unconservative. To be conservative, in the study described herein, all of the concrete decks were assumed to have finite life.

The studies by Batchelor et al. (1978), Fang et al. (1990), and Petrou et al. (1994) concluded that there was little or no relationship between overstressing and deck fatigue under service load. The displacement and reinforcement and concrete stress measurements in these studies demonstrated that no further reduction in stiffness was observed after the initial damage due to overstressing (Fang et al., 1990) and cumulative fatigue loading less than the expected fatigue life did not increase the potential for cracking by overstressing (Batchelor et al., 1978, and Petrou et al., 1994). Therefore, these two possible deterioration modes were treated as two independent phenomena discussed separately in Chapters C4 and C5.

In some of the tests performed in the laboratory environment (Azad et al., 1986, Okada et al., 1978, and Kato et al., 1978), it was demonstrated that the transverse cracks from the constructional period and water penetration during service life decreased the ultimate punching shear and fatigue strengths of the reinforced concrete deck. However, these studies have not established any quantitative interaction between the deterioration from the environmental factors and the repetitive axle load. The conclusions from those studies were limited to some qualitative observations and a few quantitative test results for very specific environmental conditions. Therefore, more laboratory tests are required to establish a general quantitative interaction between the service load and environmental factors. In the current study, both the environmental factors and repetitive mechanical loading were assumed as independent variables in deteriorating bridge decks, and only the effect of the service load fatigue was evaluated in the deterioration of the reinforced concrete decks.

Available laboratory test data is limited to a few bridge types, composite and non-composite slab-on-steel girder simply-supported bridges. There has been no data for bridge decks on prestressed concrete girders, which are another widely applied structural system in bridge construction in Minnesota. In the current study, the available fatigue equations for the case of concrete decks on steel girders were applied to the deck on the prestressed concrete girders due to the absence of data. Furthermore, even though all the bridges considered in the current study had been constructed compositely, the deck fatigue models for noncomposite bridges were also considered in selecting the most appropriate model.

The available test data showed that the measured stress range of 5 ksi (34 MPa) in the reinforcement at the presence of the cracks in the highly deteriorated deck was well below the threshold for reinforcement fatigue given by the AASHTO LRFD Design Code, 23.4 ksi (161 MPa), even under high load levels (Fang et al., 1990). Therefore, under service load, fatigue does not appear to be a problem for deck reinforcement. This conclusion corroborates the fact that fatigue of reinforced concrete decks is governed by punching failure of the concrete. It should be noted that plain concrete does not exhibit an endurance limit (ACI 215R, 1999). Therefore, the assumption of the absence of endurance limit in deck fatigue is reasonable.

In light of the discussion and assumptions above, the fatigue model obtained from the moving wheel load tests of noncomposite steel girder specimens by Petrou et al. (1994) was used for all the bridges in the current study. Although the fatigue equations were predicted for two different deck slenderness values, 7 and 10 ft (2 and 3 m) girder spacings, in the study by Petrou et al. (1994), the equation yielding the most conservative results was applied. Because all of the bridge decks in the current study had an orthotropic reinforcement pattern, the fatigue model derived from the tests of orthotropically reinforced decks was selected. The equation yielding the conservative fatigue life for orthotropically reinforced concrete decks is repeated from Chapter C2 below:

$$\text{Log}(P/P_u) = 1.022\text{-}0.243\ \text{Log}(N_{pf}) \qquad \text{(C2.4)}$$

where P_u: Ultimate strength of the deck (kips or kN)

P: Applied load range

N_{pf}: Number of cycles to failure

It should be noted that the fatigue model (Equation C2.4) was based on deck failure at the midspan. However, the same study (Perdikaris et al., 1993) and the study by Youn et al. (1998) observed lower fatigue performance at the deck regions close to the supports. Therefore, it would not be conservative to assume fatigue failure at midspan as being critical. To represent the most critical case (fatigue failure at the deck regions close to supports), a reduction of 40% in Perdikaris et al. (1993) was applied to the number of cycles to failure from Equation C2.4. This 40% reduction was the average value of largely scattered data and was more conservative than the reduction (25%) reported by Youn et al. (1998).

Regarding application of load in the fatigue models, there has not been enough information about the effect of dynamic interaction between the deck and axle load on fatigue strength. Dynamic effects in the application of the loading were absent in the previous fatigue tests. In the current study, the dynamic amplification factors specified by the design standards were applied in the selected fatigue model. The impact factor of 0.15 specified for the fatigue limit state in the AASHTO LRFD Bridge Design Code (1998) was added to the applied load range.

Because the fatigue model selected was calibrated according to measured punching shear strengths of the deck at the midspan, it was essential to predict the ultimate punching shear strength with good accuracy for evaluation purposes. In the studies by Batchelor et al. (1978), Fang et al. (1990), and Petrou et al. (1994), it was observed that compressive membrane stresses enhance the resistance to punching shear failure. Therefore, this effect should also be included in the calculations. Discussion of the methods to predict the punching shear strength and the accuracies of those methods are presented in Section C4.1.

TABLES

Applicability of Refined Methods of Analysis			
Type of Deck (fig. 2.6)	Orthotropic plate theory	Finite Element	Grillage
Slab	*	*	*
Pseudo-slab	*	*	*
Slab and beam		*	*
Cellular		*	*
Composite	*	*	*
Orthotropic	*	*	*
Box		*	*
Plan Geometry			
Right	*	*	*
Skew > 20^{o}		*	*
Curved	*	*	*
Arbitrary		*	*
Support Conditions			
Simply Supported	*	*	*
Simply Supported with Intermediate Supports	*	*	*
Arbitrary		*	*

Table 2.1 Applicability of refined methods of analysis. From Cusens and Pama (1975)

	% of Type in Overall Set (1)	Current Legal Limit (kip)	% Exceeding Legal Limit (2)	% Exceeding Legal Limit in Total (1)*(2)
Single Axle {a}	29	20	5	1
Tandem Axle {b}	70	34	9	6
Tridem Axle {c}	1	42	17	0
a+b+c				8

Table 2.2 Percentage of different types of axles in overall set, current legal load limits, percentage of axles exceeding the legal limits in each axle type, and percentage of axles exceeding the legal limits in overall set.

FIGURES

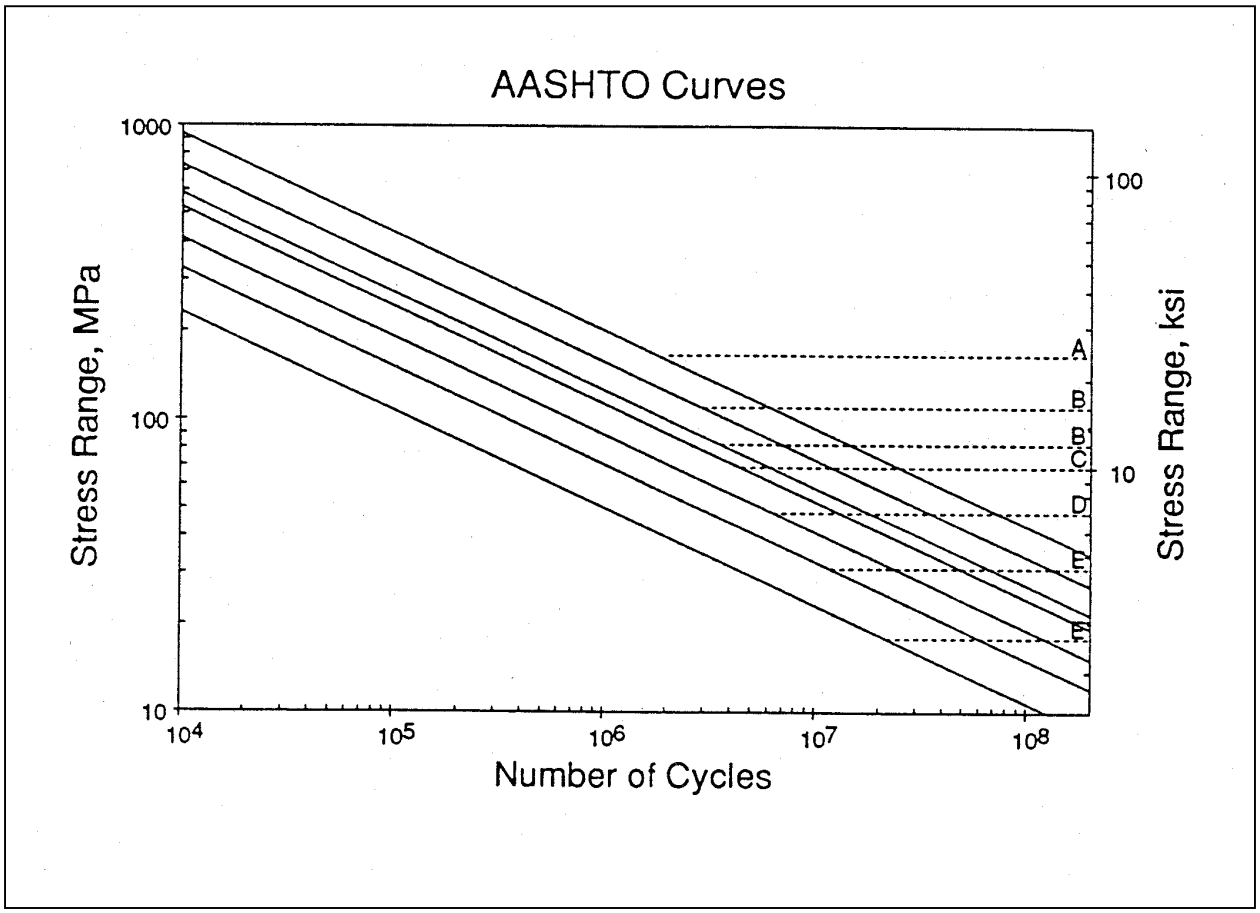

Figure 2.1 AASHTO S-N curves.

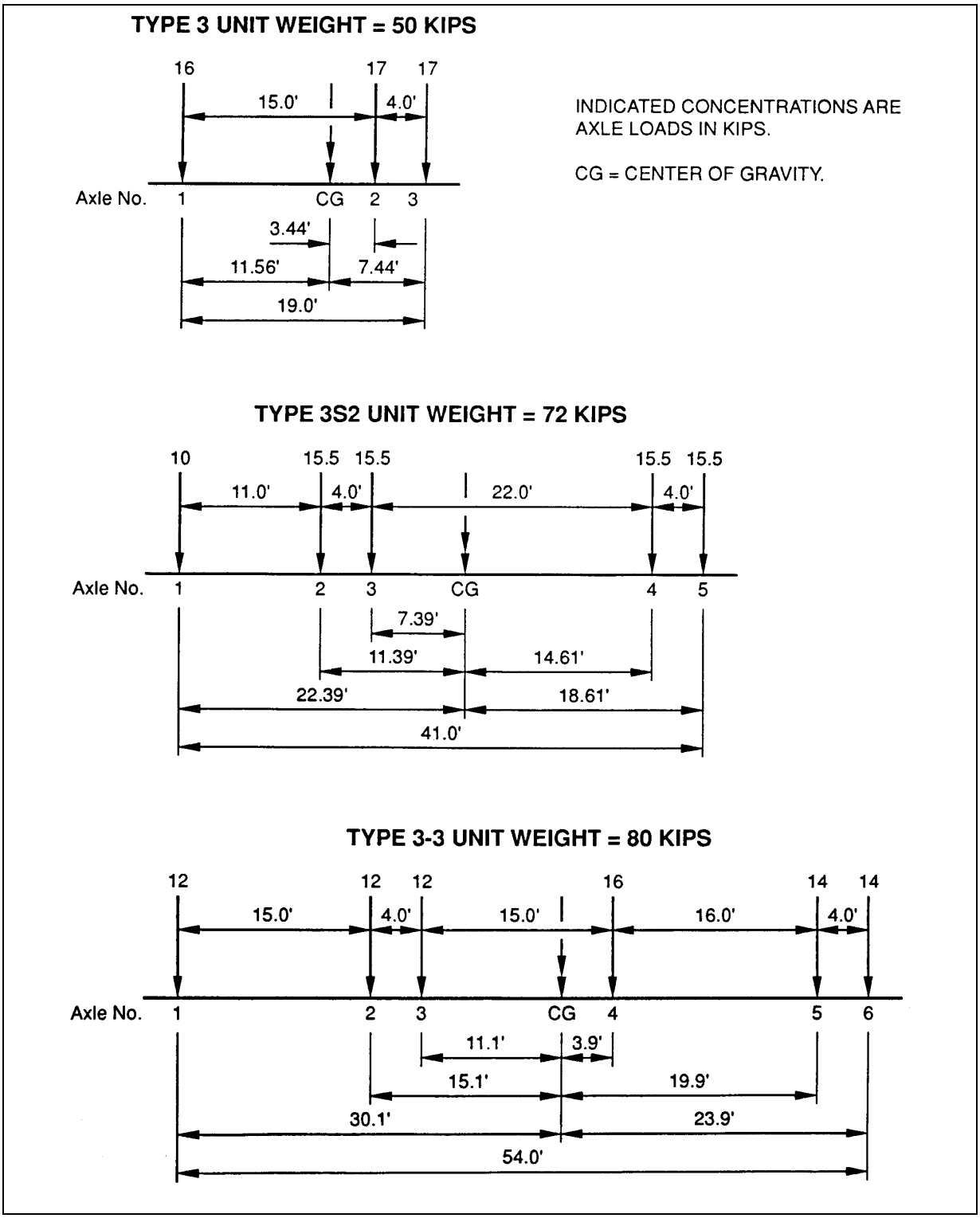

Figure 2.2 Example of rating vehicles that meet Formula B.

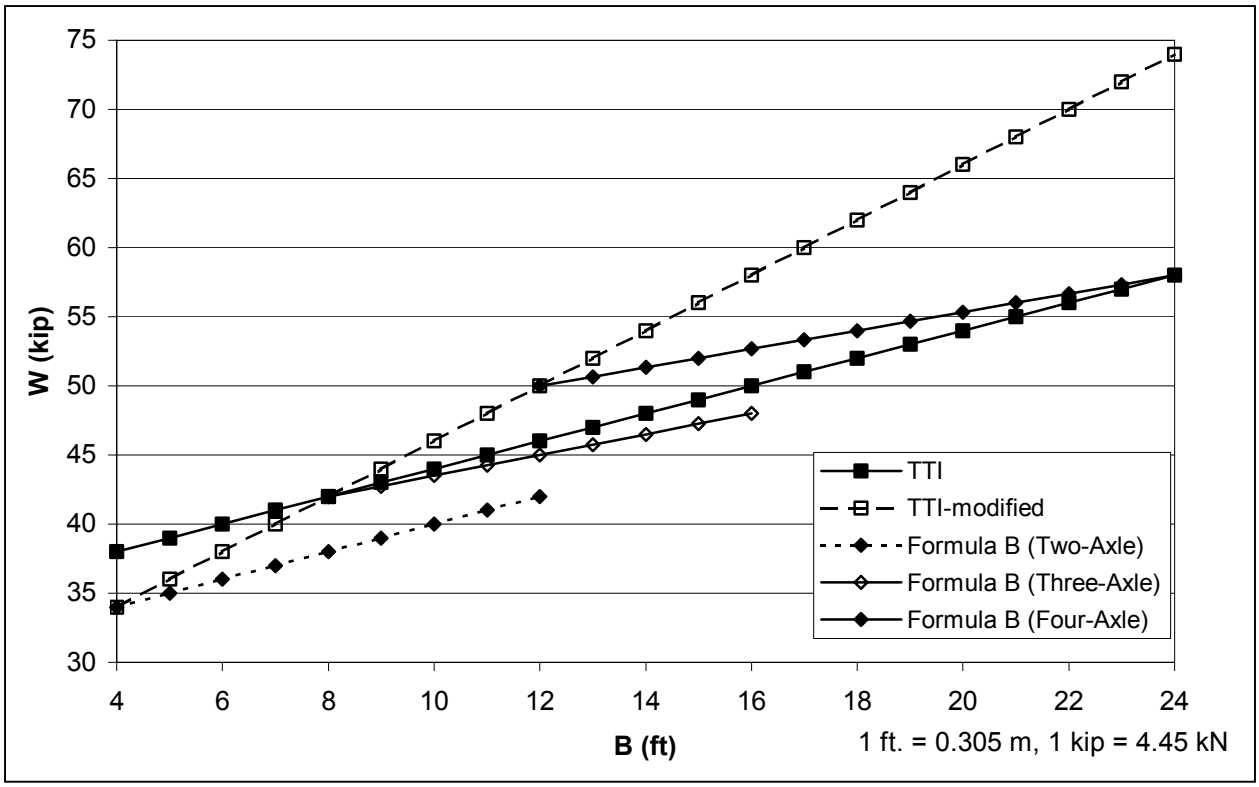

Figure 2.3 Comparison of different axle-group-weight formulas.

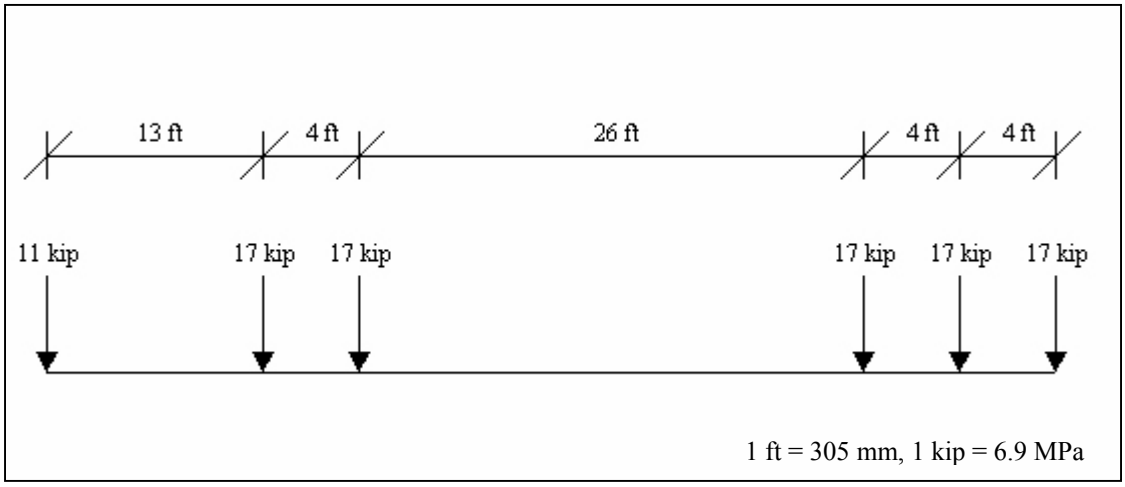

Figure 2.4 Canadian legal truck configuration.

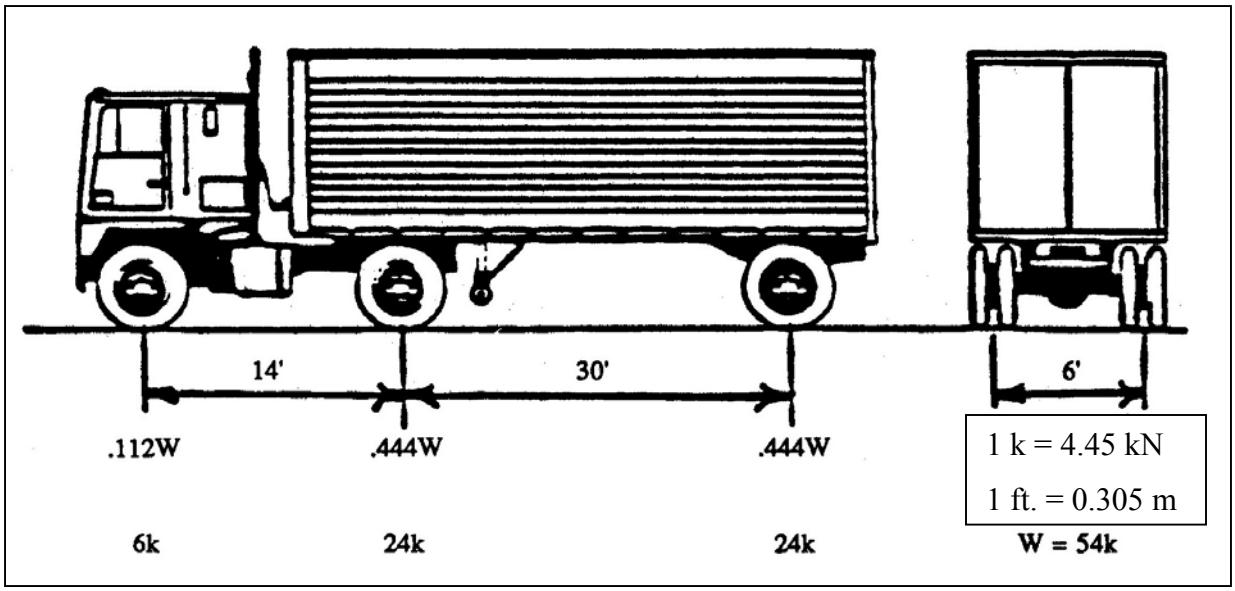

Figure 2.5 Fatigue truck. (Moses et al. 1987)

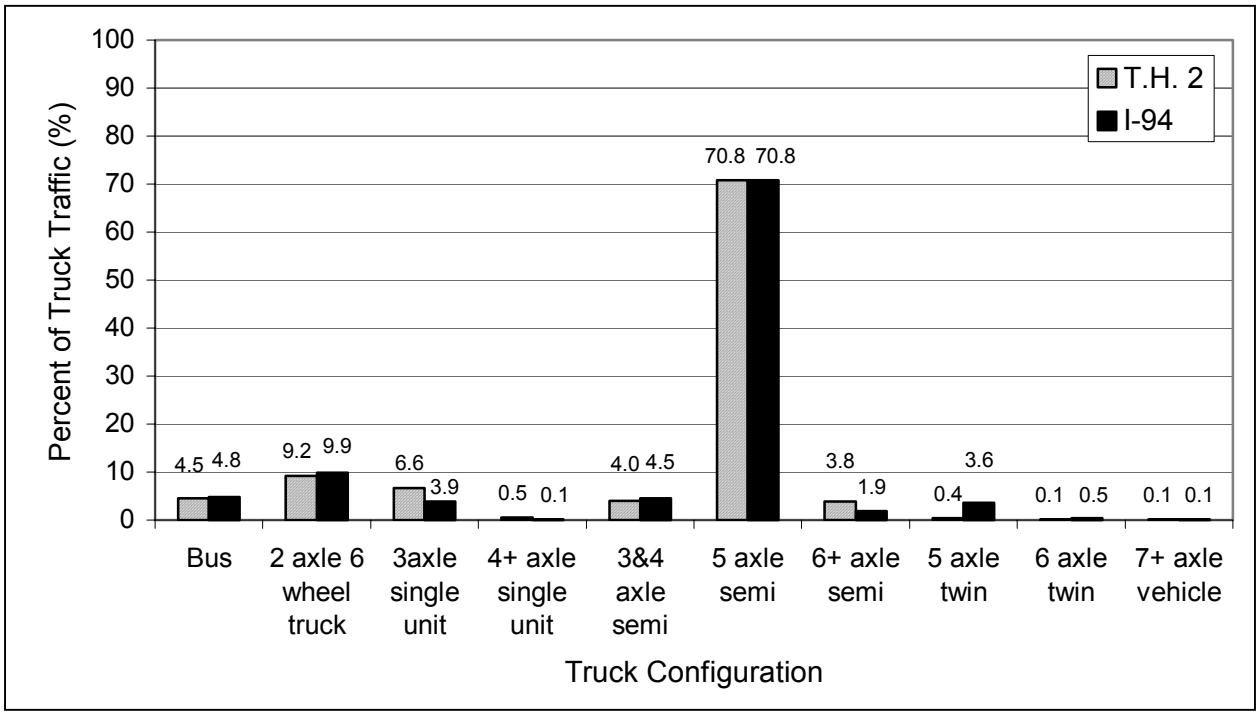

Figure 2.6 Percent of truck traffic by classification on T.H. 2 near Bemidji and I-94 at the Mn/ROAD research site from four months of 1992 WIM data.

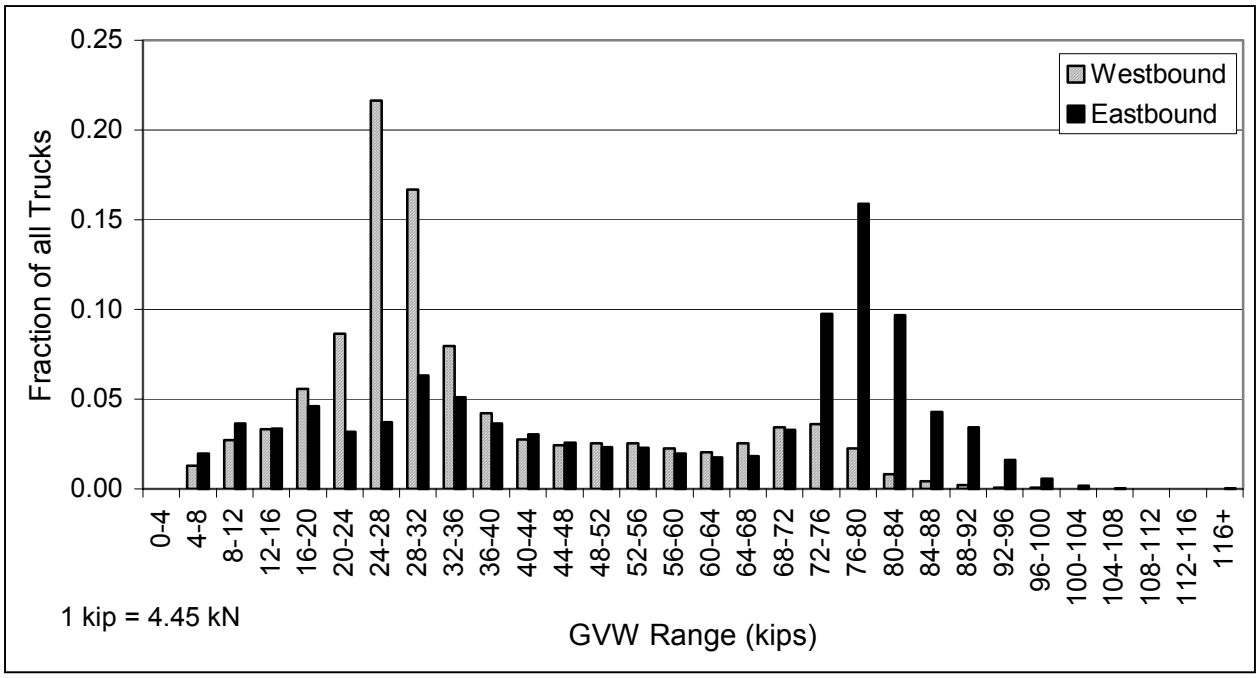

Figure 2.7 GVW histogram for T.H. 2 near Bemidji for 1992 data (from Jan., Apr., Aug, and Oct.).

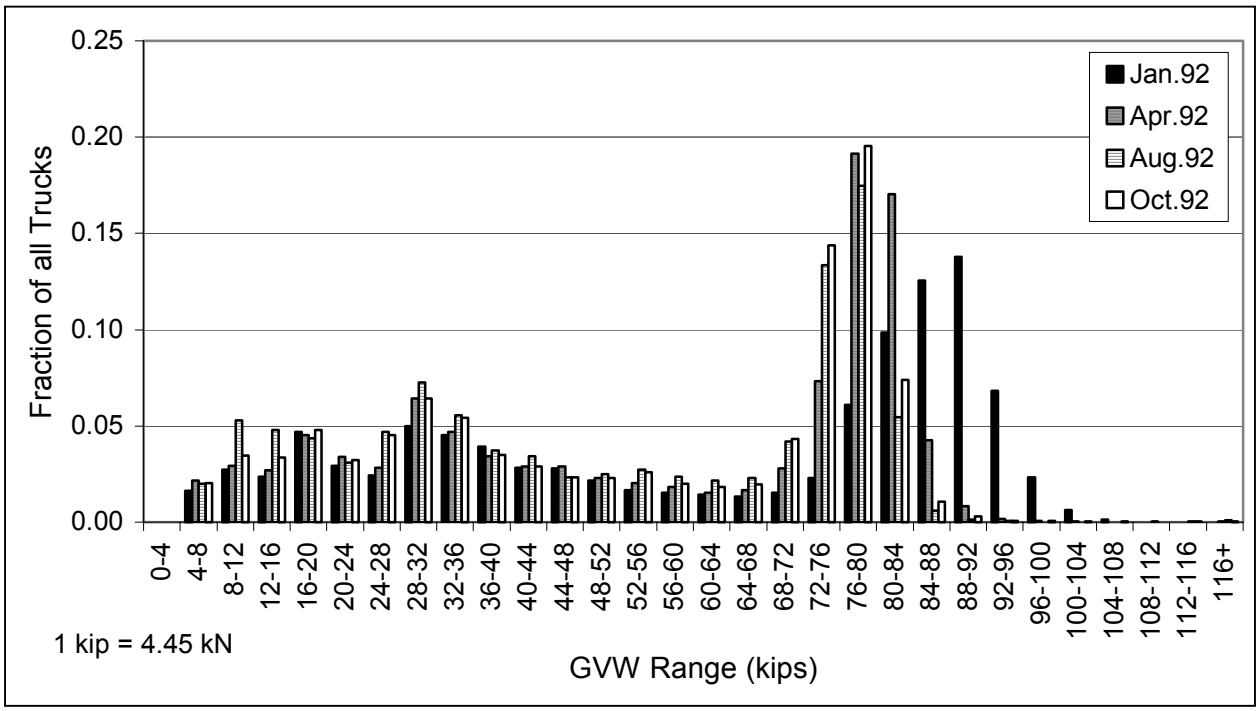

Figure 2.8 GVW histogram by month for eastbound T.H. 2 traffic for 1992 data.

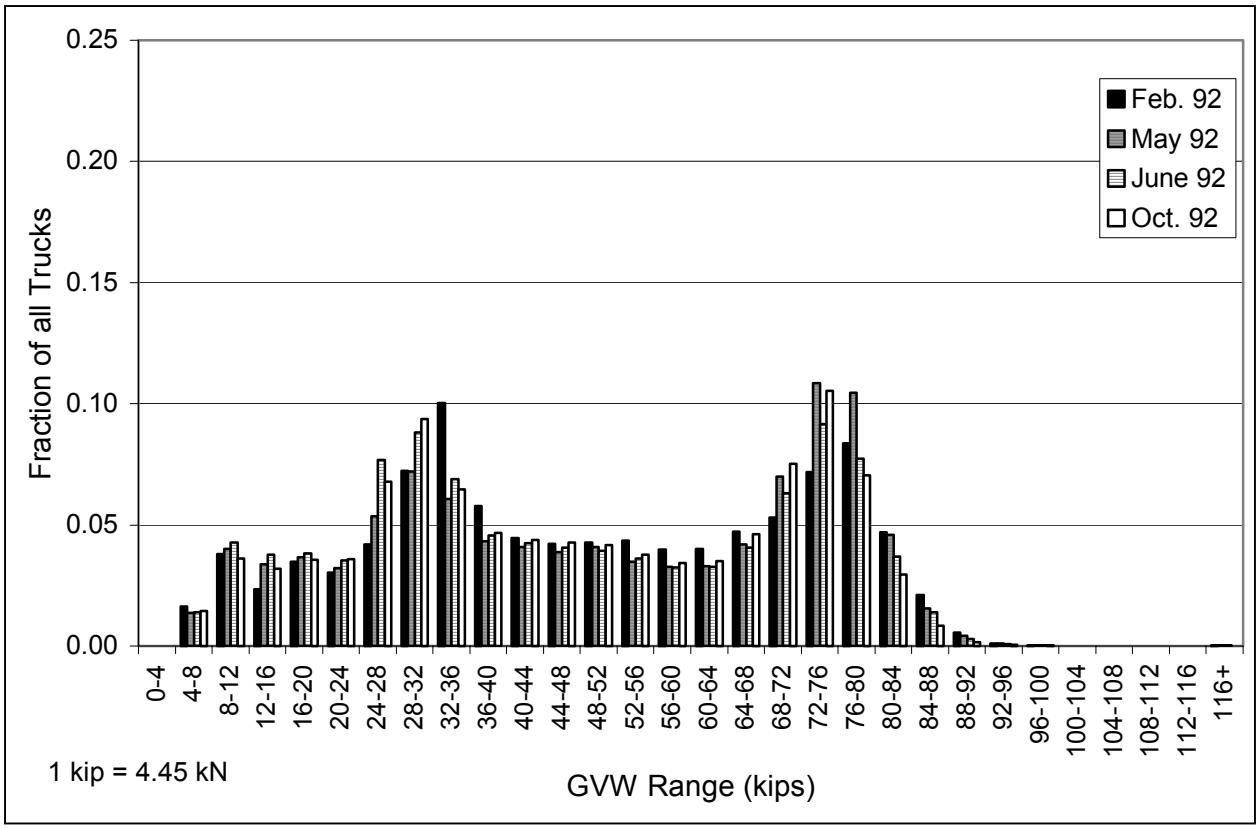

Figure 2.9 GVW histogram by month for westbound I-94 traffic for 1992 data.

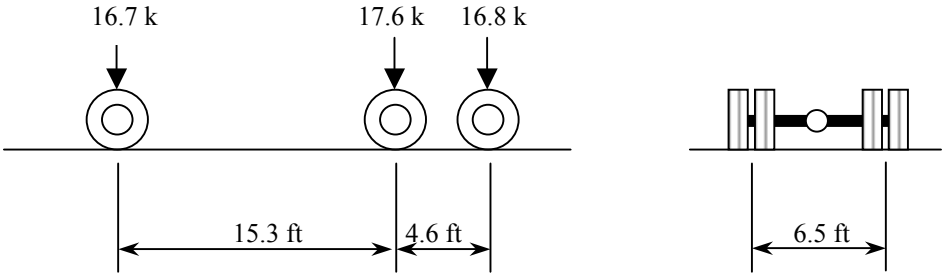

1 ft = 0.3048 m
1 k = 4.448 kN

Figure 2.10 3-axle single bodied truck (test truck) (GVW = 51.1 k (227 kN))

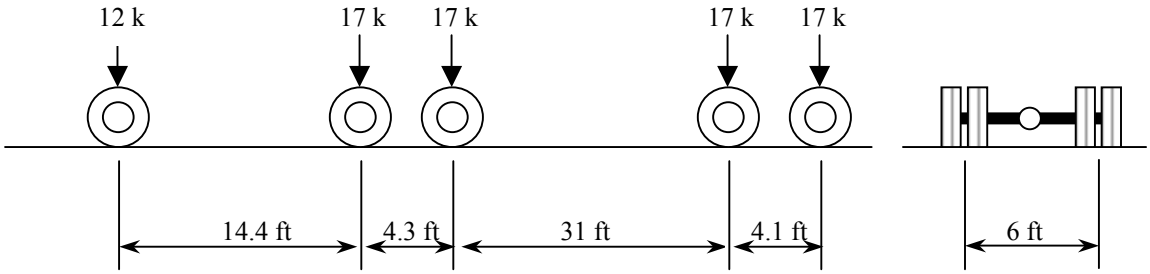

1 ft = 0.3048 m
1 k = 4.448 kN

Figure 2.11 5-axle tractor semitrailer (GVW = 80 k (356 kN))

CHAPTER 3 – FIELD TESTING AND ANALYTICAL MODELLING

3.1 BRIDGE SELECTION

To determine the effects of increasing truck weights on Minnesota Bridges, a representative sample of bridges were field-tested. The test bridges were selected from three routes: Interstate T.H. 35, U.S. T.H. 2, and Minnesota T.H. 200. Trunk Highways 2 and 200 run between Duluth and North Dakota. Characteristics of bridges along these routes and categories of bridges to be tested are described in this section. All of the data contained within this section was obtained from the Bridge Inventory and Inspection Program (BRINFO) data provided by Mn/DOT (Mn/DOT 1998).

To get a representative sample of bridges for testing, the bridges were divided into a few main categories (route, bridge type, age, traffic, fracture critical, and condition or rating) and then analyzed by looking at some of the combinations. Two separate structures for different traffic directions at one location were counted as separate bridges in this analysis, because this was how the data was organized in BRINFO.

Interstate 35, U.S. Highway 2, and Minnesota Trunk Highway 200, represent three major road systems in Minnesota. County Highways were the only highway system not examined in this study. There were a total of 297 structures (263 bridges and 34 culverts) on these selected routes. Of the 297 structures, 225, or about 86% were located on Interstate 35, while only 23 and 15 (9% and 6%, respectively) were located on U.S. 2 and Minnesota 200, respectively. Box culverts were not included in this research. Two additional bridges that were not part of the three routes were included: the Blatnik Bridge, near Interstate 35 and U.S. 2, and Trunk Highway 36 over Cleveland Avenue (#9276) near I-35W. Reasons for including these two bridges are included in Section 3.2.

3.1.1 Bridge Ages

The bridges in the three routes were built between 1922 and 1999. A large segment of these bridges were built in the 1960's (120 or almost 50%), while only 15 were built before 1957. All

of the 15 bridges built before 1957 had been remodeled or were slated for proposed improvements. The remodeling or improvements included bridge replacement, bridge widening, or deck rehabilitation or replacement. Figure 3.1 shows the number of bridges built each decade for each type of main span material. Steel was used for over two thirds of the bridges built before 1960. In the 1960's, approximately 68% of the bridges built were made of steel, while only 26% were prestressed concrete. In the 1970's, about 58% of the bridges were prestressed concrete, while 42% were steel.

3.1.2 Bridge Types

The bridge type was defined by a combination of the main span material and type. The main span material was one of the following: steel, reinforced concrete, prestressed concrete, or timber. There were also several different span types, including beam span, box girder, slab span, truss, deck girder, arch, and box culvert.

Of the 263 bridges, there were 220 beam span, 18 box girder, 10 slab span, 6 truss, 6 arch, and 3 deck girder bridges. Of the 220 beam span bridges, 138 were steel, 81 were prestressed concrete, and one was timber. The timber bridge was not included in the study because it was scheduled for replacement with a concrete continuous slab span bridge. See Table 3.1 for detailed information on the number main span types for each construction material.

For the main span material, 24 were reinforced concrete, 147 were steel, and 91 were prestressed concrete. Based on these numbers, approximately 56% of the main bridge spans were steel, 35% were prestressed concrete, and 9% were reinforced concrete.

3.1.3 Traffic

The Average Daily Traffic (ADT) and the Average Daily Heavy Commercial Truck Traffic (HCADT) varied greatly among the three routes. HCADT included all trucks, including two-axle six-wheel trucks, but it did not include pick-up trucks. Five-axle semis typically comprised 70-80% of the HCADT and two-axle six-wheel trucks were usually approximately 10% of the

HCADT. Section 2.3.3 gives more information on the distribution of truck types based on weigh-in-motion data.

Figure 3.2 shows the HCADT for the different routes. Interstate Highway 35 had the highest average ADT and HCADT (ADT ≈ 27,000, HCADT ≈ 1,750) (*note: for blank entries, the average HCADT included estimates of the HCADT by assuming it was equal to the average % of traffic that was trucks times the ADT for each route*). Interstate 35 was divided into 35W, 35E, and 35. 35W had over twice the average traffic of 35E and 35 (35W HCADT ≈ 3,800, 35E ≈ 1,200, and 35 ≈ 1,600). While Interstate 35 averaged 1,750 trucks per day, US 2 and MN 200 averaged approximately 500 and 100 trucks per day, respectively.

For steel bridges, the truck traffic volume is a major factor in estimating the remaining fatigue life. This is because for steel bridges with details that experience effective stress ranges above the variable-amplitude fatigue limit, the remaining fatigue life is directly related to the average daily truck traffic. Therefore, bridges located on I-35W are more likely to experience earlier fatigue problems than bridges on MN-200.

3.1.4 Fracture Critical

A fracture critical bridge is a bridge that contains at least one member or connection that would cause collapse of the structure if that element failed. There were six bridges along Interstate 35 that had fracture critical (FC) elements, as well as the Blatnik Bridge in Duluth on I-535. Four of the bridges on Interstate 35 were in the Twin Cities Metro Area and the other two are in the Duluth Area. Three of these bridges were steel continuous beam spans, two were steel continuous deck girders, and one was a steel continuous deck truss. One of the steel continuous beam span bridges was 35W over the Minnesota River, and the FC elements were pins in a link joint detail. For the other two steel continuous beam span bridges, the FC elements were steel pier caps. One of these bridges was 35W over T.H. 280, and the other one was in Duluth. One of the steel continuous deck girder bridges was located in Duluth and the FC element was pier caps. The other steel continuous deck girder bridge was the 35E bridge over the Mississippi River and the FC elements were pins and it was also a two-girder bridge with continuous span

welds. The truss bridge was the 35W bridge over the Mississippi River (#9340); and the FC elements were truss tension members. The tension chord on the truss of the Blatnik Bridge is also fracture critical. The Blatnik Bridge also has a link joint detail with pins. If one of the pins or the link plate fractures, the bridge could collapse.

Research was done on the fracture critical I-35W truss bridge over the Mississippi River (#9340) to determine if fatigue could be a problem for this bridge (O'Connell and Dexter 2000). Field measurements at several locations on the deck truss revealed that the stress ranges that the bridge actually experiences are less than the CAFL and infinite fatigue life is expected. A current Mn/DOT research project is examining the steel pier caps on the bridge located in Duluth on I-35.

3.1.5 Condition Ratings and Design Loads

There are several ways to rate bridges, such as the operating and inventory rating, sufficiency rating, and appraisal ratings. These ratings provide information about the level of service, or condition of the bridges.

The operating rating represents the maximum permissible load that the structure may be subjected to, or 75% of yield stress level. The inventory rating represents the load level that can safely utilize the structure for an indefinite period of time, or 55% of yield stress. The rating is given as the gross vehicle weight of an HS truck, in tons. For example an inventory rating of 25 tons represents an HS-25 truck, or a truck that has 25% heavier axle loads than an HS-20 truck. An HS-20 truck has 8 kips (36 kN) on the front axle and 32 kips (142 kN) on the second and rear axles, for a total weight of 72 kips (320 kN).

Figure 3.3 shows the number of bridges on the three routes for different design loads. The design load HS-20 and Modification means that the bridge was designed using the HS-20 vehicle as well as a military load. The figure shows that there were only 11 bridges that were designed for live loads less than HS-20, but only three of these 11 bridges were not being considered for replacement. However, these three bridges had high sufficiency ratings (above 80%) and the

structural evaluation appraisal rating was 6 or 7 (equal to or better than present minimum criteria), while the other eight bridges with lower design loads had lower sufficiency and structural evaluation appraisal ratings.

Figure 3.4 shows the average inventory and operating ratings for different design loads. As expected, the larger the design load, the larger the average rating, although there was a good deal of variation in each category. For example, the minimum HS-20 operating rating is 20, while the maximum is 80. Statistics for the inventory and operating ratings for different design loads are given in Table 3.2 and Table 3.3, respectively. Note that in Figure 3.4, Table 3.2, and Table 3.3, the design loads HS-20 and HS-20 & Modification were combined because they are similar.

The sufficiency rating is essentially an overall way to evaluate the condition of a bridge. The rating varies from 0-100%, where 100% is a completely sufficient bridge and 0% is a completely deficient bridge. The sufficiency rating is calculated from several detailed equations, of which 55% of the rating is based on structural adequacy and safety calculations, 30% is based on serviceability and functional obsolescence, and 15% is based on the essentialness of the bridge for public use, as well as up to 13% for special reductions. Some of the variables that affect the rating include, load capacity, ADT, and road width. When a bridge has a sufficiency rating below 50%, it is eligible for federal replacement funds. There were 12 bridges with sufficiency ratings below 50%, and they all had proposed improvements or were being replaced. The average sufficiency rating for the bridges on the three routes was 87%.

The structural evaluation appraisal rating is a rating that measures the overall condition of the bridge structure. This rating takes into account the superstructure, substructure, and inventory ratings. Appraisal ratings vary from 0 to 9, with 9 being superior to present desirable criteria and 0 for a closed bridge. Figure 3.5 shows the number of bridges for each structural evaluation appraisal rating. Most bridges had a rating of 6 or higher, equal to the present minimum criteria. A rating of 2 or 3 requires corrective action or replacement, while a rating of 4 or 5 means the bridge can be left in place with little or no improvement. All 20 bridges that had a rating of 4 or less were listed for proposed improvements.

Another rating is the safe load capacity appraisal. In this rating, a value of 9 is for HS-20 inventory or greater, a value of 7 is for HS-20 operating or greater, and a value of 5 is for less than HS-20 or H20 operating. Bridges rated at 5 or above do not require posting. Figure 3.6 shows the number of bridges for each safe load capacity rating. The only ratings for these bridges were 5, 7, and 9. There were only four bridges with a rating of 5, while there were 231 bridges with a rating of 9. Of the four bridges with a rating of 5, two have been replaced or were in the process of being replaced in 1999, and the other two bridges also had proposed replacements.

From the BRINFO data, it was observed that in general, the ratings were related. Bridges with low inventory and operating ratings were older and were built with lower design loads. These bridges also typically had lower sufficiency ratings, structural evaluation ratings, and safe load capacity ratings.

3.2 DESCRIPTION OF SELECTED BRIDGES

Based on the data presented in Section 3.1, and on a visual inspection of approximately 65 bridges of possible interest, eight bridges were selected for testing. The eight bridges were selected on the basis of accessibility for instrumentation and average inventory ratings. Because there was a larger proportion of bridges and larger traffic volumes on Interstate 35 than on U.S. 2 or Trunk Highway 200, six of the eight bridges selected for load testing were located on or near 35, one bridge was selected on U.S. 2, and one bridge was selected on Trunk Highway 200.

One of the bridges selected (the Blatnik Bridge in Duluth, #9030) also had a steel high truss span. While truss bridges represent only about two percent of the 263 bridges, truss bridges are generally bigger and likely more expensive to replace than the bridge types that will not be examined.

Five different deck protection strategies were observed in the set of selected bridges: new deck construction with overlay (bridge #9030), monolithic bridge deck (bridges #9731 and #54004), 2-in (50-mm) low slump concrete layer over unsound deck without repair (bridge #27939), low

slump concrete layer over sound deck (bridges #19844 and #04006), low slump concrete layer over unsound deck after scarifying (bridges #9603 and #9276).

3.2.1 Prestressed Concrete Bridges

Three prestressed concrete slab-on-girder bridges were selected for instrumentation and testing.

3.2.1.1 T.H. 35W over 31st Street (Bridge #9731)

Bridge #9731 was a single span prestressed concrete I-girder bridge with a span length of 67.3 ft (20.5 m), and girder spacing of 109 in (2,800 mm). A framing plan showing girder layout and notation is given in Figure A3.1. In addition, a cross section of the west half of the bridge showing lane location and lane notation is given in Figure A3.2. Figure A3.3 shows a cross section of the girder including reinforcement layout at midspan. A detailed description of the geometry of the bridge and the material properties is given in Section A3.2.1.

In 1965, the bridge was originally constructed as one of two separate eight girder parallel bridges with a deck thickness of 6.5 in (165 mm). In 1995, the original bridge deck was completely removed in the two parallel structures and a 9-in (230-mm) monolithic concrete deck was constructed over the 16 girders with an orthotropic reinforcement pattern. Epoxy-coated bars were used in 1995.

Bridge #9731 had the highest truck traffic volume among the selected bridges.

3.2.1.2 T.H. 35W over County Road I (Bridge #9603)

Bridge #9603 was a three-span prestressed concrete I-girder bridge. The approach span had six 35.9 ft (10.9 m) long girders spaced at 163 in (4,140 mm). The main span had nine 62.5 ft (19.1 m) girders spaced at 102 in (2,590 mm). A framing plan showing girder layout and notation is given in Figure A3.4. In addition, cross section views of the main span and approach spans are given in Figures A3.5 and A3.6, respectively. Figures A3.7 and A3.8 show cross section views of the girders in the main and approach spans, respectively, including reinforcement layout at

midspan. A detailed description of the geometry of the bridge and the material properties is given in Section A3.2.2.

In 1967, the bridge decks of the approach spans were built with a structural thickness of 8 in (203 mm), and that of the main span was constructed with a structural thickness of 6.75 in (170 mm), with a 4.5 in (115 mm) bituminous layer at both approach and main spans. In 1996, the bituminous layer was removed and a 0.5 in (13 mm) thickness of the structural concrete was scarified at all spans and a 2.5 in (64 mm) low-slump concrete layer was placed over the in-place deck. This resulted in a total thickness of the structural concrete of 10 and 8.75 in (254 and 220 mm) in the approach and main spans, respectively. The original uncoated rebars were designed orthotropically and were left in place.

3.2.1.3 Bemidji Bridge (Bridge #04006)

Bridge #04006 was a four-span skewed prestressed concrete girder bridge with staggered transverse diaphragms located on U.S. Highway 2 two miles east of downtown Bemidji. The approach spans were each 53.7 ft (16.4 m) long and had four girders spaced at 156 in (3,960 mm), while the main spans were each 87.4 ft (26.7 m) long and had five girders spaced at 114 in (2,900 mm). Only the north main span was instrumented, hence all descriptions herein refer to this span. A framing plan showing girder layout and notation is given in Figure A3.9. In addition, cross section views of the main span and approach spans are given in Figure A3.10. Figure A3.11 shows a cross section view of the main span girder, including reinforcement layout at midspan. A detailed description of the geometry of the bridge and the material properties is given in Section A3.2.3.

The bridge was built in 1978 with a total deck thickness of 9 in (230 mm) in the interior spans. The total thickness included a 2 in (50 mm) low-slump concrete wearing course. The deck was constructed with epoxy-coated bars in an orthotropic reinforcement pattern.

3.2.2 Steel Bridges

Five steel bridges were selected for testing. Three of the five had welded cover plate details which are either a fatigue detail category E or E', while a fourth bridge had riveted cover plates which is category D. The four bridges with cover plates were built in the 1960's, while the fifth bridge was built in the 1990's, and was selected partially as a comparison between current and previous fatigue design practices. A brief summary of each of the steel bridges selected is given in the following sections. Table 3.4 summarizes the important characteristics of the bridges and compares them to the averages of the bridges on the selected routes. See Chapter B3 for more detailed information about each of these bridges. A picture of each of the five steel bridges is included in Figures B3.1 through B3.5.

3.2.2.1 I-35 over 205th St. in Lakeville (Bridge #19844)

The bridge selected in Lakeville was a four-span five-girder continuous bridge. A main reason for selecting this bridge was that the second span is located over a paved walking trail. This allowed for easy access with a lift truck without interfering with any traffic. This bridge also appeared to be a typical steel bridge that was built in the early 1960's with cover plates. The positive moment cover plates were category E and the negative moment cover plate ends were category E'. This was the only bridge selected that has a fairly significant skew angle (13^{o}).

The bridge was constructed in 1965 and remodeled in 1980. The bridge originally had a 6.5 in (165 mm) thick reinforced concrete deck with uncoated rebar. In the rehabilitation of the structure in 1980, the original concrete deck was completely removed and a new 9 in (230 mm) thick bridge deck including 2 in (50 mm) low-slump concrete wearing course was constructed. The epoxy coated steel bars were installed in an orthotropic deck reinforcement pattern.

3.2.2.2 I-35W over 60th St. (Bridge #27939)

Bridge #27939 was a three-span seven-girder continuous bridge on I-35W over 60th St. in Minneapolis. This bridge is similar to the bridge in Lakeville in that it had bottom flange cover plates in the main span positive moment region and top and bottom flange cover plates in the negative moment region, although all cover plate ends were fatigue category E. Bridge #27939

had a skew angle of 3^{o}, which was considered negligible. Accessing this bridge for instrumentation was possible because 60^{th} St. was wide enough. Traffic was closed on the north half of 60^{th} St. with one lane of traffic able to flow in each direction on the south half.

The bridge was constructed in 1963 and deck protection was applied in 1996. A 2.75 in (70 mm) thick low slump concrete overlay was added over the original 6.5 in (165 mm) reinforced concrete deck without any repair. Currently, the bridge deck with a total thickness of 9.25 in (235 mm) is in service and has the original uncoated rebars in an orthotropic pattern.

3.2.2.3 Trunk Highway 200 over the Red River Near Halstad (#54004)

The Halstad bridge was a multi-span continuous plate-girder bridge with four girders. The bridge was built beginning in 1997 and opened in 1999. This was the only steel bridge tested that did not have cover plates on it. The worst fatigue detail category on this bridge was category C (transverse stiffeners). It was not possible to test the longer spans over the river, but the approach spans were easily accessible with a scissors lift from below the bridge, which was less than 20 ft (6,000 mm) above the ground in the instrumented regions.

The monolithic reinforced concrete deck without any overlay was 8.5 in (215 mm) thick. The epoxy-coated bars were installed in an orthotropic reinforcement pattern.

3.2.2.4 Blatnik Bridge (#9030)

The Blatnik Bridge was located between Duluth, MN and Superior WI on I-535. This bridge was not located on I-35, but most of the traffic on this bridge also travels on I-35, because I-535 begins off of I-35. This bridge was also originally selected because of the possibility of directional damage (because it was believed that loaded trucks deliver their goods to Superior, and then return empty on the Duluth-bound side of the bridge). However, due to the accessibility of the bridge, only one direction of traffic could be instrumented and no evidence of directional damage was found. The Blatnik Bridge was a multi-span steel continuous plate girder bridge with a steel high truss span over the St. Louis Bay.

Only one deck panel at the high truss structure was instrumented. The bounding stringers at this region were 7.8 ft (2.4 m) apart. In 1993, the original deck was removed, and the new bridge deck with a thickness of 9 in (230 mm) was reconstructed using epoxy-coated bars in the truss part. The overall thickness consisted of 2 in (50 mm) low slump concrete overlay.

3.2.2.5 Hwy. 36 over Cleveland Ave. (Bridge #9276)

Bridge #9276 was a two-span steel continuous beam span bridge with cover plates located on the bottom flanges in the positive moment region and cover plates on both flanges in the negative moment region. The cover plate ends on this bridge were fatigue category E'. This bridge was not located on I-35W, but traffic in the left lane on this bridge leads to I-35W south which is only about 300 m away (1000 ft), while traffic in the right lane leads to Trunk Highway 280. This bridge was selected because of concerns and questions about why cracking developed in some top flange cover plate locations as well as some bottom flange cover plate locations. This bridge was also included as part of a previous University of Minnesota research project (McKeefry and Shield 1999) that showed very small stress ranges at the top flange negative moment locations and therefore could not explain why there was cracking at these locations.

The bridge was built in 1963 and repaired in 1982. The original thickness of the bridge deck was 6.5 in (165 mm). In 1982, the concrete to the top of the transverse reinforcement (1.5 in (38 mm) thick concrete) was removed and a 3 in (75 mm) low slump concrete overlay was applied over the in-place deck resulting in a deck thickness of 8 in (203 mm). The original orthotropic uncoated rebars were left in service.

3.3 BRIDGE INSTRUMENTATION

The objective of the instrumentation was to accurately record the response of the girders and deck from known loads. These responses were used for the calibration of finite element models, to find the maximum response in the bridge, either in the girders or in the deck, and to estimate the location of neutral axis.

Access to the instrumented regions was gained through the use of lift trucks, scissors lifts, or snooper trucks, which were provided by the Minnesota Department of Transportation.

The total number of gages and number of spans instrumented for each bridge were limited by time constraints associated with the need for bridge maintenance crew assistance and lane closure in some instances, as well as the availability of channels on the data acquisition system. As a result, only one span was instrumented for each bridge, and not all girders in the instrumented spans were instrumented.

For the determination of the neutral axis location and the largest bending strains in the girders, single gages were placed at different heights on the same cross section on or as near as possible to the middle of the span. For several locations on each bridge, more than one gage was placed at the same location in order to corroborate test results. Gages were placed with their longitudinal axis parallel to the longitudinal axis of each girder.

In steel bridges, the weldable gages were attached by first grinding the layers of paint off of the steel to expose a smooth surface of steel to weld the gages onto. The gage was then welded onto the girder using a portable welding/soldering unit. For concrete surfaces, the surface preparation included sanding of the location where each gage was to be placed and cleaning of the location with acetone. The gages were then glued to the smoothened concrete with a fast setting adhesive. The installed strain gages were covered with caulking to protect the gage from humidity, temperature changes, and other external effects.

Instrumentation of the reinforced concrete decks to detect the flexural strains consisted of using 350-ohm resistance short [with 0.2 in (6 mm) gage length] and long [with 2 in (60 mm) gage length] concrete surface strain gages in all bridges and Linear Variable Differential Transformers (LVDT) in two of them.

The deck panels close to the instrumented girder locations were more heavily instrumented for time efficiency in placement. To monitor the distribution of the load, two adjacent panels in the transverse direction were instrumented in most cases.

The instrumented locations in the bridge decks were selected so that the most distinguishable strain peaks could be detected according to the positions of the trucks in the field-test setups. The strain gages were glued to the bottom surface of the bridge deck after obtaining a smooth surface by grinding. It was intended to measure the nominal strain ranges at the instrumented locations, rather than measuring the strain at the stress concentration spots. Therefore, the installation of the strain gages overlapping a crack and at the crack tip were avoided.

In bridge #27939 and #54004, LVDT's were installed at an 8 in (240 mm) gage length over visible transverse and longitudinal cracks to monitor the opening of these cracks under flexural action in the longitudinal and transverse directions, respectively.

The locations for each gage on the prestressed concrete girders are given in Tables A3.1, A3.2, and A3.3 for bridges #9731, #9603, and #04006, respectively. Details on the general gage notation for prestressed concrete girders are given in Section A3.3.2.

A description of the gage locations on the steel girders is presented in Section B3.2. The locations of each gage on the steel girders are presented in Tables B3.2 through B3.6.

For bridge decks, the locations of the gages are given in Figures C3.1 through C3.17. The instrumentation notation of the bridge decks is described in Section C3.2.

3.3.1 Data Collection

Data was collected from the strain gages using a Campbell PC9000 data acquisition system. The data acquisition system was controlled by a portable PC connected to it. This system allows for data collection at rates of up to 100 Hz. It was desired to have a resolution of at least one scan for every 15 in (381 mm) traveled by the trucks moving at 40 mph (64 km/hr). For each bridge, the scan rate was inversely related to the total number of gages used. As the total number of gages increased, the highest allowable scan rate decreased. As a result, data was collected at

rates varying from 50 Hz to 66.7 Hz. The exact scan rate and resulting resolution used for each prestressed concrete girder bridge is given in Section A3.3.6.

Gage noise was present when collecting strain data. Care was taken to minimize the amount of noise present in the gages during testing. All cable shielding was grounded to the data acquisition system. The data acquisition system was in turn grounded to a five foot copper rod driven almost all the way into the ground. The generator used to provide power to the acquisition system and to the portable PC was placed at least 50 ft (15 m) away from these devices, and was also grounded to a copper rod. On two bridges, it was found that running the Campbell off of the batteries reduced the noise slightly. However, the levels of noise varied from gage to gage, and from bridge to bridge. A discussion of the noise for prestressed concrete girders are given in Section A3.5.1.1, and in Sections B3.3 and B3.5 for the steel bridge girders.

For most of the instrumented bridges, there were a few gages that did not function. Possible explanations include damage during the installation process, faulty wiring, or a bad connection with the bridge surface, however the exact reason was not known. Almost all of the gages worked well, and the objectives stated at the beginning of Section 3.3 was achieved.

3.4 DESCRIPTION OF TEST TRUCKS AND TEST SETUPS

Three-axle Mn/DOT trucks were used for the truck tests on the instrumented bridges. Figure 3.7 shows a picture of the type of Mn/DOT truck that was used for the tests. Table 3.5 shows axle weights and gross vehicle weights for each of the trucks used in the live load tests of bridges #9731, #9603, #9276, and #27939. Table 3.6 shows axle weights and gross vehicle weights for each of the trucks used in the live load tests of bridge #04006. Average axle spacing for these five bridges is shown in Figure 3.8. For each bridge, four of these Mn/DOT trucks were used, with the exception of the Halstad (#54004) bridge where two trucks were used.

Because all of the instrumented bridges were located on trunk highways with moderate to very high traffic volumes, it was not possible to do static load tests on any of the bridges. Therefore most of the truck passages were performed at speeds ranging between 30 and 55 mph (48 and 88

km/hr). For bridge #54004 and bridge #04006, low traffic volumes during the day of the testing allowed for test speeds as low as 5 mph (8 km/hr). All bridges were left open to traffic during the tests. However, it was noted whenever other trucks were on the bridge at the same time as the test trucks. Data which appeared to have been affected by the presence of other trucks was ignored, and the test was repeated if possible.

All Mn/DOT truck load tests were performed in the Fall of 2000. The five bridges located in the Twin Cities Metro Area were tested at night and early morning (between 10:00 pm and 5:00 am) in order to minimize interference to and from normal traffic. The other three bridges were tested during the day. The dates of the bridge testing are listed below:

- Bridge #19844 in Lakeville was tested on the night of August 31, 2000.
- The Blatnik Bridge (Bridge #9030) was tested on October 4, 2000.
- Bridge #04006 in Bemidji was tested on October 10, 2000.
- The bridge in Halstad (Bridge #54004) was tested on October 11, 2000.
- Bridges #9731 and #27939 on I-35W over 31st St. and 60th St., respectively, were tested on the night of October 19, 2000.
- Bridge #9276 and #9603 were tested on the night of October 23, 2000.

Several different truck formations were used for the tests in each bridge. These different truck formations remained approximately the same from bridge to bridge. Any variation in the test formations was primarily due to the differences in the deck geometry, such as number and type of lanes, and the number of trucks available, either two or four. The basic formations that were used at all or nearly all of the bridges were:

- One truck on the bridge at a time in the center of a lane. This formation represents the usual case of a single heavy truck crossing the bridge at a time.
- Two trucks driving side-by-side in adjacent lanes (if there were more than two lanes, tests with more than two trucks side-by-side were also performed).
- All four trucks in a 2 x 2 formation (see Figure 3.9).

- Two trucks driving in the same lane with the second truck following close behind the first truck.
- Other formations, such as one truck at a time on the bridge with a wheel line over or near a painted lane or shoulder line.

More information on the truck tests for the different aspects of the research can be found in the corresponding appendices.

3.5 MN/DOT TRUCK TEST RESULTS

In this section, the most important results obtained from the live load tests are discussed.

3.5.1 Prestressed Concrete Bridge Results

From the live load tests, the most important variable for flexural cracking was the magnitude of the flexural live load strains. For each tested bridge it was observed that multiple trucks side-by-side presented a more critical loading case than trucks closely following each other or single trucks. It was also observed that as the spacing between trucks increased to 40 ft (12.2 m) the maximum response generated by pairs of trucks was approximately the same as that generated by single trucks. This was determined from the measured data, in combination with the visual estimates of spacing between trucks as recorded during the testing of each bridge. Furthermore, these observations were only valid for the three tested bridges, as it was recognized that the bridge response due to multiple trucks following each other was a function of span length.

The largest measured strains for the three bridges were: 66 με for bridges #9731 and #9603 (Tests 9 and 10, respectively), on girders G6 (gage G6_Sh_0) and G5 (gage G5_Lo_0), respectively, due to all four trucks crossing the bridges in a side-by-side configuration, and 43 με for bridge #04006 (Test 9) on G3 (gage G3_Sh_0) for two trucks traveling side-by-side.

Using the adjusted values for E_c introduced in Section A3.2, the largest measured strains were converted to stresses: 0.29 ksi (200 MPa) for bridge #9731; 0.28 ksi (193 MPa) for bridge #9603; and 0.18 ksi (124 MPa) for bridge #04006.

The influence of test truck speed on the bottom fiber response of the girders was investigated for bridge #04006. For the other two tested bridges, the speed of the trucks was not varied, hence the data from these latter bridges could not be used to characterize dynamic effects.

Two tests involving two trucks driving side-by-side were used to characterize the dynamic response of bridge #04006. For the first test (Test 9 from Table A3.9) the trucks were traveling at a nominal speed of 15 mph (24 km/hour). For the second test (Test 10 from Table A3.9) the trucks were traveling at a nominal speed of 40 mph (64 km/hour). Figure 3.10 and Figure 3.11 shows the bottom fiber strain reading from each test. The error bars shown in both figures illustrate possible error due to the noise present in the gages at the time of testing, as well as error due to possible lateral and longitudinal variations in the position of the test truck.

For Test 10, the first pair of trucks traveling at 40 mph (64 km/hour) generated bottom fiber strains that were 12% smaller than those generated by those same two trucks crossing the bridge in the same configuration, but at 15 mph (girder G3) (Figure 3.10). This same effect was also observed in the other girders, although the difference between responses was smaller. The second pair of trucks traveling at 40 mph (64 km/hour) generated smaller bottom fiber strains on two of the five girders (Figure 3.11).

It was concluded that the observed decreased strains with increased speed was within the range of reading error due to gage noise and possible variations in the position of the trucks (see error bars in Figure 3.10 and Figure 3.11). As a result of these observations, it was concluded that the truck speed did not have a significant influence on the measured strains for the three tested prestressed concrete bridges.

3.5.2 Steel Bridge Results

For steel bridges, the most important data is the range of stresses. For each truck or group of trucks passage, the minimum and maximum-recorded strain values were recorded. Because all trucks were nearly the same, the results of each identical test formation were averaged into one value for each formation. Also, whenever applicable, the reported values include the average of two gages that were in the same location, so that there would only be one recorded stress range for each test formation and gage location.

Table 3.7 lists the maximum center of span stress ranges caused by a single Mn/DOT truck. The values in the table are the average stress range from several (four to eight) passages. The values shown are from the gaged location on the bottom of the bottom flange near the center of the instrumented span. The girder that had this recorded stress range was the girder directly below or nearest to the lane that the truck was in.

Table 3.8 summarizes the maximum average center span stress ranges that were recorded during the Mn/DOT truck tests with any truck configuration. The Mn/DOT truck formation that caused that stress range is also listed.

More information on the results of the truck tests on the steel bridges is included in Chapter B3. Additional information in this appendix includes distribution factors, neutral axis locations, and some graphs of the recorded stress histories.

3.5.3 Reinforced Concrete Deck Results

In the investigation of the susceptibility of bridge decks to longitudinal cracking, the analytical models were calibrated using the field test results. Although the maximum tensile strain in transverse direction was the most important criterion to determine the susceptibility to overstressing, the longitudinal strain variations from the field test data were also compared to the analytical results to validate the analytical models.

In the field tests, the maximum transverse tensile strains in the passages of test trucks were observed at the midpoint gage locations between the girders when one of the wheel lines was at the closest position to the corresponding gage location. Table 3.9 summarizes the observed maximum strains in longitudinal and transverse directions for single-truck, side-by-side, and two-by-two formation (if applied) test setups.

The highest maximum transverse deck strain was observed in the field test of bridge #9276, which had the thinnest deck (8 in (200 mm) thick) among the instrumented bridges. Even for this bridge, the observed maximum transverse strain (58 μstrain) was lower than the concrete tensile cracking strain (132 μstrain).

3.6 COMPARISON OF ANALYTICAL RESULTS WITH TEST RESULTS.

This section summarizes the comparison between the analytical results and the test results. For a more detailed discussion, see the respective appendices (Appendix A for prestressed concrete results, Appendix B for steel bridge results, and Appendix C for reinforced concrete decks).

3.6.1 Analytical and Experimental Results for Prestressed Concrete Bridges

Section A3.4 contains a detailed discussion of the analytical models for each bridge, including a description of each model and a description of how the test trucks were idealized for each model.

The models were calibrated by reproducing several tests within the model and comparing the numerical results to the measured strain readings at the bottom fiber of the girders. The measured and analytical values used in the calibration process were those corresponding to the maximum bottom fiber strains produced by each individual truck or groups of trucks in a test. For all tests used in the validation process, the trucks were assumed to be perfectly centered in their lanes, and in every case the trucks were applied as static loads on the model. No factor was used to account for dynamic effects. A typical comparison between measured and analytical results for the same test is shown in Figure 3.12 for bridge #9731. Additional comparisons between measured and analytical results are given in Figures A3.34 through A3.36.

3.6.1.1 Additional Considerations for Each Tested Prestressed Concrete Bridge

The analytical models were used to determine the effect of the following variables on bridge response: deck continuity over the supports, variability in the longitudinal and transverse position of the test truck, deck strength, and the presence of railings. Each variable is discussed in more detail in Section A3.4.6. In addition, Figures A3.25-A3.27 show the effects of the variables on bottom fiber strains for each bridge, for a single lane loaded.

It was found that deck continuity had the largest effect on maximum bottom fiber girder strains bridges #9731, #9603, and #04006. Removing the deck continuity for bridges #9731, #9603, and #04006 increased the midspan bottom fiber strain for the most heavily loaded girder in each bridge (G4, G6, and G2, respectively) by approximately 3, 8, and 3 με, respectively. These values represented 5.7, 20.9, and 8.8% of the peak strain values for bridges #9731, #9603, and #04006, respectively, for a single lane loaded. For the other girders in each bridge, the increases in bottom fiber strains were slightly lower.

Variability in the longitudinal and transverse position of the test truck changed the midspan bottom fiber strain in the most heavily loaded girder of each bridge by values ranging between 0.5 and 2 με. The effect of deck strength on girder response was negligible for the three tested bridges. Similarly, the effect of J-rails was negligible for bridges #9731 and #9603. For bridges #04006, the effect of J-rails was more noticeable than for the other two bridges because bridge #04006 was a narrow structure and the traffic lanes were close to the edges of the bridge. However, the variation in bottom fiber strain due to the J-rails for bridge #04006 was still within the noise level of the girders (described in Section A3.5.1.1).

Analytical distribution factors (DFs) were computed for each tested prestressed concrete bridge. Two different approaches were used to compute DFs (Approaches 1 and 2, as explained in Section A3.5.8). Approach 2 was a better method for calculating live load distribution factors because it was based on normalizing the stresses from a line girder analysis to those of the girder stresses in the full SAP model ,therefore only those results are discussed herein. For each analytical model, the DFs were calculated for the models with and without diaphragms. In addition, DFs were computed according to the 1989 AASHTO Standard and 1994 AASHTO

LRFD Bridge Design Specifications. All details for the computation of the DFs are given in Section A3.5.8.

The one-lane DFs obtained from the AASHTO standard and AASHTO LRFD specifications exceeded the values calculated analytically by at least 64% and 41% for each tested bridge for the models with and without diaphragms, respectively (Approach 2, Table A3.19). The multiple-lane DFs obtained from the specifications exceeded the values calculated analytically by at least 36% and 21% for the models with and without diaphragms, respectively, , for the case in which all lanes were loaded simultaneously for each bridge (Approach 2, Table A3.20). For the case of multiple-lane DFs due to only two lanes loaded simultaneously on each bridge, the DFs obtained from the specifications exceeded the values calculated analytically by at least 86% and 56% for the models with and without diaphragms, respectively (Approach 2, Table A3.20).

Part of the difference between AASHTO distribution factors and distribution factors calculated from SAP for each tested bridge was due to the diaphragms. It is likely that the remaining difference in DFs for each bridge was due to the load distribution provided by the deck.

A more detailed discussion on live load distribution factors for the three tested prestressed concrete bridges is provided in Section A3.5.8.

3.6.2 Analytical and Experimental Results for Steel Bridges

The analytical models included a finite element grillage analysis using the software program SAP 2000 and a variety of lateral distribution factors for single girder analysis. After the models were compared with the Mn/DOT truck test data, the models were used to estimate the remaining fatigue lives of the tested bridges using the procedures outlined in NCHRP 299 (or the 1990 AASHTO Guide Specifications for the Fatigue Evaluation of Existing Steel Bridges), which are described in Section B2.1.2.1.

A finite element grillage model was created for each of the five steel bridges that were instrumented and field-tested. The models consisted of frame elements for both the girders and

deck elements. The deck elements and girder elements were separated by the distance between their neutral axes and were connected by rigid links. Moving loads were used on the models to determine the maximum and minimum stresses at each location of interest. Descriptions of how the models were created and how the loads were applied is included in Appendix B.

Figure 3.13 compares the measured and grillage model stresses at the gage location near the center of the second span of bridge #54004 near Halstad from a Mn/DOT truck traveling across the first two spans. The grillage model stresses were calculated from the influence lines of the bridge at that location. This figure shows that the grillage model did a good job of predicting the measured stresses for this bridge and it verifies that the moving loads were applied correctly on the grillage models.

Because only the stress ranges are important for fatigue of steel, only the grillage model stress ranges were analyzed for the other bridges at locations of interest and not the influence lines. Figure 3.14 presents an example of the graphs that were used for comparison between the measured and grillage stress ranges (Section B3.6.1.2 has a couple of these graphs for each of the five steel bridges). Table 3.10 summarizes the maximum average stress ranges from the measured results and the percent of measured for the grillage analysis models.

Overall, there was some variability between the measured results and the grillage models, but most of the results were relatively close. There are two main reasons that could explain the slight differences between the two results. First, the grillage models may not accurately represent all of the actual properties of the real bridge even though it was attempted to model the bridges with the correct properties.

The other main reason that could account for the differences between the two results is due to the variability of the measured data. This is especially true if the measured results were larger than the model, because electrical noise could have amplified the stress ranges for the gages with relatively large noise. The variability of the measured data was reduced by averaging the stress ranges from several truck passes and from gages that were located at the same locations on the

bridges. Another factor in the differences could be that the actual transverse positions of the trucks in the lanes were not known, although this is considered a minor factor.

The measured and analytical (both grillage and line girder) stress ranges are summarized in Table 3.11. This table presents the maximum average stress ranges that were recorded or found from the grillage analysis for a Mn/DOT truck in the lane specified (the lane that was used for fatigue evaluation). The stress ranges from the line girder analysis with no distribution factor were used to calculate the measured and grillage model distribution factors by dividing the maximum stress ranges by this line girder stress range. The line girder stress ranges are also compared using the NCHRP 299 and AASHTO LRFD distribution factors.

Section B3.6.2 describes and summarizes the results of the line girder analyses and the distribution factors from different methods. It was found that the distribution factors from the AASHTO Standard Specifications are too conservative for fatigue evaluation. The line girder distribution factors using AASHTO LRFD and NCHRP 299 were similar for most of the tested bridges, but still larger than measured and from the grillage models. For bridge #9030 (Blatnik Bridge) the AASHTO LRFD and NCHRP 299 line girder stress ranges could not be computed because the large difference in stiffness between the plate girders and stringers violates the assumptions used in calculating the distribution factor.

The stress ranges from the grillage analysis were the closest to the measured stress ranges, although some of the stress ranges were somewhat smaller than the measured results. The stress ranges from the AASHTO LRFD and NCHRP 299 distribution factors were similar to each other, but conservative compared to the measured stress ranges.

The analytical stress ranges in Table 3.11 do not include an impact factor. According to the AASHTO LRFD Specifications, for fatigue evaluation an impact factor of 0.15 should be applied to increase the stress range. For the NCHRP 299 procedures, an impact factor of 0.10 should be used to increase the gross weight of the fatigue truck for smooth road surfaces, however, if an inspection of the roadway reveals unusual surface conditions, then it is allowed to increase the impact factor, but not more than 0.30.

Also for the NCHRP 299 procedures, it is specified that the moment of inertia for the composite section in the positive moment region should be increased by 15% (this has the effect of reducing the stress by 15%). The 15% increase is to account for the differences between field tests and the typical analysis procedures that conservatively neglect beneficial effects such as contributions from nonstructural elements, unintended partial end fixity at abutments, and unintended composite action (see Section B2.2.1 for a discussion on the differences that have been found between field tests and normal analytical procedures). However, because the stress ranges from the line girder analysis with the NCHRP 299 distribution factor were still larger than the measured stress ranges, a 15% reduction may not be enough for fatigue evaluation.

Because of these factors, the stress ranges in Table 3.11 from the AASHTO LRFD distribution factor would need to be increased by 15% for fatigue, while the stress ranges from the NCHRP 299 distribution factor would be multiplied by 1.10/1.15, which is about 0.96. After these factors are included, the stress ranges from the AAHSOT LRFD distribution factors will be larger and even more conservative than the stress ranges from the NCHRP 299 distribution factors. When these factors are applied to the line girder stress ranges, the AASHTO LRFD line girder stress ranges would be about 50% to 80% larger than the measured stress ranges and the NCHRP 299 line girder stress ranges would be about 25% to 50% larger than the measured stress ranges with the exception of the Blatnik Bridge (#9030), in which distribution factors could not be computed.

For the fatigue evaluation of steel bridges, the grillage analysis results were treated as the most accurate and the best estimate of remaining fatigue life. Because the procedures of NCHRP 299 were used to estimate the remaining fatigue lives of the steel bridges, the grillage model stresses were increased by 10% to account for impact (although the positive moment sections were not increased by 15% as is done for the line girder analysis because the finite element grillage models are a more accurate way to predict stresses). When the grillage model stresses are increased by 10%, they are even closer to the measured results. In Chapter 4, the results from the line girder analyses with the NCHRP 299 distribution factor are also included to give a comparison of the effect on the estimated fatigue life, because the line girder analysis can be used as a first step to determine if fatigue is a problem for a certain bridge. If a bridge is

expected to have an infinite fatigue life from the more conservative line girder analysis, then the creation of a more complicated finite element model is not necessary.

3.6.3 Analytical and Experimental Results for Bridge Decks

In Section C5.1, the important variables in terms of deck overstressing (i.e. susceptibility to longitudinal cracking) were determined. Among the variables investigated, the ones affecting the flexibility of the deck were more important. These variables can be listed as:

- Girder spacing,
- Deck thickness,
- Transverse crack spacing,
- Degradation at the cracks.

Although the first three variables could be determined from the bridge plans and visual inspections at site, the last one, continuity at the cracks, was difficult to determine by visual inspections or simple calculations.

In the parametric study in Section C5.1, it was observed that it was important to model the full-depth transverse cracks to simulate the critical case for transverse tensile strains. The highest level of degradation (free-end crack simulation) at these cracks was assumed in most of the cases to save in computational time. However, in the case of the comparison of different crack simulations in Section C5.1.3, it was observed that there was an abrupt difference in transverse stress predictions between the free-end crack simulation and the crack simulation with degraded stiffness with $1/7^{th}$ of original deck thickness, which simulated the continuity between the crack faces. Indeed, although the transverse cracks from the construction period are called ‘full-depth cracks’, it was believed that there was considerable continuity between the crack faces from the longitudinal reinforcement and aggregate interlock. Therefore, it was necessary to investigate the degree of the continuity at the crack faces in the field.

For this purpose, the strain measurements at the bottom surfaces of the decks were compared to the results of the finite element analyses. As in the parametric study in Section C5.1, linear

elastic models of the bridges were subjected to the applied load to simulate the field tests. Because there were many variables related to the loading of the test setup, and material and geometric properties of the structural system, it was difficult to predict the continuity at the cracks directly. In Chapter C5, important variables affecting the deck stresses were investigated for bridge #9276 (the most deteriorated one among the other bridges considered) in Section C5.2.1 through C5.2.4 by comparing the analytical and field test results. The variables considered were: (1) concrete contribution at the negative moment region in continuous bridges, (2) concrete modulus of elasticity, (3) transverse position of the test trucks, (4) presence of transverse cracks, and (5) linearity of structural response.

In Section C5.2.5, the continuity at the crack locations was determined. The reasons that bridge #9276 was deemed the most critical in terms of deterioration and overstressing were:

- Full-depth transverse cracks spaced at 5 ft with considerable leaching, which was one of the smallest crack spacings observed in the preliminary on-site bridge survey,
- Smallest deck thickness observed in the metro area.

In the parametric study in Section C5.1, it was observed that the longitudinal stresses were not critical in terms of overstressing. However, because it was demonstrated that the longitudinal strains were more susceptible to the presence of cracks and more indicative for investigating the continuity at the crack location compared to the transverse strains as demonstrated in Section C5.2.5, in which the field test and analytical results for longitudinal strains at different locations at the bottom surface of the deck were compared in addition to the transverse strain results.

The analytical models incorporating simulated cracks with degraded stiffness (1/8 of the original deck thickness) approached the results of the field tests, especially in the longitudinal direction and the same models conservatively predicted the transverse tensile strains. Detailed comparison of field test and analytical results is given from Figure C5.48 to Figure C5.68. Consequently, it was judged that the applied degree of degradation at the cracks (1/8 of the original deck thickness) was a reasonable assumption for conservative estimations of transverse strains.

In summary, an efficient linear analytical modeling to analyze the bridge deck with a conservative approach was developed to investigate the overstressing (susceptibility to longitudinal cracking) in bridge decks.

It was observed that the transverse cracks from construction period increases the maximum transverse strain controlling the susceptibility to longitudinal cracking. The comparison of the field test and analytical results gave a reasonable prediction for the degradation at the crack locations.

TABLES

	Main Span Material					
Main Span Type	Reinforced Concrete	Steel Simple Span	Steel Continuous Span	Prestress or Precast	Timber	Total
Beam Span	0	11	127	81	1	220
Low Truss	0	1	0	0	0	1
High Truss	0	3	0	0	0	3
Deck Truss	0	1	1	0	0	2
Deck Girder	0	0	3	0	0	3
Box Girder	16	0	0	2	0	18
Slab Span	4	0	0	3	0	7
Voided Slab Span	1	0	0	2	0	3
Arch	3	0	0	0	0	3
Pipe Arch	0	0	0	3	0	3
Total	24	16	131	91	1	263

Table 3.1 Number of bridges by type and material on I-35, U.S. 2, and MN 200

	HS15 & Less	*H20*	*HS20*	*HS25*
Mean	11.5	21.3	24.7	29.9
Standard Deviation	4.3	7.4	5.6	4.7
Minimum	6	11.3	14	22
Maximum	18	28.8	54	37
Count	6	5	233	19

Table 3.2 Inventory rating value statistics

	HS15 & Less	*H20*	*HS20*	*HS25*
Mean	20.6	34	42.2	52.4
Standard Deviation	3.5	14.1	8.8	10.5
Minimum	18	16.3	20	25
Maximum	27.4	47.9	80	62
Count	6	5	233	19

Table 3.3 Operating rating value statistics

	Bridge #					average of selected bridges	average of bridges on 35, 2, and 200
Bridge#	19844	27939	54004	9030	9276		
Year Built	1965	1963	1997	1961	1963	1970	1969
Route #	35	35W	200	535	36		
City	Lakeville	Minneapolis	Halstad	Duluth	Roseville		
Feature Crossed	205th St. and trail	60th St.	Red River	St. Louis Bay	Cleveland Ave.		
Truck ADT	1510	4875	120	2000	1480	1997	1740
# of Lanes	2	3	2	4	2	2.6	2.6
# of Girders	5	7	4	4	6	5.2	?
Girder Size	W33x118 & W33x130	W27x84	45 in web (1.1 m)	9 ft web (2.7 m)	W36x150		
Girder Spacing	9 ft (2.7 m)	9 ft (2.7 m)	11.5 ft (3.5 m)	8 ft* (2.4 m)	8.2 ft (2.5 m)	9.1 ft (2.8 m)	?
Instrumented Span Length	65.3 ft (19.9 m)	58.6 ft (17.9 m)	100 ft (30.5 m)	173 ft (53 m)	82 ft (25 m)	96 ft (29.2 m)	84 ft (25.7 m)
Number of Spans	4	3	13	54	2	15.2	4.6
Skew Angle	13°	3°	0°	0°	0°	3	17
Design Load	HS20+	HS20+	HS25	HS20	HS20+		
Inventory Rating	14.8	20.2	25	18	25.3	20.7	24.7
Operating Rating	24.6	33.7	25**	31	42.2	32.9	42.3
Sufficiency Rating	86.4	58.6	86.5	80.1	58.7	74.1	86.8
Structure Evaluation	5	4	9	7	5	6.0	6.4
Cover plates present?	Yes	Yes	No	Yes, but riveted	Yes		
Worst Fatigue Category	E'	E	C	D	E'		

** Blatnik Bridge stringer spacing is listed, the main girder spacing is 30.7 ft (9.3 m).*

*** Bridge #54004's operating rating was recorded as 25 (same as inventory), which appears to be an error.*

Table 3.4 Summary of selected steel bridges

Test Truck #	MN/DOT Truck #	Front Axle (lbs)[1]	Middle Axle (lbs)[1]	Rear Axle (lbs)[1]	Tandem Axles (lbs)[1]	GVW (lbs)[1]
1	97437	16,100	17,290	16,590	33,880	49,980
2	99052	16,560	17,200	16,480	33,680	50,240
3	97803	16,630	17,870	17,140	35,010	51,640
4	97801	15,760	17,520	16,780	34,300	50,060
5	99053	16,450	17,670	16,960	34,630	51,080
Average Truck[2]		16,260	17,470	16,750	34,220	50,480

[1] 1 lb = 0.454 kg

[2] Average based on trucks one through four.

Table 3.5 Mn/DOT trucks used for testing bridges #9731, #9603, #9276, and #27939

Test Truck #	MN/DOT Truck #	Front Axle (lbs)[1]	Middle Axle (lbs)[1]	Rear Axle (lbs)[1]	Tandem Axles (lbs)[1]	GVW (lbs)[1]
1	94189	17,000	17,400	16,800	34,200	51,200
2	96039	16,400	17,800	17,200	35,000	51,400
3	96408	17,200	17,700	16,600	34,300	51,500
4	93734	16,000	17,500	16,700	34,000	50,200
Average Truck		16,650	17,600	16,825	34,425	51,075

[1] 1 lb = 0.454 kg

Table 3.6 Mn/DOT trucks used for testing bridge #04006

Bridge #	Max Avg Stress Range (MPa)	Max Avg Stress Range (ksi)	Lane The Truck Was In
19844	23	3.3	Right Lane
27939	20	2.9	Center Lane
54004	20	3.0	East-Bound Lane
9030	13	1.9	Right Lane
9276	25	3.6	Left Lane

Table 3.7 Maximum center of span steel bridge stress ranges recorded from a single Mn/DOT truck

Bridge #	Max Avg Stress Range (MPa)	Max Avg Stress Range (ksi)	Mn/DOT Truck Formation That Caused This Stress Range
19844	36	5.2	2 Trucks Side-by-side (1 in each lane)
27939	35	5.0	3 Trucks Side-by-side (1 in each lane)
54004	33	4.8	2 Trucks in the WB lane & shoulder
9030	22	3.3	2 x 2 Truck Formation
9276	38	5.5	2 x 2 Truck Formation

Table 3.8 Maximum center of span steel bridge stress ranges recorded in any configuration

Bridge #	Gage Location	Single-Truck Test	Side-by-side Test	2x2 Formation Test
9731	IN3-M-tr	30	27	N/A
9603 (Approach)	App2-M-tr	12	8	8
9603 (Central)	Cen3-M-tr	41	22	24
4006	EX1-M-tr	44	14	N/A
19844	IN4-M-tr	30	28	26
27939	EX1-M-tr	18	15	15
54004	EX2-M-tr, EX3-M-tr	25	20	N/A
9030	T1, T3	16	14	16
9276	EX2-M-tr	40	51	58

Table 3.9 Maximum transverse strains measured in the field tests of the selected bridges

	Right Lane		Left/Center Lane**		Side-by-side in all lanes***	
Bridge # and Gage Cross-Section*	Measured Stress Range (ksi)	% of Measured for Grillage	Measured Stress Range (ksi)	% of Measured for Grillage	Measured Stress Range (ksi)	% of Measured for Grillage
19844						
Cross-section A	3.3	83%	2.9	109%	5.2	94%
Cross-section B	2.9	98%	3.2	100%	4.6	106%
27939						
Center	2.9	81%	2.9	85%	4.7	95%
Approach	2.6	70%	-	-	-	-
54004**						
2nd Span - 10 mph	2.8	93%	3.0	87%	4.1	101%
2nd Span - 50 mph	2.6	98%	3.6	72%	-	-
1st Span - 10 mph	2.6	98%	-	-	3.7	109%
1st Span - 50 mph	2.7	95%	-	-	-	-
9030						
Cross-section 1	1.9	82%	1.5	76%	2.7	92%
Cross-section 2	1.6	70%	1.3	65%	2.1	79%
9276						
Center	3.0	104%	3.6	102%	4.8	116%

**See Tables 3.2 through 3.6 in Appendix B for descriptions of the cross-sections.*
*** Left lane, except center lane for bridge # 27939.*
**** 2 trucks side-by-side, except for bridge # 27939 where 3 trucks were side-by-side.*
***** For bridge # 54004, right lane is westbound direction and left lane refers to eastbound, also, there were two speeds that were recorded.*
Other Notes:
Reported values are the average bottom flange stress range on the girder with the largest stress range. If an entry is blank, either a girder that was not instrumented would have recorded the largest stress or that test was not performed at that speed.
1 ksi =6.9 MPa, 1 mph = 1.61 km/hr

Table 3.10 Summary of measured and comparison with grillage results for Mn/DOT trucks

Bridge #	Lane	Stress Range (ksi) *(1 ksi = 6.9 MPa)*				
		Measured Stress Range	Grillage Analysis Stress Range	Line Girder Stress Range		
				LRFD Dist. Factor	NCHRP 299 Dist. Factor	No Distribution Factor
19844	Right	3.3	2.7	5.3	5.1	10.9
27939	Right	2.9	2.4	3.7	3.8	7.9
54004	WB	2.8	2.6	3.6	4.4	7.6
9030	Right	1.9	1.5	NA	NA	4.6
9276	Left	3.6	3.6	4.6	4.7	11.6

Table 3.11 Summary of maximum bottom flange center of span stress ranges from a Mn/DOT truck

FIGURES

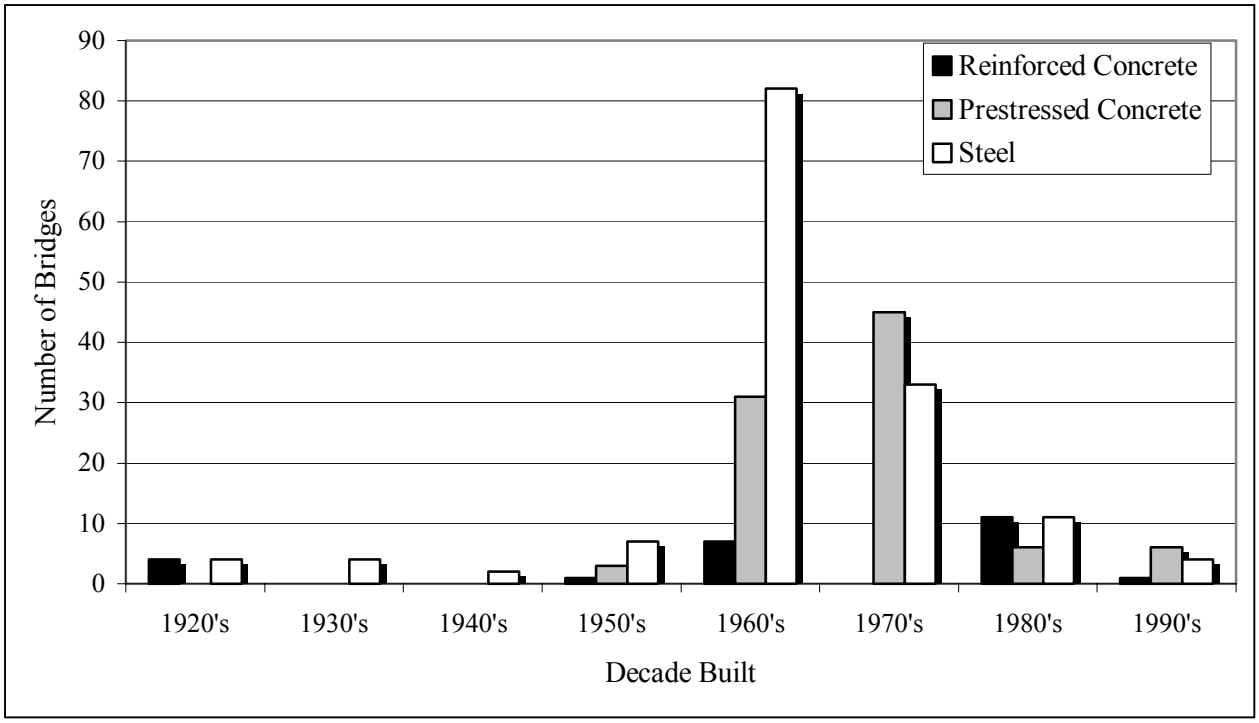

Figure 3.1 Number of bridges built each decade by main span material on highways 2, 200, and 35

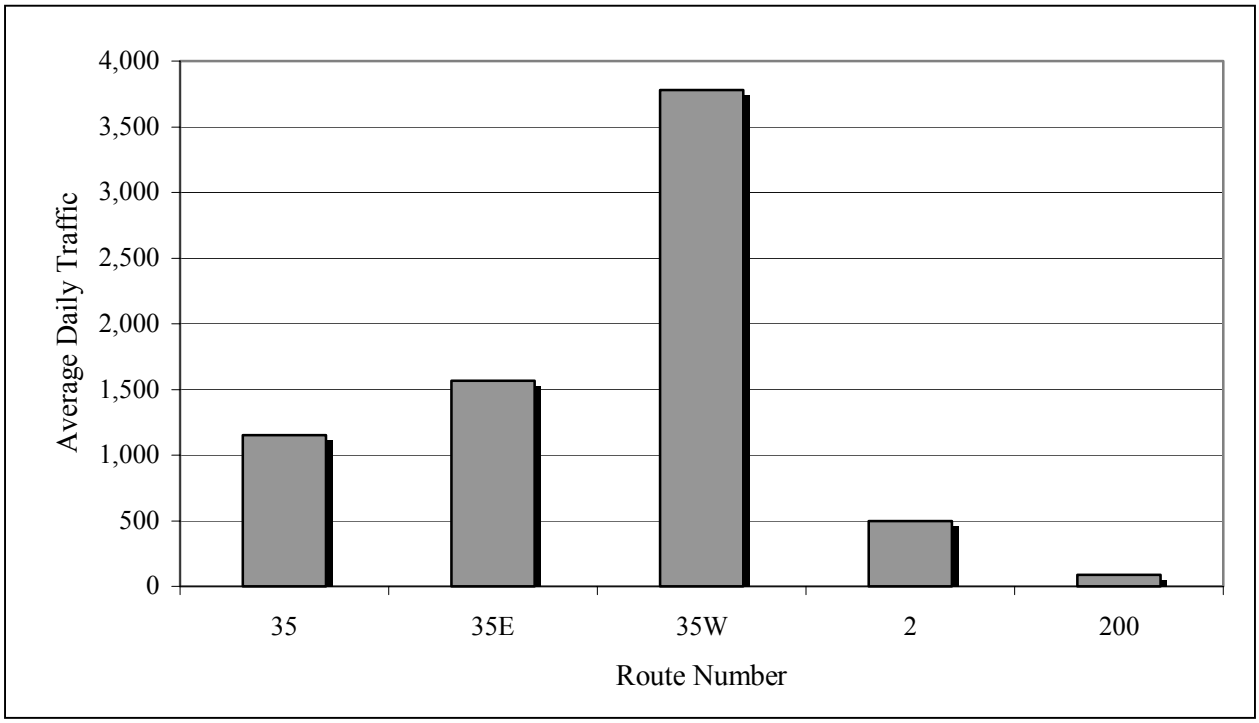

Figure 3.2 Mean average daily heavy commercial truck traffic (HCADT) for selected routes

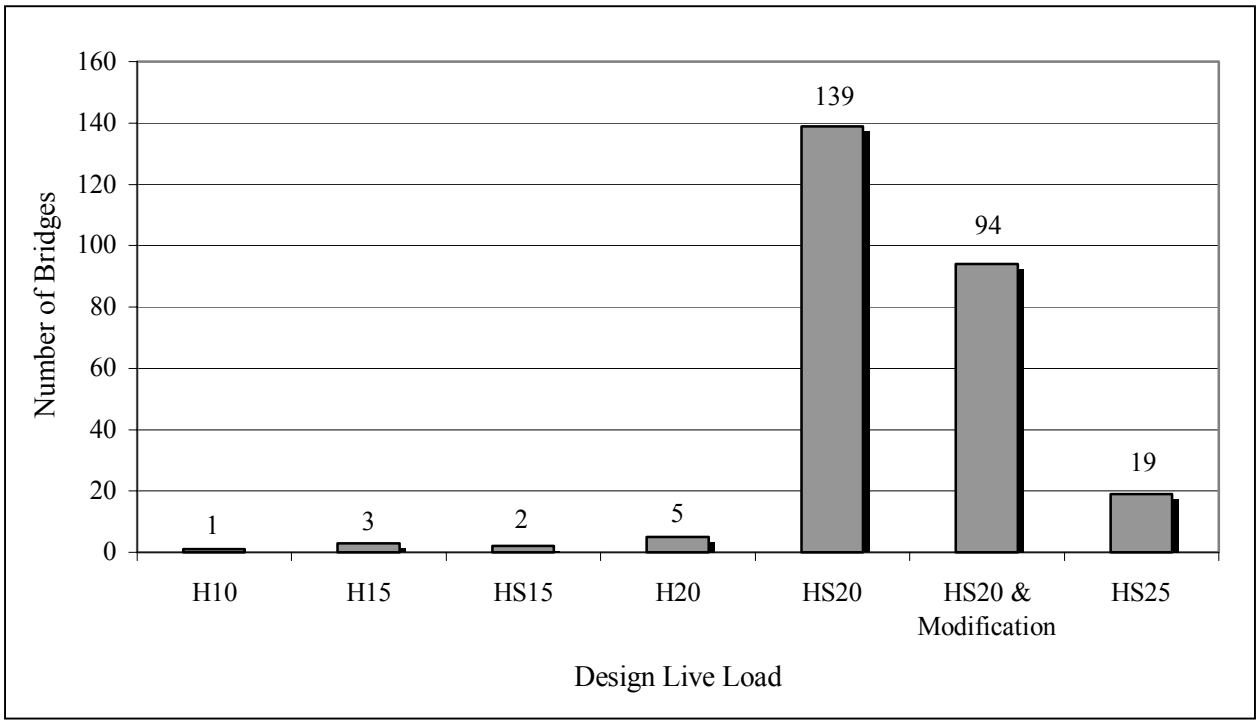

Figure 3.3 Number of bridges on the three selected routes for each design live load level

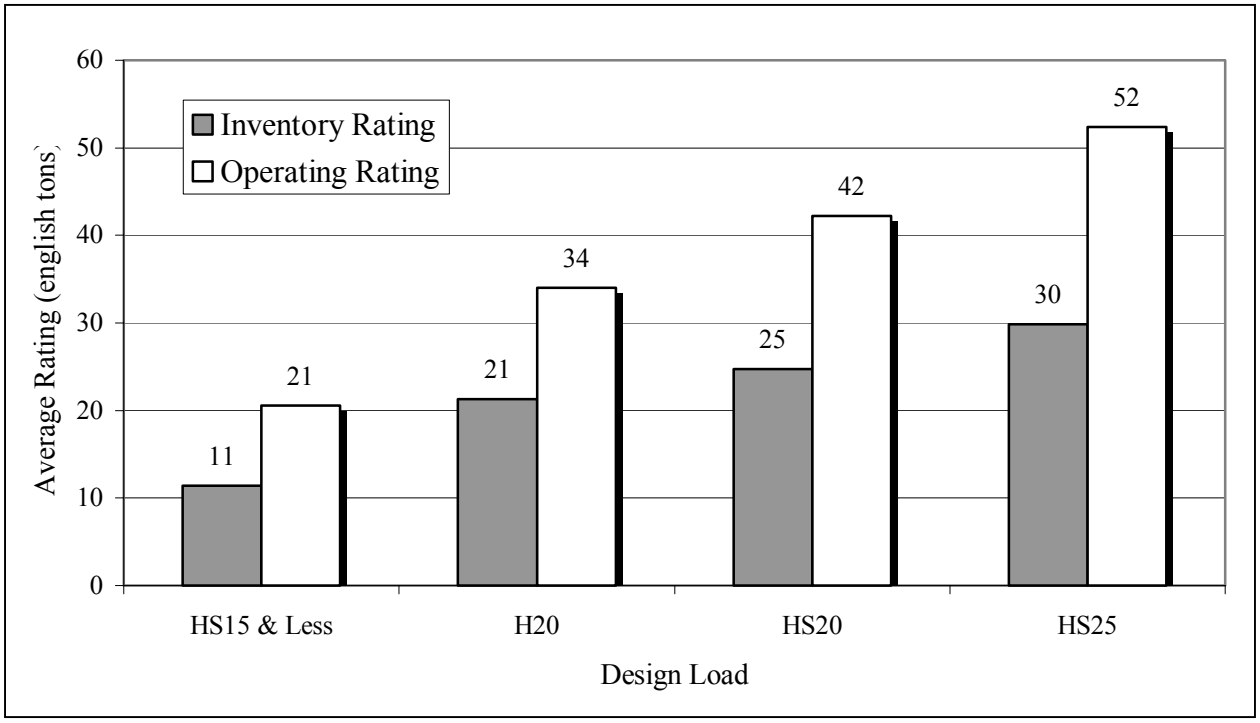

Figure 3.4 Average inventory and operating ratings for different design loads

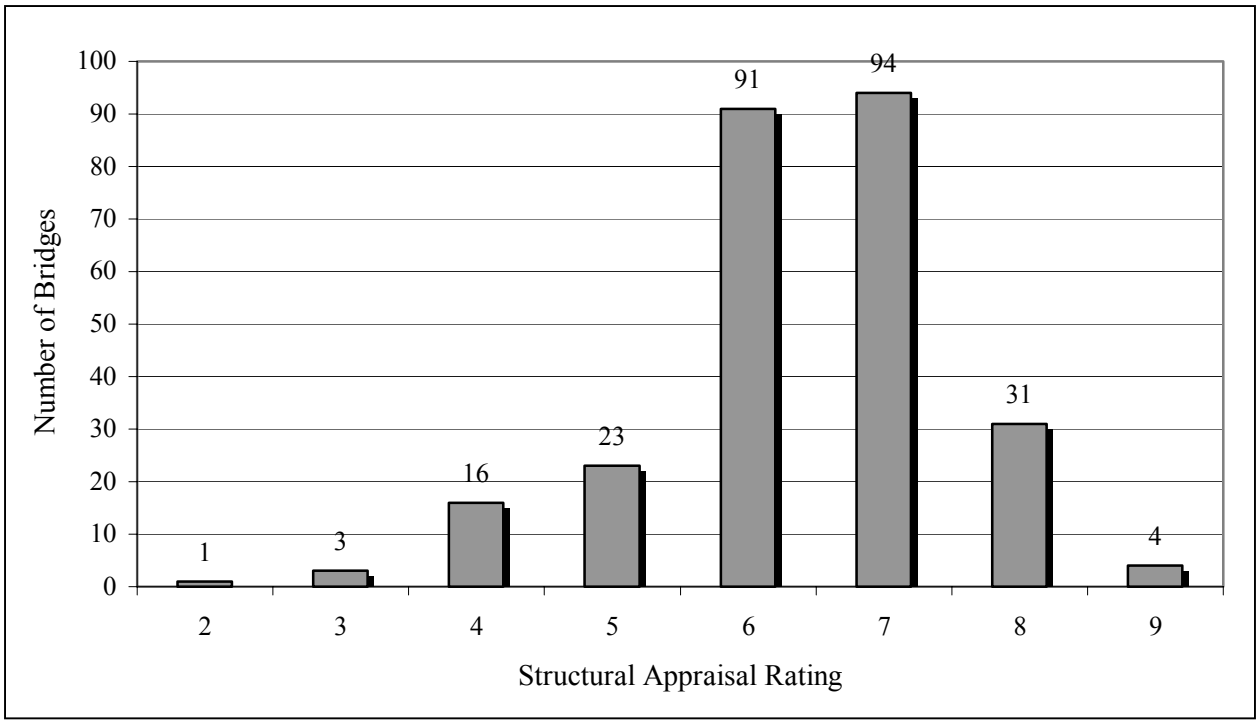

Figure 3.5 Structural valuation appraisal rating for bridges on the selected routes

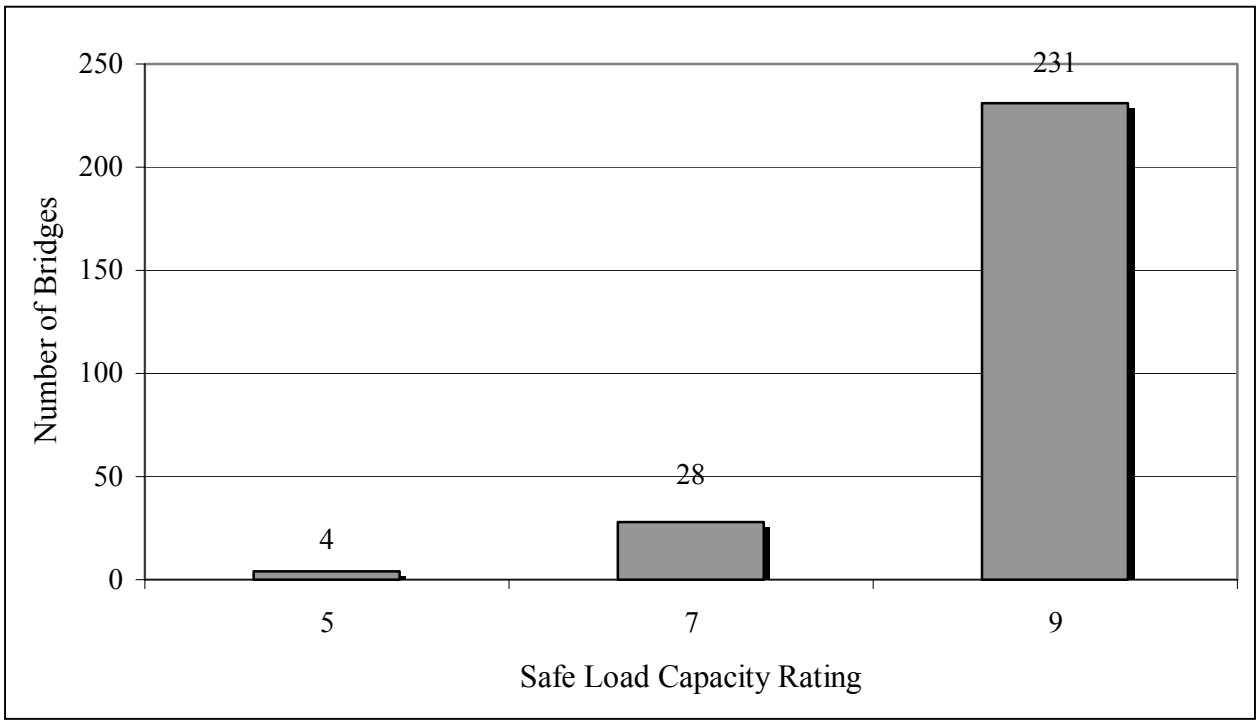

Figure 3.6 Safe load capacity rating

Figure 3.7 Typical 3-axle Mn/DOT truck used for live load tests

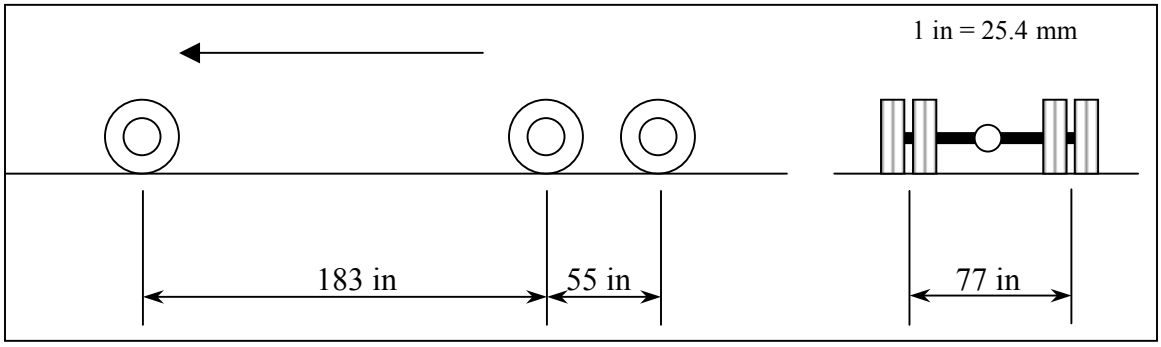

Figure 3.8 Average axle spacing of test trucks

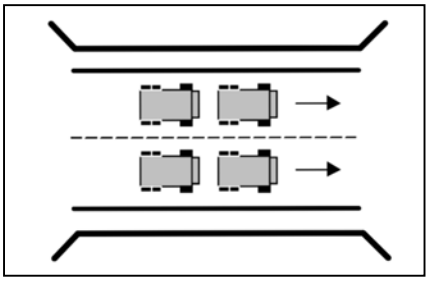

Figure 3.9 Illustration of 2 x 2 truck formation

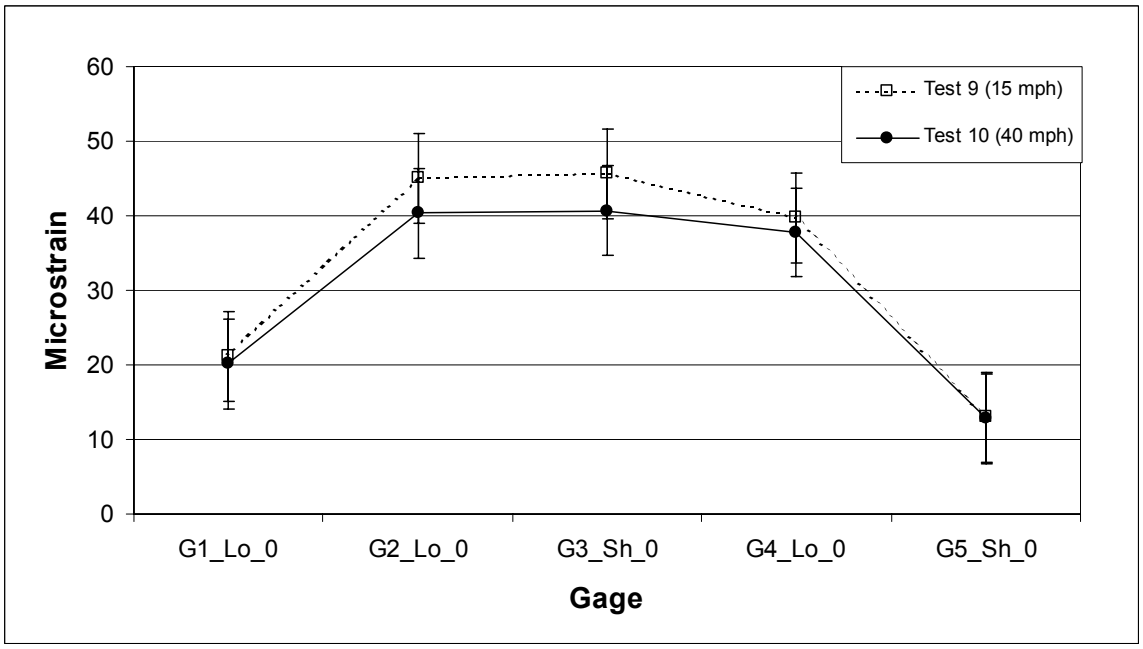

Figure 3.10 Dynamic response of bridge #04006 – Trucks 1 and 2 (measured)

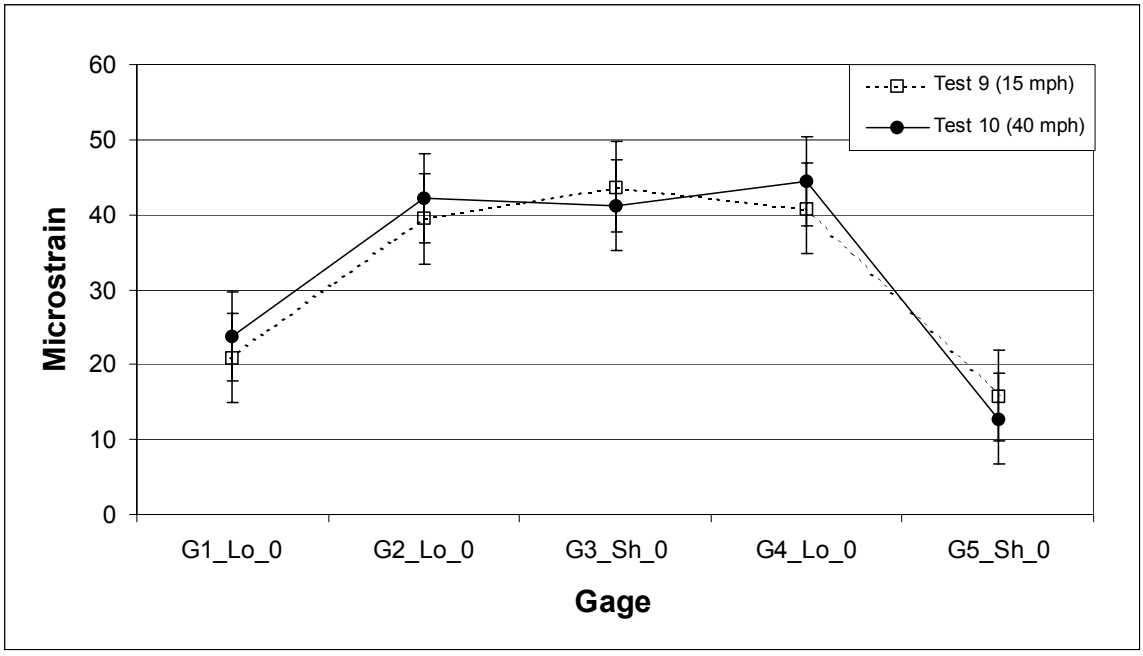

Figure 3.11 Dynamic response of bridge #04006 – Trucks 3 and 4 (measured)

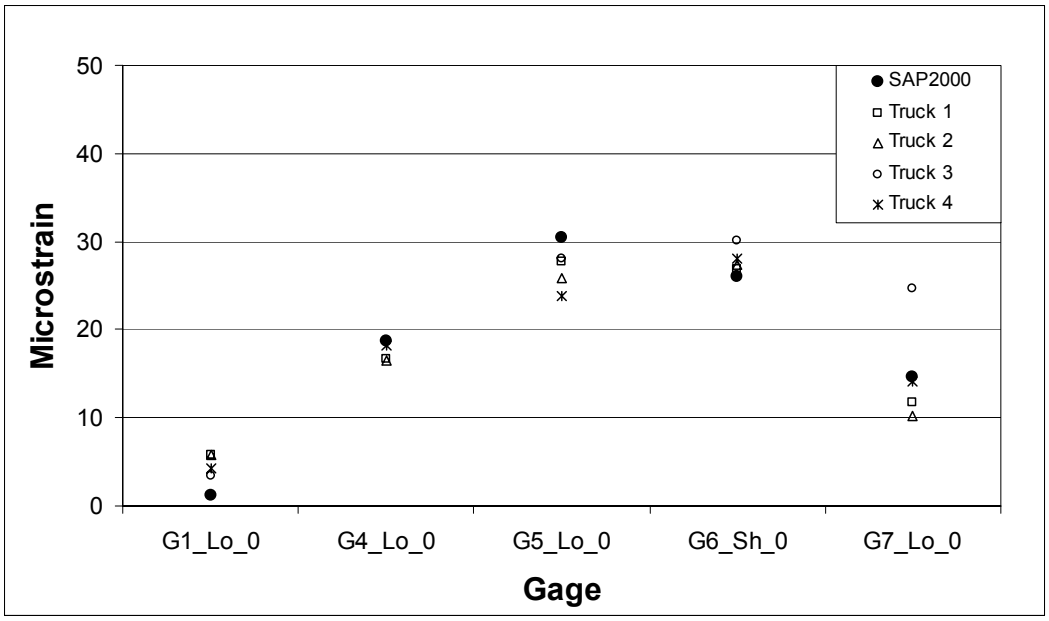

Figure 3.12 Bridge #9731 – Bottom fiber strains for Test 3 (test truck in lane 2)

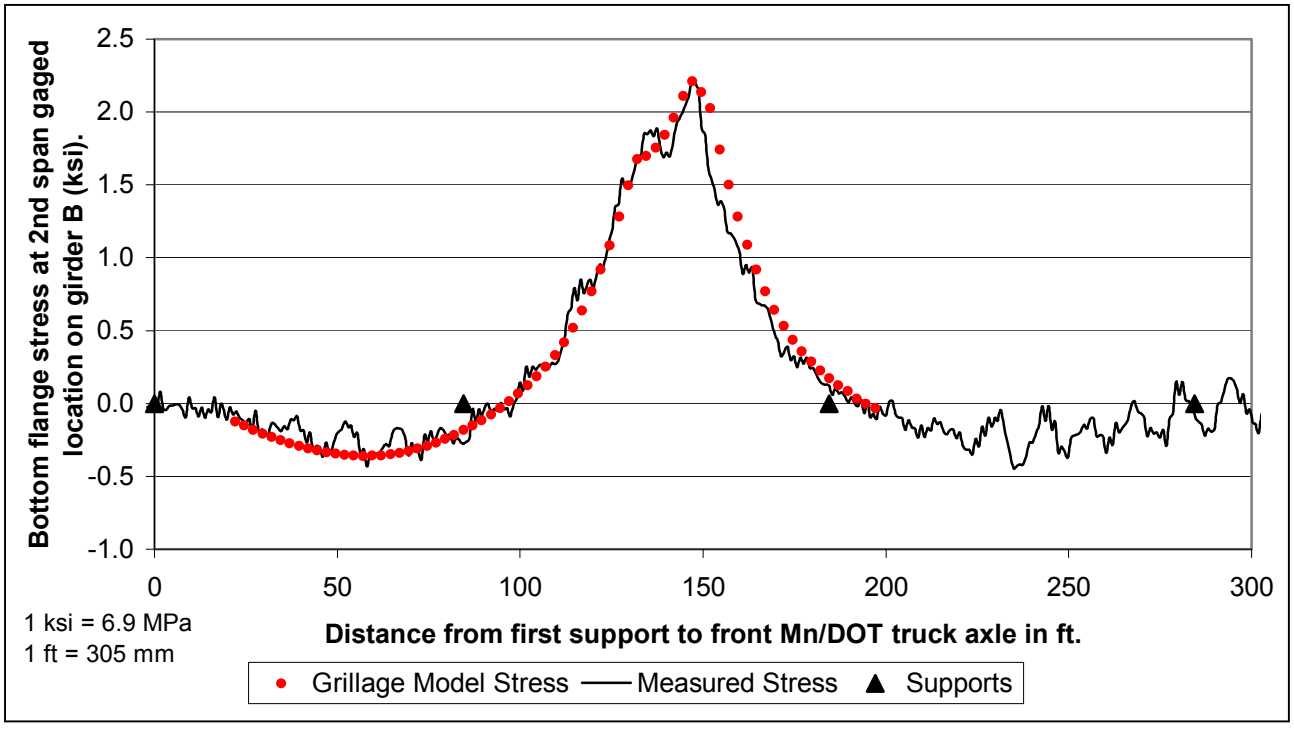

Figure 3.13 Bridge #54004 over the Red River Stress at 2nd span gaged location vs. Mn/DOT truck position traveling in the westbound lane

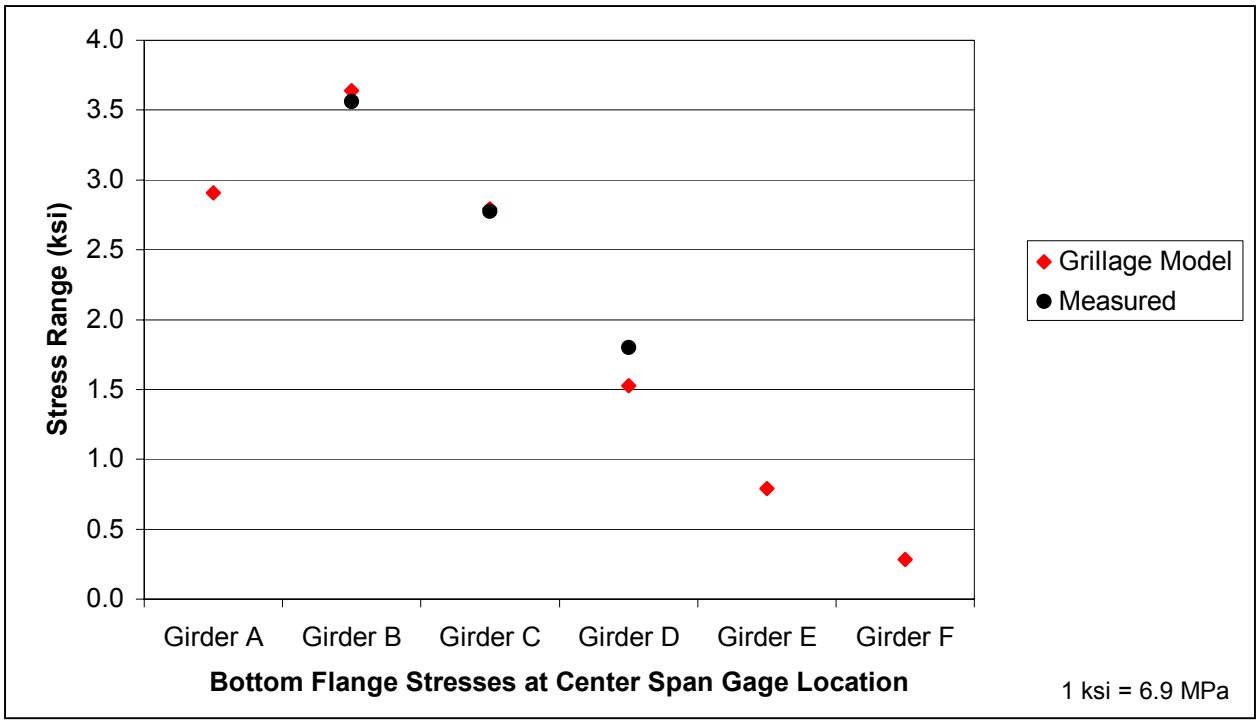

Figure 3.14 Bridge #9276, grillage analysis model and measured results for a Mn/DOT truck in the left lane

CHAPTER 4 – EFFECT OF INCREASING TRUCK WEIGHT

In this chapter, the effects of increasing the allowable truck weight in the remaining service life of the tested bridges are investigated.

4.1 REMAINING LIFE CALCULATIONS FOR THE TESTED PRESTRESSED CONCRETE BRIDGES

In order to determine the cracking load for the prestressed concrete girders in each tested bridge, it was necessary to determine the current stress state and modulus of rupture of the girders. The current stress state of the girders was composed of two main parts: stress due to dead loads and stress due to prestress. The stress due to the dead load was computed by using the current geometry of each bridge to determine the amount of dead load supported by each girder. To determine the stress due to the prestress it was necessary to compute prestress losses, which were subtracted from the original prestress to obtain the service level prestress. Prestress losses for the three tested bridges were calculated using the refined method present in both the AASHTO Standard and LRFD specifications (see Section A2.1.4.3). The modulus of rupture of the girders was assumed to be equal to $7.5\sqrt{f'_c}$. Live load stresses were computed for the two different truck configurations shown in Figure 2.10and Figure 2.11.

The final concrete bottom fiber girder stresses for each bridge, and for each truck configuration, are given in Table 4.1a and Table 4.1b. For each tested bridge, the results corresponded to an interior girder. The details of the calculations are given in Sections A4.1 and A4.2.

The results showed that the final bottom fiber concrete stresses for each tested bridge were below the target design value of zero for bridges #9731 and #9603, and 0.46 ksi (3.17 MPa) for bridge #04006. The reasons for the difference in results between analytical and design values are explained in Section A4.2.1.1.

On the basis of these results, the needed percent increases in GVWs that would lead to flexural cracking of each tested bridge were calculated, and are shown below:

3-axle single unit truck:	Bridge #9731	239%
	Bridge #9603	222%
	Bridge #04006	447%
5-axle tractor semitrailer:	Bridge #9731	259%
	Bridge #9603	287%
	Bridge #04006	447%

Shear calculations were also performed for an interior girder for each tested prestressed concrete bridge. The 5-axle truck shown in Figure 2.11 was used in the calculation of the nominal concrete shear resistance to cracking and nominal shear demands because it was found to generate larger shear stresses than the 3-axle truck shown in Figure 2.10. AASHTO LRFD multiple-lane DFs for shear were used to distribute the live load to the interior girders.

The nominal concrete shear resistance to cracking of the girders in the three tested bridges was computed using the sectional design model, or modified compression field theory, as found in the 1998 AASHTO LRFD Specifications.

In order to find the percent increase in GVW that would lead to shear cracking for each bridge, an iterative procedure was used because both the shear resistance of the concrete, and the shear demand, depended on the level of loading. In this way, it was found that in order to prevent shear cracking for each bridge, the increase in the GVW of the 5-axle trucks should be limited to the following values:

Bridge #9731	140%
Bridge #9603	95%
Bridge #04006	130%

Because the 3-axle truck generated smaller shear stresses than the 5-axle truck, increasing the GVW of the 3-axle truck by the percentages given above will not lead to shear cracking for the three tested bridges. All details of the shear calculations are given in Section A4.3.

Fatigue life was calculated for each of the bridges on the basis of strand stress ranges and Equation A2.30, repeated here for convenience (Equation A2.30a for SI units).

$$\text{Log } N = 11.0 - 3.5 \text{ Log } S_r \qquad \text{(A2.30)}$$

$$\text{Log } N = 13.93 - 3.5 \text{ Log } S_r \qquad \text{(SI units)} \qquad \text{(A2.30a)}$$

where: N = fatigue life in number of cycles
S_r = strand stress range; maximum stress - minimum stress, ksi (MPa)

Live load strand stress ranges were only calculated for the lowest layer of strands in each bridge, as this was the layer of steel that experienced the largest stress ranges. The live load stresses used corresponded to the stresses generated by multiple 3-axle trucks (given in Table 4.1a), however, in order to calculate strand stress ranges, the axle loads of the 3-axle trucks were increased by 95%, which was the maximum allowable increase in GVW that was obtained from the shear calculations for bridge #9603. The calculated strand stress ranges for bridges #9731, #9603, and #04006, were 4.4, 4.6, and 2.8 ksi (30.3, 31.7, and 19.3 MPa), respectively. These strand stress range values were inserted into Equation A2.30, and the number of cycles to fatigue failure were calculated for each bridge. The number of cycles to fatigue failure for bridges #9731, #9603, and #04006 were found to be 560 $x10^6$, 479 $x10^6$, and 2,700 $x10^6$, respectively. All details on these calculations are given in Section A4.4.

On the basis of the results reported in this section, the following conclusions were made on the effects of increased truck weight on the three tested prestressed concrete bridges:

- For the three bridges it was concluded that no flexural or shear cracking would occur under current legal 3- and 5-axle truck loads.

- A 20% increases in allowable GVW will not lead to shear cracking, flexural cracking, or fatigue of the three tested prestressed concrete bridges.

- In one bridge, shear cracking could occur for the Standard C permit truck with the presently allowable GVW of 159 kips.

4.2 REMAINING FATIGUE LIFE CALCULATIONS FOR STEEL BRIDGES

In this section, the remaining fatigue lives of the five instrumented steel bridges are presented for both current loads and future load increases (Chapter B4 contains a more detailed discussion on this topic). The procedures of NCHRP 299 were used to estimate the remaining fatigue lives of the bridges and both the safe remaining life (2.3% or 0.1% probability of developing cracks before that time) and the mean remaining life (50% chance of developing cracks by that time) were calculated. The mean remaining life is the best available estimate of the actual remaining fatigue life of a detail on a bridge, while the safe life estimate should be used to determine which bridges are the most susceptible to fatigue damage and deserve closer inspection.

Because the exact effective weight was not known for each of the bridge locations, the 54 kip (240 kN) fatigue truck of NCHRP 299 (and the 1998 AASHTO LRFD), which is based on extensive nation-wide weigh-in-motion (WIM) data, and a similar fatigue truck with a larger gross vehicle weight based on the WIM data from two Minnesota sites (discussed in Section 2.3.3). For the three bridges located in the Twin Cities area, the 58 kip (260 kN) effective weight found on I-94 was used. For the two other bridges, located on T.H. 200 in Halstad (#54004) and on I-535 in Duluth (#9030), the high effective weight of 66 kips (293 kN) from the eastbound traffic on T.H. 2 was used. Although it was found that even with this conservative load fatigue was not a problem for these two bridges. The reason for using the heavier WIM-based fatigue truck was to provide a more conservative calculation and to compare the effect of different loads on the remaining life.

For each of these load cases, the remaining fatigue lives were estimated from grillage analyses and also from a conservative line girder analysis with distribution factors. These latter

calculations were included even though they are not accurate due to significant overestimation of the stress ranges, because this method is often used in practice, at least as a preliminary assessment. In many cases this preliminary line girder analysis may be sufficient, because a sufficiently long remaining life may be predicted despite the conservatism. For example, this is the case with most bridges built since the 1980's that have only good fatigue details (e.g. bridge #54004 near Halstad over the Red River).

The safe and mean remaining fatigue lives for the five instrumented steel bridges are presented in Table 4.2 and Table 4.3 respectively for assuming current truck weights over the entire bridge life. These estimations include an assumed constant compound traffic volume growth rate up to a limiting value (see Section B2.3.1 for discussion and tables on traffic volume) and when applicable a change in stress range in the past due to deck rehabilitation which increased the deck thickness and reduced the girder stress ranges. The values in the tables indicate the remaining lives at the location with the shortest estimated remaining fatigue life.

Table 4.4 and Table 4.5 present the remaining safe and mean fatigue lives for the five steel bridges after a future 10% increase in truck GVW. It should be noted that an increase of the maximum allowable truck weight limits of 10%, would lead to an increase in effective truck weight that is smaller than 10%. The reason for this is that not all truck traffic will take advantage of this increase. Most trucks will still have to travel empty for some of their trips. Also, loaded trucks that currently travel at weights below the limits are not going to be affected by an increase in truck weight limits. Although, the increase in effective truck weight from a 10% increase in the weight limits is going to be less than 10%, it is difficult to determine how much less it will be. Therefore, it is conservative to use the full 10% increase in the effective fatigue truck GVW.

Bridge #9276, Highway 36 over Cleveland Avenue, had the worst estimated remaining fatigue life. The reason why this bridge had the worst estimated fatigue life was because it had the worst fatigue details (category E' cover plates) with the largest stress ranges. The safe life was already exhausted before an increase in truck weight was applied. Bridge #9276 was the only bridge that had a mean remaining fatigue life based on the grillage analyses that was less than 75 years. An

increase in truck weight will only accelerate the fatigue damage on this bridge. To make sure that fatigue does not become a serious problem on this bridge, it is recommended that the cover plate ends are regularly inspected for cracks (possibly more than once every two years) and that any cracks that are found are repaired.

The other two bridges with welded cover plate details (#19844 in Lakeville and #27939 in Minneapolis over 60th St.) had the remaining safe lives reduced to about a decade or two (for the grillage model estimate) or by about 20 to 25% from the 10% increase in truck weight. However, for these two bridges, the remaining mean lives were still sufficient (over 75 years).

The two bridges with C or D details (C for bridge #54004 with transverse stiffeners, and D for bridge #9030 for rivets) are not expected to have fatigue problems even under the increased truck weights. It was found that these bridges could tolerate an increase in truck weight much larger than 20%. For example, the effective truck weight would need to be increased to over 100 kips (450 kN) (about a 50% increase over the already conservative 66 kip (293 kN) effective weight truck) for the remaining safe life from the grillage analysis to be 75 years.

4.3 BRIDGE DECK FATIGUE

Among the deck fatigue models, the model developed by Petrou et al. (1994) was applied to determine the fatigue life of the bridge decks because (1) it represented the most recent research on this topic; (2) the physical models tested in that study simulated field boundary conditions better than other tests; (3) it had been observed that the tests simulated the repetitive truck loading in the field better than other research; and (4) it had the most conservative results among the fatigue models.

As in all of the deck fatigue models available in the literature (Batchelor et al., 1978, Petrou et al., 1994, and Youn et al., 1998), the model by Petrou et al. (1994) to determine the service life of the deck slabs was based on the relative ratio of the applied load to the nominal punching shear strength of the slab. The prediction of the number of cycles and equivalent weight of axle

loads was presented in Section C4.2. Also, two different methods for estimating the nominal punching shear strength of the slab-on-girder bridges, (i.e. AASHTO conventional punching shear strength formula and the algorithm proposed by Hewitt et al., 1975), were given in Section C4.1.

The punching shear strength of the reinforced concrete decks of the five metro area slab-on-girder bridges studied in this report were calculated using the two methods. Although only the thickness of the slab and the compressive strength of the concrete were the input for the conventional AASHTO punching shear strength formula; the lateral and torsional stiffness of the slab boundary, the contribution from the reinforcement, and in-plane stiffness of the slab were also considered in the latter algorithm. Because the AASHTO formula had been developed for design purposes within the building design code body, it was reported to yield highly conservative estimates for bridge decks due to the neglect of compressive membrane action and dowel effect enhancements. On the other hand, it was demonstrated that the Hewitt algorithm predicted well-correlated punching shear strength values with the bridge deck ultimate strength test results (Petrou et al., 1994, Hewitt et al., 1975, and Mufti et al., 1998). Therefore, the Hewitt algorithm in Section C4.1 was thought to yield more realistic punching shear strength predictions for the bridges considered. The input values for the Hewitt algorithm and the conventional punching shear strength formula are given in Table C4.9. The modulus of elasticity of the reinforcement and concrete were assumed as 29,000 ksi (200 GPa), and 4,000 ksi (27.5 GPa), respectively, for all bridges considered.

The load histogram obtained from the analysis of the WIM data for Interstate Route I-94 was applied as the distribution of the truck traffic for the specific bridges in Twin Cities metro area (Section C4.2). The load histogram from this analysis was implemented into the fatigue model selected from the study by Petrou et al. (1994). There were histograms for different axle types, i.e. individual single axle different from front axle, front axle, and tandem and tridem axles. The third power-weighted average of these different axle types with their number of repetitions were calculated. Also, the third power-weighted average weight, (i.e. effective axle weight), of the whole set of axles was calculated (Equation C4.27).

As described in Section C4.1.3, the presence of consecutive axles decreases the ultimate shear strength calculated with the Hewitt algorithm. The reductions in tandem and tridem groups were applied during the calculation of damage accumulation in the fatigue model for different bridges and scenarios. Equations C4.24 and C4.25 were implemented to investigate the tandem and tridem axle groups, respectively, with the girder spacing of the bridge and minimum axle spacing of 4 ft. The reductions for different bridges are shown in Table C4.10 as percentage.

Although no dynamic amplification was observed in flexural strains during the field tests, an impact factor was included in the applied load, because the dynamic interaction between the bridge and the truck may be bridge-specific and dependent on the dynamic characteristics of the individual trucks in traffic. There is not a clear statement in bridge design codes that addresses the dynamic allowance factor for deck slabs specifically. An impact factor of 0.15 specified for the fatigue limit state in the AASHTO LRFD bridge design code was applied to the axle loads. The tire pressure of 125 psi (0.86 MPa) including the impact from dynamic effects was assumed as being uniformly distributed to the patch area, as the AASHTO LRFD bridge design code specifies. The tire patch width was assumed to be 20 in (500 mm) and constant for all wheel load levels. Three different load cases were analyzed: the Base Case represented the current traffic in the bridge system, and the Alternative Scenarios 1 and 2 were the cases when the truck weight limits were increased by 10 and 20% in the system, respectively.

The P/P_u values were input into the fatigue model by Petrou et al. (1994) given by Equation C2.4, and the number of cycles to failure obtained as output. For a specific bridge, three different P/P_u ratios were applied for the base case and alternative scenarios: the ratio normalized with ultimate strength from the conventional formula, the ratio normalized with ultimate strength from the Hewitt algorithm without reduction for the axle group interaction, and the ratio normalized with ultimate strength from the Hewitt algorithm with reductions for the axle group interaction.

Regardless of the 10 or 20% increase in Scenarios 1 and 2, service lives calculated using the Hewitt algorithm for punching shear strength resulted in service lives much longer than the expected design life. If the conventional formula from the AASHTO specifications was used,

the computed service lives were considerably smaller. However, only three bridges had a result of less than 50 years of service life. In general, the 20% increase in legal weight limits resulted in an approximate 50% decrease in service life. The fatigue curve from the regression analysis of test results from the study by Petrou et al. (1994) had an inverse relationship between the ratio P/P_u and the service life with a power of 4.1. In other words, if the average applied load decreased to half of the original value, the cycles to failure increases to $2^{4.1} = 17.15$ times the original computed life. The 20% increase in load should correspond to $1.2^{4.1}$ or a factor of 2.0 decrease as observed.

In summary, the loading can be predicted from the weigh-in-motion data as was done in this study. The difficulties in the estimation of loading may be in the prediction of the future loads and the response of the truck traffic to the changes in truck weight regulations. Reasonably conservative approaches were applied to approximate these issues. It was observed that there was a great difference between the punching shear strength predictions from the different models. The literature (Hewitt et al., 1975, and Mufti et al., 1998) has verified that the conventional AASHTO formula gave more conservative values for the reinforced concrete bridge decks than the Hewitt model. When the Hewitt algorithm was applied for deck fatigue evaluation, regardless of the assumptions used in the analysis (i.e. the assumptions related to loading and material strength) and possible range in the input values (i.e an applied load up to 10% of the punching shear strength of the deck slab), the result was that the service life would not be limited by deck fatigue. Details on the application of the deck fatigue model are given in Section C4.3.

4.4 EFFECT OF INCREASING ALLOWABLE TRUCK WEIGHT ON OTHER MINNESOTA BRIDGES

In this section, the effects of increasing the allowable truck weight on other Minnesota bridges are investigated. In addition, approaches are provided to extend the findings from this study to other Minnesota bridges.

4.4.1 Prestressed Concrete Bridges

Other prestressed concrete bridges in the three selected routes were considered in an attempt to find a more critical bridge for flexural and shear cracking than the three tested bridges.

For the purpose of this study, a critical bridge for the three routes is defined as a bridge that is close to cracking due to live loads.

The variables considered important in selecting a possible critical bridge for flexure for the three routes were (in order of importance): number of loaded lanes, ratio of live to dead load stresses, design allowable bottom fiber stress for the girder concrete, and number of intermediate diaphragms. These variables are discussed in more detail in Section A5.1.

After considering all 81 prestressed concrete bridges in the three routes, bridge #9603 emerged as a possible critical bridge for flexural cracking. Because bridge #9603 had already been analyzed for flexure, no further considerations were given to it.

For shear, the important variables were girder depth and girder spacing (see Section A5.2.1). Approximately 30 of the 81 total prestressed concrete bridges were considered. On the basis of the girder depth and girder spacing, a possible critical bridge for shear was Mn/DOT bridge #11006, which had 36 in (914 mm) deep girders and a girder spacing of 10 ft (3.05 m). A description of this bridge is given in Section A5.2.1.

For this bridge it was found that the 3-axle truck shown in Figure 2.10 generated larger shear stresses than the 5-axle truck shown in Figure 2.11, therefore, the 3-axle truck was used to calculate the shear capacity and the shear demand.

Through iteration, it was found that increasing the GVW of the 3-axle truck shown in Figure 2.10 by more than 35% could lead to shear cracking of bridge #11006. All details on these calculations are given in Section A5.2.2. Obviously, this bridge is susceptible to shear cracking under presently allowed permit loads.

4.4.2 Steel Bridges

If truck weight is increased, a reduction in fatigue life can be expected for some of the steel bridges. The steel bridges that will be most affected by an increase in truck weight are the bridges with poor fatigue details, such as cover plates, and are located on routes with high truck traffic. Although a number of the bridges will have reduced fatigue lives, some steel bridges will not have fatigue lives that are reduced below the useful bridge life.

Of the five bridges that were tested, the two bridges that did not have E or E' details had infinite fatigue lives under all situations including a 10% increase in truck weight. If a 20% increase is applied on these two bridges, the only case where the bridge would not have an infinite fatigue life is when the conservative line girder analysis is used with the conservative 66 kip (294 kN) fatigue truck increased by 20%, the conservative safe remaining life estimate would still be about 70 years on bridge #54004 over the Red River. This suggests that bridges with category D or better details and with connection plates attached to both flanges are not as susceptible to fatigue.

The bridge on Highway 36 over Cleveland Avenue (#9276) had the worst fatigue life of the five instrumented bridges. The main reasons why this bridge had the shortest fatigue life is that it had the largest stress ranges (both measured and analytical) with the worst fatigue detail, category E' cover plates. This combination of relatively high stress ranges with poor fatigue details is probably close to the worst-case scenario. There are not likely to be many if any Minnesota bridges that have much higher stress ranges at E' details, although there probably are some other

metro area bridges that have a higher truck volume than the current approximately 1,500 trucks per day per lane on bridge #9276. Because this bridge is already having fatigue problems, an increase in truck weight will only accelerate the damage on this and similar bridges.

From the results of the two bridges with category E positive moment cover plates (bridge #19844 in Lakeville and #27939 over 60th St. in Minneapolis), it can be concluded that fatigue will become a problem for only a few of the bridges with similar details under increased truck weight. This is because the remaining safe lives using stress ranges from the grillage analyses for these bridges were under 25 years, but the remaining mean lives were over 75 years. The safe life indicates a 97.7% probability that the actual fatigue life will exceed the calculated safe life for redundant members. However, the problem with a short remaining safe life, even if the mean life is adequate, is that these bridges deserve increased inspections, which increases costs.

In summary, some steel bridges currently have fatigue problems and an increase in truck weight will amplify those problems. Some steel bridges may be on the cusp of having fatigue problems, and an increase in truck weight will cause an increase in the number of bridges requiring immediate repairs or replacement. However, some bridges, especially the ones with long spans (because the dead load dominates) and/or good fatigue details, will not have fatigue problems even under truck weight increases of over 10% or 20%. The five steel bridges that were instrumented are an example of the different effects of increased truck weights.

- One of the bridges is beginning to have fatigue cracking under current truck weights.
- Two of the bridges are not expected to have fatigue problems, even from increased truck weight.
- Two of the bridges could have fatigue problems decades in the future and an increase in truck weight would increase the likelihood of fatigue problems, although the mean remaining lives for a 10% or 20% increase in truck weight were still adequate (over 75 years for the more accurate grillage model stresses).

The characteristics of steel bridges that are an indication of potential fatigue problems include poor fatigue details, relatively short spans, high truck traffic volume, and high stress ranges.

Poor fatigue details include cover plates, especially on flanges that are thicker than 0.8 in (20 mm) which is category E'. Bridges that have high truck traffic volume are generally located near or in between large metropolitan areas. It is typically difficult to determine which bridge is going to experience the highest stress ranges without performing a detailed analysis for each bridge. However the stress ranges are primarily a function of span length, girder size, and girder spacing.

4.4.3 Bridge Decks

The results for the selected group of bridges were extended in terms of deck fatigue and deck overstressing.

In Chapter C4, it was observed that the most important variable affecting the predicted fatigue life for Minnesota bridges was the Annual Daily Truck Traffic (ADTT) of the bridge. Most of the bridges in the Twin Cities metro area have similar structural deck thicknesses, which range from 8 to 10 in (203 to 254 mm) including the low slump concrete overlay. Within this limited range of variation, the deck thickness was not a significant variable. Although some bridge decks in Minnesota were constructed with deck thicknesses of 6.5 to 7 in (165 to 178 mm), they have been rehabilitated (as described Chapter C3) or redecked so that the structural deck thickness was increased to at least 8 in (203 mm). Other variables, such as girder spacing, girder size and material type were not found to affect the fatigue life significantly (Petrou et al. 1994).

Even though the fatigue lives of the bridge decks constructed or rehabilitated after 1975 in Minnesota under any reasonable scenario are predicted to be greater than the design life of 75 years, in Chapter C4, it was useful to examine the effects of certain variables (e.g. ADTT, deck thickness, girder spacing, and deck reinforcement) on the computed lives when the fatigue limit was ignored. The analyses did not indicate that any of the variables had an effect of immediate concern because the predicted outcome was still the same, that is, the predicted deck life was still in excess of 75 years (the design life). However, if there were a change in the design practice or there were a drastic increase in wheel loads -- and consequently there were to be finite fatigue

lives (less than 75 years), this analysis provides information with regard to the likely effects of these variables.

The most critical bridge among those that were instrumented as part of this project (in terms of deck fatigue) was one of the prestressed concrete bridges, #9731. The thickness of the deck was 9 in (230 mm) and the girder spacing was 109 in (2.8 m). Although these dimensions were typical of the group of bridges in the study, bridge #9731 had the highest truck traffic volume amongst the others, which was the critical factor in determining the most susceptible bridge. Bridge #9731 also had the highest ADTT in the metro area and probably in the state. Even, in the most critical bridge, deck fatigue due to the loadings in the Base Case and Alternative Scenarios (10 and 20% increases) were not a governing factor for determining the service life (>75 years), even though the fatigue limit was ignored (i.e. finite life was assumed), which was very conservative assumption. In fact, this analysis indicated that it would require doubling of the axle weights to cause deck fatigue to begin to govern the service life.

The criterion for overstressing a bridge deck was concrete cracking by reaching the tensile stress level in the transverse direction (that is longitudinal cracking). It was found that the stresses in the transverse direction were more susceptible to overstressing than longitudinal stresses. The bottom fiber at the midspacing between girders and the top fiber over the girders were the potentially susceptible regions to overstressing as verified in the parametric study described in Chapter C5.

In the field tests, it was observed that the measured transverse strains in the bottom surface of the concrete decks near midspan between girders were always well below the concrete cracking strain, even after including the effect of the estimated dead load strains and even for the most critical bridge in this group, bridge #9276. The tandem axle load for the test trucks was presently at the legal tandem axle load limit. Based on the field measured strains and the analyses, it was concluded that the legal axle load limits would have to double in order for cracking due to overstressing to be a significant problem.

To extend the results of overstressing to all of the bridges in the system, the critical characteristics of a bridge structural system leading to overstressing were determined (see Section C5.1). As demonstrated in Section C5.3.2, the maximum transverse strain increased as the crack spacing decreased, in other words the slab behavior approached to the one-way action (Figure C5.71). Therefore, the bridge decks with small crack spacings (less than 5 ft (1.5 m)) formed one of the risk groups susceptible to overstressing in the bridge system.

Other risk group was investigated by combining the possible worst cases in the structural system of a bridge to maximize the strain at midpanel and over the girders. In this investigation, typical crack spacings observed in the field were simulated. The transverse strain over the girders was maximized when the torsional stiffness of the girders was relatively high, and when the truckload was applied so that a relatively high differential deflection of the girders occurred (Case 1). Furthermore, it was demonstrated that the midpoint transverse strain at the bottom surface of the deck was maximized when the torsional stiffness of the girders was relatively low and when one of the wheel lines coincided with the midspacing between the girders (Case 2). For both cases, the maximum practical girder spacing was modeled to simulate high flexibility in the deck.

For both of these cases, the current legal limit loads for single, tandem, and tridem axles were applied as uniformly distributed loads over specific patch areas according to the guidelines in Section C5.1.1. The total transverse strains (i.e. including the dead load) were calculated at two locations (over the girder and at the midpoint between the girders).

For both hypothetical bridge models, critical crack configurations representing the typical conditions found in the study by Eppers et al. (1998) were analyzed including no cracks and two different crack spacings: 9 ft (2.7 m) and 5 ft (1.5 m). The spacings were chosen so that tridem and tandem axles just fit between two cracks in the cases of 9-ft (2.7-m) and 5-ft (1.5-m) crack spacings, respectively. Using the method described in Section C5.1, the cracks were modeled with degraded stiffness shell elements to simulate the continuity between the crack faces due to the reinforcement and aggregate interlock.

Although, with the presence of the cracks, a 20% increase in axle weights, which represents the legal load limit of the truck traffic from Canada and the allowable increase due to the application of the TTI truck weight formula, would not cause overstressing problems at the top surface of the critical bridge deck (over girder), such an increase may cause problems at the bottom surface of the deck (between girders) for the hypothetical bridge simulating Case 2.

Further analyses were performed to determine the extent of the overstressing risk to bridge group incorporating initial transverse cracks in case 2. The analyses demonstrated that the risk group for overstressing includes the bridges with relatively flexible girder cross sections (typically cross sections smaller than 27 in (690-mm) deep), thin bridge decks (deck thicknesses less than 9 in (230 mm)), and large girder spacings (spacings of more than 10 ft (2.7 m)) in the system. These bridges are susceptible to longitudinal cracking at the bottom surface of the deck between the girders. Therefore, such bridges should be inspected and maintained more frequently.

In conclusion, a 20% increase in axle weights enabling the routing of the legal load limits of Canadian truck traffic and TTI truck weight formula can be tolerated on most bridge decks in the system. Such an increase would not have a detrimental effect on a typical bridge in Minnesota. The typical deck thicknesses in recently constructed bridges are 9 in (230 mm), and typical girder spacings are about 8 to 10 ft (2.4 to 3.0 m). Also, the typical spacing of full-depth penetrating transverse cracks from the construction period is approximately 6 ft from the review of the study by Eppers et al. (1990). Relatively flexible bridge decks with transverse cracks spaced less than 5 ft (1.5 m) may be sensitive to overstressing even under the present load regulations.

4.5 RECOMMENDED METHODOLOGY FOR MN/DOT

4.5.1 Prestressed Concrete Bridges

The following methodology is recommended as a way of extending the results presented in this study to other Minnesota prestressed concrete bridges. Two levels of evaluation are provided. The first level of evaluation is more general and should be applied to any prestressed concrete bridge that could appear critical for cracking. The second level of evaluation is a more detailed method of evaluation and should only be applied to bridges that fail the first level of evaluation, where failure is defined as a bridge reaching girder cracking due to the live load considered. The two levels of evaluation do not provide guidelines on the selection of the critical live load for each bridge. This is left to the discretion of the user.

4.5.1.1 First Level of Evaluation

This first level of evaluation consists of a line girder analysis, and it can be broken down into eight steps.

Step 1. Selection of Possible Critical Bridge for Cracking

Select a prestressed concrete bridge. Bridges likely to experience shear cracking will likely have small girder depths and large girder spacing. It is likely that a bridge could be critical for flexural cracking if it has four or more lanes of traffic and if the ratio of live to dead load stresses is above the value of 0.2 found for bridge #9603. In addition, bridges designed for allowable bottom fiber stresses of $3\sqrt{f'_c}$ or $6\sqrt{f'_c}$ ksi ($0.25\sqrt{f'_c}$ and $0.5\sqrt{f'_c}$ MPa) are more likely to experience flexural cracking than bridges designed for an allowable bottom fiber stress of zero. Finally, fewer intermediate diaphragms could lead to increased bottom fiber stresses and more propensity for flexural cracking.

Step 2. Calculation of Prestress Losses and Stress Due to Prestress

Estimate prestress losses by using the refined method provided in the AASHTO Design Specifications (described in Section A2.1.5.3 of this report). Subtract prestress losses from initial prestress values, and use the resulting prestress force to compute girder bottom fiber stresses by using Equation A4.1.

Step 3. Calculation of Dead Load stresses

Calculate dead load due to the deck on the basis of tributary areas (include all wearing courses present at the time of the evaluation). Assume that the weight of the edge barriers is equally supported by all girders in the bridge. Calculate midspan moments due to the total dead load. Finally, calculate girder bottom fiber stresses at midspan due to the total dead load by using Equation A4.2.

Step 4. Estimation of Modulus of Rupture

Compute the modulus of rupture on the basis of the design concrete strength values by using Equation A4.3. Using the design concrete strength is conservative, because concrete strength increases with time, thereby increasing the modulus of rupture.

Step 5. Calculation of Live Loads Stresses

Select a live load and compute live load moments by assuming the girder to be simply supported, and by applying the entire weight of the truck to the line girder. The live load should be placed on the span so as to generate maximum live load moments. Compute live load stresses by using

$$\sigma_{live} = \frac{M_{live} \cdot DF \cdot c_{comp}}{I_{comp}} \qquad \text{A5.1}$$

Equation A5.1.

where: σ_{live} = stress due to live load, ksi (MPa)
DF = AASHTO LRFD live load distribution factor for multiple lanes loaded
M_{live} = midspan moment due to the live load loads, k-ft (N-mm)
c_{comp} = height of composite section neutral axis from the bottom of the girder, in (mm)
I_{comp} = moment of inertia of composite section, in^4 (mm^4)

Step 6. Flexural Cracking Calculations

Use Equation A4.5 to determine if the live load considered will lead to flexural cracking of the bridge. If the results from the first level analysis indicate that the bridge will experience flexural cracking under the selected live load, go to a second level evaluation.

Step 7. Shear Cracking Calculations

Shear cracking should be investigated by following the guidelines provided in the AASHTO LRFD Specifications. The nominal shear capacity of the girders should be determined by using Equation A4.6. The nominal shear demand due to dead and live loads should be determined at the critical section for shear. AASHTO LRFD multiple-lane DFs for shear should be used to distribute the live load to the individual girder.

The second level analysis does not address shear. Therefore, if the results from the first level analysis indicate that the bridge will experience shear cracking under the selected live load, it is up to the Engineer or Bridge Owner to decide on the course of action to be taken. However, it is recommended that prestressed concrete girders not be allowed to reach cracking, as the presence of cracks may lead to increased corrosion and increased strand stress ranges.

Step 8. Number of Cycles to Fatigue Failure

Strand stress ranges should be computed on the basis of Equation A4.9. The number of cycles to fatigue failure can then be computed from Equation A2.30.

4.5.2 Second Level Evaluation

The second level evaluation is similar to the first level evaluation, except that for Step 5, the live load stresses should be determined directly from a more refined method of analysis, by means of a grillage or other suitable method of analysis. By using a more refined method of analysis to compute live load stresses, the conservatism typically present in the AASHTO live load distribution factors is avoided, thereby obtaining a more accurate assessment of live load stresses.

4.5.3 Steel Bridges

To estimate the remaining fatigue life of a critical steel bridge detail, the procedures of NCHRP 299 should be used. There are two levels of analysis that can be done. The first level would involve using a line girder analysis with the NCHRP 299 distribution factor to estimate the stress ranges at the critical detail. The second level would require a more accurate evaluation of the stress ranges; such as creating a finite element grillage model or collecting measured stress data (which could be used as a third level of evaluation if necessary). If the remaining life is adequate after the line girder analysis, it can be assumed that the bridge should have an infinite fatigue life.

The procedure for calculating the NCHRP 299 distribution factor is repeated here for convenience and is discussed further in Section B2.1.2. The distribution factor for interior I-shaped members is $DF_i = S/D$ but not more than $(S - 3)/(S)$, where S is the girder spacing in feet and D is based on the span length distance between points of dead load contraflexure and is listed in Table 4.6. However, if there are only two girders on the bridge, assume the deck acts as a simple beam supporting the fatigue truck in the center of the lane. There is also an equation for exterior girders in NCHRP 299, but is not given here because it has been found that the largest effective stress ranges are typically measured on the interior girder that is nearest to the left wheels of traffic in the right lane (Laman and Nowak 1996).

It is possible to simply estimate the reduction in remaining fatigue life for any change in truck weight based on the fact that the remaining fatigue life is inversely proportional to the cube of the stress range (or fatigue truck weight). This is shown in Equation 4.1, where Y_x is the remaining fatigue life after an increase in truck GVW, x (expressed as a decimal), and Y_0 is the remaining fatigue life assuming no future increase in truck weight. This equation can be used to estimate the percent reduction in fatigue life from a change in truck weight by x percent as shown in Equation 4.2.

$$Y_X = \frac{1}{(1+x)^3} \cdot Y_0 \qquad 4.1$$

$$\left(\frac{Y_0 - Y_X}{Y_0}\right)\cdot 100\% = \left(1 - \frac{1}{(1+x)^3}\right)\cdot 100\% \qquad 4.2$$

These equations will only give accurate results if the truck volume is assumed constant in the future. If the truck volume is assumed to be increasing, the percent reduction will be less than what Equation 4.2 would indicate because more fatigue damage would be done by the large traffic volumes near the end of the fatigue life. If the effect of traffic growth is desired to be included, the procedures of NCHRP 299 for two or more periods of constant traffic growth can be used, which are described in Section B2.1.2.1.2. However, typically, this is a good estimate; for example, there was a 20-25% reduction in remaining fatigue lives for the instrumented bridges with finite remaining lives for a 10% increase in GVW, while Equation 4.2 would estimate a 25% reduction in life for this increase.

To identify which steel bridges are more susceptible to fatigue damage there are some characteristics that should be looked for. The characteristics of steel bridges that are an indication of potential fatigue problems include poor fatigue details, high truck traffic volume, high stress ranges, and relatively short spans. Poor fatigue details include cover plates, especially on flanges that are thicker than 0.8 in (20 mm) which is category E'. Typically bridges with poor fatigue details were built before the fatigue provisions that were developed in the 1970's or bridges built before 1985 for distortion induced fatigue. Bridges that have high truck traffic volume are generally located near or in between large metropolitan areas. It is typically difficult to determine which bridge is going to experience the highest stress ranges without performing a detailed analysis for each bridge. However the stress ranges are primarily a function of span length, girder size, and girder spacing.

4.5.4 Bridge Decks

Different approaches for two different problems in bridge decks (deck fatigue and deck overstressing) were proposed in Chapter C6.

Although the deck fatigue is not concern for the current loads and future load scenarios studied, a quick screening method for deck fatigue is recommended to further extend the results of this study to specific bridge decks of concern. Further detailed approaches are described in the case of the failure with the quick screening method.

In the quick screening method, the legal axle load (e.g. 20 kips for current traffic) can be assumed as the applied load and the punching shear strength can be computed using the conventional AASHTO punching shear strength formula (Equation C4.1 and C4.2). Noting that the legal axle load is much higher than the effective axle load in fatigue and the conventional formula predicts 1/3 to 1/2 actual punching shear strength of the bridge deck slabs, the outcome of the implementation of these into deck fatigue model will be conservative. If the resulted fatigue life is higher than the service life of the bridge, no further refined method is required. Otherwise, the refinements result in more realistic predictions for service life of the bridge in terms of deck fatigue.

In the case that the fatigue life calculated by the quick screening method is smaller than the bridge service life of 75 years, the refinements listed below should be applied:

- Application of Hewitt algorithm, which includes the enhancement from the compressive membrane forces, to calculate the punching shear strength of the bridge deck as described in Section C4.1,
- Calculation of effective axle weight from site-specific WIM data as described in Section C4.2.1, and
- Application of a shifting algorithm for load histogram as described in Section C4.2.4.

In this study, the extension of deck overstressing problem (i.e. susceptibility to longitudinal cracking) was studied based on reaching cracking strain level under legal load. The approach applied herein can be applied for different specific loads and specific bridge decks of concern.

As described in Section C5.1.1, the models with shell elements in the loaded area and grillage outside of the loaded area should be used. The methodology given in Section C5.1.1 should be followed in the investigation of maximum transverse strains at midpanel and over girders.

The maximum transverse strain over girders shall be calculated using three-girder model of the bridge concerned. The full effective deck width should be modeled with shell elements in the loaded area or beam elements in the grillage. The loading should be applied in the position so that the maximum differential deflection between one of the edge girders and the middle girder can be obtained. In that case, the maximum transverse strain is calculated over middle girder.

In the investigation of the maximum transverse strain between the girders, the model with two girders bounding the panel of concern can be used. The methodology described to create finite element models in Section C51.1.1 should be followed as indicated for the three-girder model. Only one wheel line should be applied along the midline between the girders.

In both the three-girder and two-girder models, the cracks observed in the field or the imaginary ones causing the critical case should be modeled with the reduced thickness at the crack locations. In both of the models, the maximum transverse strain occurs at the transverse crack edge when the loading is located at the closest position to the crack edge.

It is important to model the transverse cracks with reasonable stiffness reduction. In the present study, for the most deteriorated situation observed in the field, the reduction to $1/8^{th}$ of the original deck thickness resulted in a good correlation with the field test data. It is thought that the reduction in the range of $1/10^{th}$ to $1/8^{th}$ of original deck thickness gives reasonably conservative predictions of maximum deck transverse strains. Then the maximum transverse strain resulted should be compared with the concrete cracking level of 132 μstrain. If the slab

fails in this check, the inspections and maintenance should be performed more frequently than those of typical bridges.

TABLES

	σ_{pr} (ksi)[a]	σ_{dead} (ksi)[a]	σ_{live} (ksi)[a] 3-axle Single Unit Truck (Test Truck)	$\sigma_{pr} + \sigma_{dead} + \sigma_{live}$ (ksi)[a]	Modulus of Rupture, $7.5\sqrt{f'_c}$ (ksi)[a]
Bridge 9731[c]	-2.47[b]	1.89	0.36[d]	-0.22	0.64
Bridge 9603[c]	-2.33[b]	1.77	0.36[d]	-0.20	0.6
Bridge 04006[c]	-2.81[b]	2.24	0.21[e]	-0.36	0.58

Table 4.1a Summary of concrete bottom fiber stresses for 3-axle truck

	σ_{pr} (ksi)[a]	σ_{dead} (ksi)[a]	σ_{live} (ksi)[a] 5-axle Tractor Semitrailer	$\sigma_{pr} - \sigma_{dead} - \sigma_{live}$ (ksi)[a]	Modulus of Rupture, $7.5\sqrt{f'_c}$ (ksi)[a]
Bridge 9731[c]	-2.47[b]	1.89	0.34[d]	-0.24	0.64
Bridge 9603[c]	-2.33[b]	1.77	0.30[d]	-0.26	0.6
Bridge 04006[c]	-2.81[b]	2.24	0.21[e]	-0.36	0.58

[a] 1 ksi = 6.89 MPa
[b] Negative numbers indicate compression
[c] Girder properties used included transformed areas to account for prestressing reinforcement
[d] Live load stress corresponding to four trucks crossing the bridge side-by-side
[e] Live load stress corresponding to two trucks crossing the bridge side-by-side

Table 4.1b Summary of concrete bottom fiber stresses for 5-axle truck

Remaining Safe Life	54 kip Fatigue Truck Analysis Model		WIM Fatigue Truck Analysis Model	
Bridge #	Line Girder Analysis	Grillage Analysis	Line Girder Analysis	Grillage Analysis
19844	-2	30	-5	23
27939	5	17	-1	12
54004	> 75	> 75	> 75	> 75
9030	NA	> 75	NA	> 75
9276	-24	-11	-26	-15

1 kip = 4.45 kN

Table 4.2 Remaining safe life for the instrumented bridges assuming the fatigue truck weight does not change over time

Remaining Mean Life	54 kip Fatigue Truck		WIM Fatigue Truck	
	Analysis Model		Analysis Model	
Bridge #	Line Girder Analysis	SAP 2000	Line Girder Analysis	SAP 2000
19844	33	> 75	26	> 75
27939	> 75	> 75	> 75	> 75
54004	> 75	> 75	> 75	> 75
9030	NA	> 75	NA	> 75
9276	3	29	-2	20

1 kip = 4.45 kN

Table 4.3 Remaining mean life for the instrumented bridges assuming the fatigue truck weight does not change over time

Remaining Safe Life	54 kip Fatigue Truck		WIM Fatigue Truck	
	Analysis Model		Analysis Model	
Bridge #	Line Girder Analysis	Grillage Analysis	Line Girder Analysis	Grillage Analysis
19844	*	24	*	18
27939	4	12	*	9
54004	> 75	> 75	> 75	> 75
9030	NA	> 75	NA	> 75
9276	*	*	*	*

1 kip = 4.45 kN

** Remaining safe life already exhausted under current conditions.*

Table 4.4 Remaining safe life for the instrumented bridges with a fatigue truck GVW increase of 10%

Remaining Mean Life	54 kip Fatigue Truck		WIM Fatigue Truck	
	Analysis Model		Analysis Model	
Bridge #	Line Girder Analysis	Grillage Analysis	Line Girder Analysis	Grillage Analysis
19844	26	> 75	21	> 75
27939	> 75	> 75	68	> 75
54004	> 75	> 75	> 75	> 75
9030	NA	> 75	NA	> 75
9276	2	22	*	15

1 kip = 4.45 kN

** Remaining mean life already exhausted under current conditions.*

Table 4.5 Remaining mean life for the instrumented bridges with a fatigue truck GVW increase of 10%

Span (ft)	D
30 or less	17
40	19
60	20
90	22
120 or more	23

1 ft = 0.305 m

Table 4.6 D factor for lateral distribution. (Moses et al. 1987)

CHAPTER 5 – SUMMARY AND CONCLUSIONS

Five steel and three prestressed concrete bridges were selected and instrumented to determine the effect of increasing truck weight on steel and prestressed concrete bridges in Minnesota, including both the girders and deck. Tests were performed on these bridges with known loads (50 kip (222 kN) Mn/DOT sand trucks) so that analytical models could be compared with the measured results. With the analytical models that produced results similar to the measured results, the remaining service lives of bridge components could be estimated for both current truck loads and increased truck loads. The results from the eight tested bridges were then used to determine which bridges are more susceptible to deterioration from load increases. The conclusions for each of the three main bridge components that were studied are presented in the following sections.

5.1 PRESTRESSED CONCRETE BRIDGES

- Shear cracking (not incipient shear failure) was the first phenomena to occur with increasing truck weight that could significantly affect service life for prestressed concrete I-girder bridges in the State of Minnesota.

- It is likely that up to 20% increases in allowable gross vehicle weight (GVW) will not lead to shear cracking and associated decrease in the remaining life.

- Certain presently allowed permit load configurations such as Standard C with a GVW of 159 kips could lead to shear cracking in several Minnesota prestressed concrete I-girder bridges. The maximum GVW of these permit vehicles should not be increased and further consideration should be given to the impact of these permit vehicles on deterioration of prestressed concrete I-girder bridges.

- Prestressed concrete I-girders in bridges with four or more lanes of traffic, and a large ratio of live load stresses to dead load stresses were at a higher risk of experiencing flexural cracking.

- Minnesota prestressed concrete I-girder bridges should not be susceptible to fatigue, even with a 20% increase in GVW.

- Girders in the three tested bridges were not cracked.

- Live load distribution factors found from both AASHTO specifications were found to be conservative for the three tested bridges.

- The presence of interior reinforced concrete diaphragms had a significant effect on live load distribution factors and live load bottom fiber girder stresses. For bridge #9731, the effect of the diaphragms was more pronounced because bridge #9731 had two more lines of interior diaphragms than bridges #9603 and #04006.

5.2 STEEL BRIDGES

- Fatigue is the deterioration mechanism that is most affected by an increase in truck loads. Since fatigue is not sensitive to loads that occur less frequently than 0.01% of truck traffic, fatigue is not sensitive to permit loads unless they exceed this frequency at a given location.

- Modern steel bridges (built with the improved fatigue design specifications that were developed in the 1970's) should tolerate increases in GVW greater than 20% before they would experience a safe fatigue life less than 75 years. A possible exception to this is web-gap cracking on bridges built before it was specified in 1985 that connection plates be connected to both girder flanges. The results of Berglund and Schultz (2002) can be used to identify bridges that are more susceptible to this type of cracking. It can be estimated that the frequency of the repairs will increase 33% if the legal GVW increased by 10%; and the frequency of the repairs will increase 73% if the legal GVW increased by 20%. The present costs for maintenance and repairs of bridges already experiencing

web-gap cracking would be expected to increase at least as much as the repair frequency increases.

- Steel bridges that have high truck traffic volumes and poor fatigue details, such as welded cover plates (especially when it is category E'), are the most likely to have increased fatigue problems if truck weight were increased. A few of these bridges are presently experiencing fatigue cracking and therefore cannot tolerate any increase in truck weight. For bridges that have a finite fatigue life (less than 75 years), an increase in truck weight of 20% would lead to a reduction in the remaining fatigue life of up to 42% (a 10% increase would lead to a 25% reduction in fatigue life).

- The grillage method produced stress ranges that were closest to the measured results. Therefore, the estimated fatigue lives from this method are considered to be the most accurate.

- Line girder analyses are conservative for typical multi-girder bridges (i.e. ones that do not contain stringers and floor beams). The NCHRP 299 distribution factors produced stresses that were about 25 – 50% larger than the measured stress ranges, while the AASHTO LRFD distribution factors gave stress ranges that were about 50 – 80% larger than the measured stress ranges. Although line girder analyses are conservative, they can still be used as a preliminary analysis. For example, for bridge #54004 (over the Red River) the remaining safe life was still over 75 years for 10% increased truck weights using the line girder analyses. If the estimated remaining life is not adequate, then a more detailed method can be used. This included using the grillage method or collecting measured field-test data.

5.3 BRIDGE DECKS

- Axle weights are the important loading characteristic affecting bridge decks rather than GVW.

- Longitudinal cracking is the first the first phenomena to occur in bridge decks with increasing truck weight that could significantly affect service life. Fatigue is not expected even at 20% greater axle loads.

- Transverse cracks in bridge decks are primarily a consequence of shrinkage of the concrete during the construction period and are unrelated to the mechanical loading from the traffic.

- Recently constructed bridge decks in Minnesota (i.e. decks with typical 9-in thickness) should not be affected by a 20% increase in axle loads.

- Relatively flexible bridge decks (i.e. girder spacings greater than 10 ft (3.0 m) and deck thicknesses less than 9 in (225 mm)) with transverse cracks spaced less than 5 ft (1.5 m) may be sensitive to longitudinal cracking even under the present load regulations. Therefore, such bridge decks should be inspected and maintained more frequently.

- The analytical methods used in this study (i.e. the multi-girder and simplified models including the combination of Grillage and 3D finite elements) predicted the measured strains with a good agreement.

REFERENCES

Altay, A.K. (2002). "Effects of Increasing Truck Weight on Reinforced Concrete Decks." Thesis, Master of Science in Engineering, Department of Civil Engineering, University of Minnesota, May.

American Association of State Highway and Transportation Officials (AASHTO) (1990). *Guide Specifications for the Fatigue Evaluation of Existing Steel Bridges*. Washington, D.C.

American Association of State Highway and Transportation Officials (AASHTO) (1994). *LRFD Bridge Design Specifications*. Washington, D.C.

American Association of State Highway and Transportation Officials (AASHTO) (1998). *LRFD Bridge Design Specifications*. Washington, D.C.

American Association of State Highway and Transportation Officials (AASHTO) (1989). *Standard Specifications for Highway Bridges*. Washington, D.C.

American Association of State Highway and Transportation Officials (AASHTO) (1994). *Manual for Condition Evaluation of Bridges, 2nd Edition*. Washington, D.C.

Arabbo, D.S. (2002). "Effects of Increasing Truck Weight on Prestressed Concrete Bridges." Thesis, Master of Science in Engineering, Department of Civil Engineering, University of Minnesota, May.

Azad, A. K., Baluch M.H., Al-Mandil M.Y., and Al-Suwaiyan, "Static and Fatigue Tests of Simulated Bridge Decks," *Experimental Assessment of Performance of Bridges*, Proceedings of ASCE Convention, Boston, Mass., Oct. 1986, pp. 30-41.

Bakht, B. and Jaeger, L.G. (1985). *Bridge Analysis Simplified*. McGraw-Hill, Inc.

Batchelor, B., Hewitt B.E., Csagoly, P., "An Investigation of the Fatigue Strength of Deck Slabs of Composite Steel/Concrete Bridges," *Transportation Research Record 664*, TRB, National Research Council, Washington, D.C., Vol.1, 1978, p.153-161.

Berglund, E. and Schultz, A.E. (2002). "Girder Differential Deflection and Distortion-Induced Fatigue in Skewed Steel Bridges." Transportation Research Board, 81st Annual Meeting, Washington, D.C., January 13-17, 2002, Paper No. TRB 02-3412.

Clough, R.W. (1965). *Stress Analysis*. ed. O.C. Zienkiewicz and G.S. Holister (Wiley), Chapter 7, 1965.

Corwin, E.B. (2002). "Effects of Increasing Truck Weight on Steel Bridges." Thesis, Master of Science in Engineering, Department of Civil Engineering, University of Minnesota, May.

Cusens, A.R., and Pama, R.P. (1975). *Bridge Deck Analysis*. Wiley-Interscience, Great Britain.

Dexter, R.J. and Fisher J.W. (1997). "Fatigue and Fracture." *Handbook of Structural Engineering*, Chen, W.F. ed., CRC Press LLC, New York, Chapter 24.

Dexter, R.J. and Fisher, J.W. (1999). "Fatigue and Fracture." *Handbook of Bridge Engineering*, Chen W.F. ed., CRC Press LLC, New York, Chapter 53.

Fang, I. K., Tsui C. K. T., Burns N. H., and Klinger R. E., "Fatigue Behavior of Cast-in-Place and Precast Panel Bridge Decks with Isotropic Reinforcement," PCI Journal, Vol. 35, No.3, May-June 1990, pp.28-39.

Federal Highway Administration (FHWA) (1994). *Bridge Formula Weights*. Publication No. FHWA-MC-94-007, Washington, D.C.

Fisher, J.W. (1984). *Fatigue and Fracture in Steel Bridges.* John Wiley and Sons, New York.

Fisher, J.W. (1997). "The Evolution of Fatigue Resistant Steel Bridges." 1997 Distinguished Lectureship, Transportation Research Board, 76th Annual Meeting, Washington, D.C., January 12-16, 1997. Paper No. 971520: 1-22.

Fisher, J.W., Albrecht, P.A., Yen, B.T., Klingerman D.J., and McNamee B.M. (1974). "Fatigue Strength of Steel Beams With Welded Stiffeners and Attachments." *National Cooperative Highway Research Program Report 147*, Transportation Research Board, Washington, D.C.

Fisher, J.W., Frank, K.H., Hirt, M.A., and McNamee, B.M. (1970). "Effect of Weldments on the Fatigue Strength of Steel Beams." *National Cooperative Highway Research Program Report 102*, Highway Research Board, Washington, D.C.

Fisher, J.W., Jian, J., Wagner, D.C., and Yen, B.T. (1990). "Distortion-Induced Fatigue Cracking in Steel Bridges." *National Cooperative Highway Research Program Report 336*, Transportation Research Board, Washington, D.C.

Ghosn, M. (2000). "Development of Truck Weight Regulations Using Bridge Reliability Model." *Journal of Bridge Engineering*, ASCE, 5(4), pp 293-303.

Hewitt, B.E., "An Investigation of the Punching Strength of Restraint Slabs with Particular Reference to the Deck Slabs of Composite I-Beam Bridges," Thesis Presented to Queen's University at Kingston, Ontario, Canada, in Partial Fulfillment of the Requirements for the Degree of Doctor of Philosophy.

Hewitt, B.E., and Batchelor, B.deV., "Punching Shear Strength of Restraint Slabs," *Journal of the Structural Division*, ASCE 101 (5T9), 1975, pp.1837-1853.

Jajich, D., Schultz, A.E., Bergson, P.M., and Galambos, T.V. (2000). "Distortion-Induced Fatigue in Multi-Girder Steel Bridges." Minnesota Department of Transportation, Final Report.

James, R.W., Noel, J.S., Furr, L.H., and Nutt, R.V. (1986). "Proposed New Truck Weight Limit Formula." *Journal of Structural Engineering*, ASCE, 112(7), pp 1589-1604.

Kato, T., and Goto Y., "Effect of Water Infiltration of Penetration Deterioration of Bridge Deck Slabs," *Transportation Research Record 950*, National Research Research Council, Washington, D.C., 1978, pp. 202-209.

Laman J.A. and Ashbough J.R. (2000). "Highway Network Bridge Fatigue Damage Potential of Special Truck Configurations." *Transportation Research Record No. 1696*, Fifth International Bridge Engineering Conference, April 3-5, 2000, Tampa Bay, Florida, Volume 1.

Laman, J.A. and Nowak, A.S. (1996). "Fatigue-Load Models for Girder Bridges." *Journal of Structural Engineering*, 122(7), pp 726-733.

McKeefry, J. and Shield, C. (1999). "Acoustic Emission Monitoring of Fatigue Cracks in Steel Bridge Girders." Minnesota Department of Transportation, Final Report, 1999-36, September 1999.

Minnesota Department of Transportation (1998). *BRiNFO Users Manual*, Office of Bridges and Structures, Bridge Management Unit, October 1998 revision.

Moses, F. and Bakht, B. (1988). "Lateral Distribution Factors for Highway Bridges." *Journal of Structural Engineering,* ASCE, 114(8), pp 1785-1803.

Moses, F., Schilling, C.G., and Raju, K.S. (1987). "Fatigue Evaluation Procedures for Steel Bridges." *National Cooperative Highway Research Program Report 299*, Transportation Research Board, Washington, D.C.

Newmark, N.M. (1948). "Design of I-beam bridges." Highway Bridge Floor Symposium, *Journal of Structural Division,* ASCE, 74(2), pp 141-161.

Nordby, G.M., "Fatigue of Concrete-A Review of Research," *Journal of the American Concrete Institute*, Vol. 30, No. 2, Detroit, MI, August, 1958, pp. 191-219.

Nowak, A.S. and Al-Zaid, R. (1989). "Fatigue Reliability of Prestressed Concrete Bridges." *Proc. ICOSSAR 89 5th International Conference on Structural Safety and Reliability*. publ. by ASCE, New York, NY, USA. pp 1939-1942.

O'Connell, H.M. and Dexter, R.J. (2000). "Fatigue Evaluation of the Deck Truss of Bridge 9340." Minnesota Department of Transportation, Final Report.

Okada, K.; Okamura H.; and Sonada K. "Fatigue Failure Mechanism of Reinforced Concrete Deck Slabs," *Transportation Research Record 664*, TRB, National Research Council, Washington, D.C., 1978, pp.136-144.

Ontario Highway Bridge Design Code, 3rd Ed. Ministry of Transportation of Ontario, Downsview, Ont., 1991.

Overman T.R., Breen J.E., and Frank K.H. (1984). "Fatigue Behavior of Pretensioned Concrete Girders." *Final Research Report 300-2F,* Center for Transportation Research, Bureau of Engineering Research, University of Texas at Austin, Austin, TX.

Perdikaris, P.C.; Petrou M.F.; and Wang A., "Fatigue Strength and Stiffness of Reinforced Concrete Bridge Decks," *Final Report FHWA/OH-93/016*, Ohio Department of Transportation, March 1993.

Petrou, M., Perdikaris P. C., and Wang A., "Fatigue Behavior of Non-composite Reinforced Concrete Bridge Deck Models," *Transportation Research Record 1460*, TRB, National Research Council, Washington, D.C., 1994, pp.73-80.

Sanders, W.W., and Elleby, H.A. (1970). "Distribution of Wheel Loads on Highway Bridges." *National Cooperative Highway Research Program Report 83*, Transportation research Board, Washington, D.C.

Transportation Research Borad (TRB) (1990). "Truck Weight Limits: Issues and Options." *Special Report 225*.